Aus der Medizinischen Klinik und Poliklinik IV der

Ludwig-Maximilians-Universität München

Direktor: Prof. Dr. med. Martin Reincke

Role of murine double minute-2 in diabetic kidney disease

Dissertation

Zum Erwerb des Doktorgrades der Medizin

an der Medizinischen Fakultät der

Ludwig-Maximilians-Universität München

vorlegt von

Anaïs Rocañín Arjó

aus Barcelona, Spanien

2017

Mit Genehmigung der Medizinischen Fakultät

der Universität München

Berichterstatter:	Prof. Dr. med. Hans-Joachim Anders
Mitberichterstatter:	Prof. Oliver Schnell
	PD Heike Pohla
	Prof. Peter Weyrich
Mitbetreuung durch den promovierten Mitarbeiter:	
	Dr. Satish Devarapu
Dekan:	Prof. Dr. med. Reinhard Hickel

Tag der mündlichen Prüfung: 26.10.2017

To my beloved family

A la meva estimada família

Meiner geliebten Familie

TABLE OF CONTENTS

ZUSAMMENFASSUNG

„Murine double minute 2“ (Mdm2) ist eine E3-Ubiquitin-Ligase, die das Zellwachstum via Inhibition des Tumorsupressorproteins p53 fördert. Die Blockade dieses Enzyms durch das Kleinmolekül Nutlin-3a wird derzeit wegen seines potentiellen Nutzens in der Krebstherapie in klinischen Studien getestet. Die möglichen Nebenwirkungen von Nutlin-3a in gesunden Geweben, bedingt durch die Störung der Zellhomöostase auf Grund Konzentrationsverschiebungen zwischen p53 und Mdm2, geben jedoch Anlass zur Sorge. In einem acute-kidney-injury(AKI)-Mausmodell zeigte die Verabreichung von Nutlin-3a eine verminderte Heilungsfähigkeit. Zudem zeigte die spezifische *Mdm2*-Deletion in Podozyten und Tubuluszellen eine signifikante Beeinträchtigung der Nierenfunktion, einhergehend mit der Einleitung von Podoptosis (p53-overexpression dependent cell death). Auf Grund dieser Beobachtungen stellten wir die Hypothese auf, dass die Gabe von Nutlin-3a in gesunden Mäusen die Nierenfunktion durch Podoptosis der Podozyten und Tubuluszellen schädigt.

Im Einklang mit der Hypothese beobachteten wir durch die Stimulation von Mauspodozyten- und Maustubuluszell-Kulturen mit Nutlin-3a vermehrten Zelluntergang. Zudem verursachte die Nutlin-3a-Verabreichung in gesunden Mäusen die Stabilisierung von p53 mit resultierender Funktionsbeeinträchtigung der glomerulären Filtrationsbarriere und Albuminurie aufgrund einer Podocytopenie. Es konnte weiterhin eine vermehrte Makrophageninfiltration, eine Hochregulation von Markern der Tubulusschädigung und Entzündungsreaktion, sowie erhöhtes Blut-Harnstoff-Stickstoff beobachtet werden. Bei der Planung einer Nutlin-3a-Therapie, muss deshalb eine potentielle Nierenschädigung nach Blockade von Mdm2 Berücksichtigung finden.

Da sich eine Mdm2-Blockade in chronischen Glomerulopathien durch die Inhibition der mitotischen Katastrophe auch positiv auswirken kann, stellten wir die Hypothse auf, dass Nutlin-3a die diabetischen Nephropathie verbessern kann, indem Entzündungsreaktion und die mitotische Katastrophe in Podozyten unterdrückt werden. Erwartungsgemäß zeigte sich nach Nutlin-3a Gabe in diabetischen Mäusen reduzierte Inflammation und Fibrose, aber die Schädigung von Podozyten war nicht vermindert

und die Nierenfunktion dadurch nicht verbessert. Entgegen der ursprünglichen Annahme, wurde im Vergleich zu Plazebo eine schlechtere Nierenfunktion hinsichtlich Blut-Harnstoff-Stickstoff, als auch eine signifikantere Podozytopenie beobachtet. Diese unerwarteten Ergebnisse unterstützen jedoch eine neuere Arbeit in metabolomics und computational network analysis von Saito et al., in welcher Mdm2 als ein wichtiges heruntergeregeltes Protein bei diabetischer Nierenerkrankung aufgezeigt wurde.

Zusammenfassend kann die therapeutische Mdm2-Blockade eine Schädigung der Nierenfunktion sowohl in Nierengesunden, als auch in Patienten mit diabetischen Nephropathien begünstigen.

SUMMARY

Murine double minute 2 (Mdm2) is an E3 ubiquitin ligase that promotes cell growth through negative regulation of the tumour suppressor p53. Its blockade with the small molecule antagonist Nutlin-3a is currently tested on clinical trials for its potential benefit as cancer treatment. The crucial equilibrium between p53 and Mdm2 in the cell homeostasis raises however concern on the effect of this drug in healthy tissues. Its administration in a mouse AKI model showed a diminished capacity of healing and the specific deletion of *Mdm2* in both podocytes and tubular cells induced p53-overexpression dependent cell death (podoptosis). For this reason we hypothesized that the administration of Nutlin-3a to healthy mice damages renal function by promoting podoptosis in podocytes and tubular cells.

Consistent with the hypothesis, we observed that stimulation with Nutlin-3a increased cell death in cultured mouse podocytes and tubular cells. In addition, treatment with Nutlin-3a caused in healthy mice stabilization of p53 levels and subsequent podocytopenia, promoting albuminuria and impaired glomerular filtration barrier. Moreover, increased macrophage infiltration was observed together with upregulation of inflammatory and tubular injury markers and augmented blood urea nitrogen levels. Therefore, renal damage after blockade of Mdm2 needs to be regarded when considering Nutlin-3a therapy.

As blockade of Mdm2 can at the same time be beneficial in chronic glomerulopathies by inhibiting podocyte mitotic catastrophe, we hypothesized that Nutlin-3a could ameliorate diabetic nephropathy by preventing mitotic catastrophe and inhibiting inflammation; effect that has been previously observed in different disease models, where inflammation plays a central role in the pathogenesis. The administration of Nutlin-3a to diabetic mice did indeed decrease inflammation and fibrosis but it did not improve podocyte injury or renal function; contrary to the original hypothesis, increased podocytopenia and decreased renal function in terms of BUN compared to the placebo group. These results could further support a recent work on metabolomics and computational network analysis from Saito et al., where Mdm2 was revealed as a relevant downregulated protein in the diabetic kidney disease.

In conclusion, therapeutic Mdm2 blockade may hold the risk of damaging renal function in patients with no underlying kidney diseases and also in those with diabetic nephropathy.

1. INTRODUCTION

1.1 Chronic kidney disease

Chronic kidney disease (CKD) is a gradual and progressive loss of kidney function, caused by abnormalities of kidney structure or function present for 3 months or longer (Levey AS 2012). Renal abnormalities include albuminuria (albumin/creatinine ratio >30mg/g), urine sediment abnormalities, electrolyte imbalance due to tubular disorders, histological abnormalities and decreased glomerular filtration rate (GFR) <60 ml/min/1,73m^2 (KDIGO 2012).

CKD severity can be classified according to the GFR in five different stages (table 1) (Levey AS 2005). However, the inclusion of albuminuria and clinical diagnosis to the classification defines more precisely the severity of the disease and helps to predict the prognosis (figure 1) (Levey AS 2011, KDIGO 2012). The need of kidney replacement therapy to ensure the survival of patients defines end-stage renal disease (ESRD), the most advanced form of CKD.

Table 1. Severity of kidney disease.

Stage	Description	GFR (ml/min/1,73m^2)	Related terms
1	Kidney damage with normal or increase in GFR	≥90	Albuminuria, proteinuria, haematuria
2	Kidney damage with mild decrease in GFR	60-89	Albuminuria, proteinuria, haematuria
3	Moderate decrease in GFR	30-59	Chronic renal insufficiency, early renal insufficiency
4	Severe decrease in GFR	15-29	Chronic renal insufficiency, early renal insufficiency, pre-ESRD
5	Kindey failure	<15 (or dialysis)	Renal failure, uraemia, ESRD

GFR = glomerular filtration rate; ESRD = End-stage renal disease. Adopted from (Levey AS 2005).

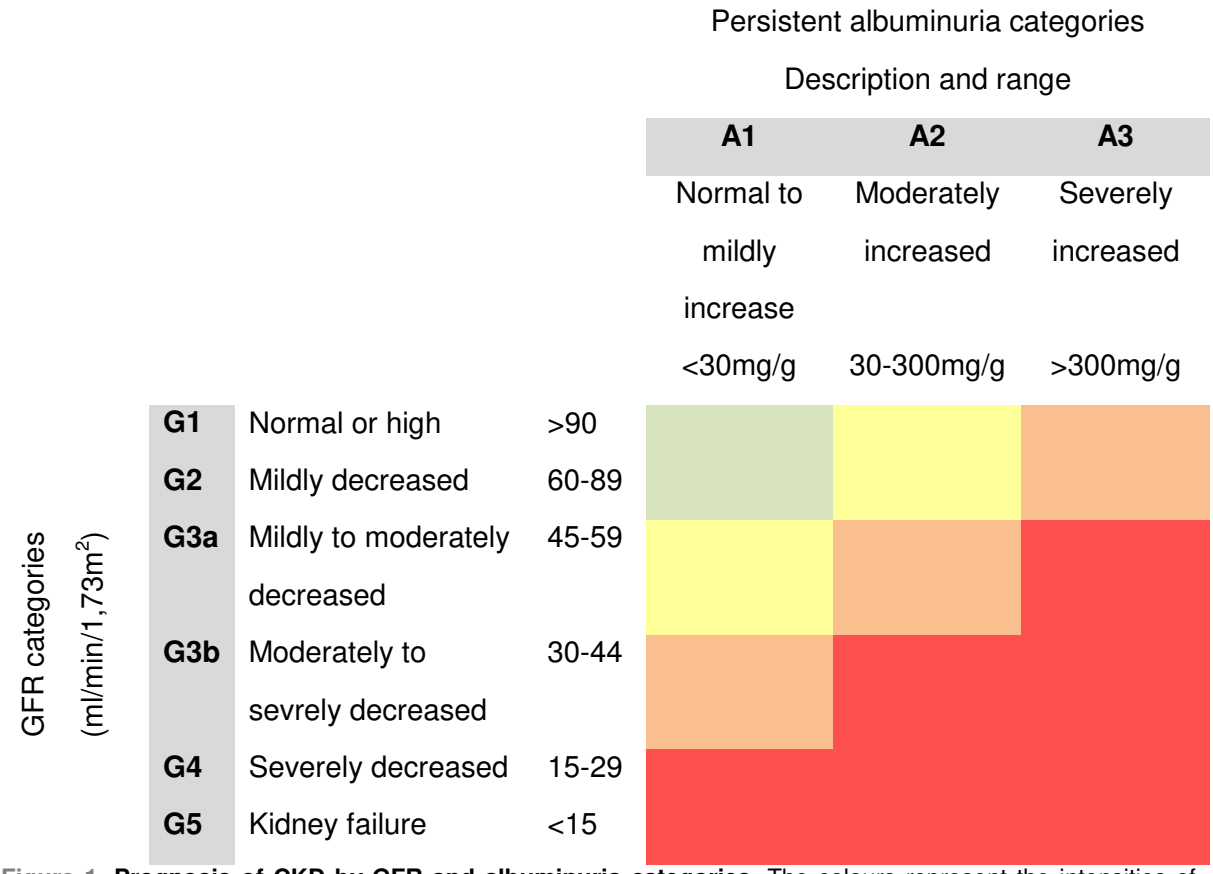

Figure 1. Prognosis of CKD by GFR and albuminuria categories. The colours represent the intensities of risk. Green: low risk; yellow: moderately increased risk; orange: high risk; red: very high risk. Adapted from (KDIGO 2012).

The prevalence of CKD accounts for approximately 14% of the adult US population, being the main risk factors cardiovascular disease and diabetes mellitus, followed by hypertension and obesity (Levey AS 2010, USRDS 2015). The prevalence of CKD showed an increasing tendency in the nineties (Ju W 2012), but it stabilized in the last years mostly due to the reduction of percent of individuals at target blood pressures, percent of individuals not smoking and percentage of diabetics with glycosylated hemoglobin <7% (USRDS 2015).

1.2 Diabetic kidney disease

1.2.1 Diabetes Mellitus

Diabetes mellitus (DM) refers to a group of common metabolic disorders that shares the phenotype of hyperglycemia (Powers AC 2008). According to the pathophysiological process that leads to hyperglycaemia, DM can be classified into different types (table 2) from which type 2 diabetes (T2D), involving around 90% of DM, and type 1 diabetes (T1D) are the most prevalent. While in T1D there is a total lack of insulin due to destruction of

pancreatic β cells, in T2D the pathophisiology combines peripheral insulin resistance, impaired insulin secretion and increased glucose production (Powers AC 2008). The aetiology of T1D and T2D combines both genetic predisposition with environmental factors. The environmental triggers of T1D in genetically predisposed individuals are not well known. In T2D, it has been shown that lifestyle habits contribute greatly to the development and progression of the disease, involving mainly high fat diet and physical inactivity (ECDCDM 2002).

Table 2. Classification of diabetes types.

Types of diabetes
1.Type 1 diabetes
A. Immune-mediated
B. Idiopathic
2. Type 2 diabetes
3. Other specific types of diabetes
A. Genetic defects of βcell function
MODY 1 (hepatic nuclear transcription factor 4α, HNTF-4α)
MODY 2 (glucokinase)
MODY 3 (HNF 1α)
MODY 4 (insulin promoter factor 1)
MODY 5 (HNF 1β)
MODY 6 (NeuroD1)
Mithocondrial DNA
Subunits of ATP-sensitive potassium channels
Proinsulin or insulin conversion
B. Genetic defects to insulin action: type A insulin resistance, Leprechaunism, Rabson-Mendenhall syndrome, lipodystrophy syndromes
C. Diseases of the exocrine pancreas: pancreatitis, pancreatectomy, neoplasia, cystic fibrosis, hemchromatosis, fibrocalculous pancreatopathy, mutations in carboxyl ester lipase
D. Endocrinopathies: acromegaly, Cushing's syndrome, glucagonoma, pheocromocytoma, hyperthirodism, somatostatinoma, aldosteronoma

E. Drug or chemical induced: vacor, pentamidine, nicotininc acid, glucocorticoids, thyrid hormone, diazoxide, βadrenergic agonists, thazides, phenytoin, α-interferon, protease inhibitors, clozapine.

F. Infections: congenital rubella, cytomegalovirus, coxsackie

G. Uncommon forms of immune-mediated diabetes: 'stiff-person' syndrome, anti insulin receptor antibodies.

H. Other genetic syndromes sometimes associated with diabetes: Wolfram's syndrome, Friedreich's ataxia, Huntington's chorea, Laurence Moon-Biedl syndrome, myotonic dystrophy, porphyria, Prader-Willi syndrome.

4. Gestational diabetes mellitus (GDM)

Adapted from (Powers 2008).

The prevalence of DM worldwide was around 10% in 2013; that is 347 million people, of which 60 million are affected in Europe. By 2025, the number of people with diabetes is expected to increase and even to double in regions such as North Africa, Eastern Mediterranean and South-East Asia. Moreover, many countries are now reporting that the onset of type 2 diabetes in young people is also raising, due to increased sedentary lifestyles and obesity (WHO 2015). These figures imply a very high rate in morbidity and mortality: in 2013, around 5 million people died as a result of disease complications (WHO 2015). Diabetic complications are generally classified in macrovascular and microvascular. Macrovascular complications comprise coronary artery disease, peripheral artery disease and cerebrovascular disease, whilst microvascular complications include retinopathy, neuropathy (sensory and motor and autonomic) and nephropathy.

1.2.2 Diabetic kidney disease

Diabetic kidney disease (DKD) is a microvascular complication of long-standing diabetes characterized by persistent albuminuria (>300mg/24h), declined GFR and elevated blood pressure (Alpers CE 2007). The natural history of DKD has been mostly studied in type 1 diabetes (T1D), because the onset is usually evident and it occurs earlier in life, so the duration of diabetes is longer as for those with T2D. Back in 1983 a conceptual division of the natural history of DKD was described by Mogensen. This one starts with a nephron hypertrophy and hyperfiltration, followed by a thickening of the glomerular basal membrane and the expansion of mesangial matrix. In later stages, microalbuminuria can be detected,

first isolated and then together with the decline of glomerular filtration rate (GFR), the augment of blood pressure and the presence of other diabetic complications such as retinopathy (Mogensen CE 1983). Microalbuminuria is therefore one of the major predictive factor for the development of DKD in diabetic patients (Wolf 2007). However, other factors like sex, age, glucose control, duration of diabetes, obesity, hypertension and other comorbidities, above all in T2D, play also a significant role in the progressive deterioration of kidney function (Atsuhito T 2005, Dong Z 2016). Therefore a more complex natural history than the one presented by Mogensen should be considered.

1.2.3 Pathophysiology of diabetic kidney disease

The increased glomerular filtration rate (GFR) at early stages of DKD has been recognized as a pivotal event in the progression of DKD since many years, but the pathomechanism behind was unclear. It had been related to impaired autoregulation and the activation of the local intrarrenal renin-angiotensin aldosterone system (RAAS), being its cause hyperglycaemia (Kanwar YS 2011). The link between these events was recently unveiled thanks to a new oral antidiabetic drug with renoprotective properties, Empagliflozin (see section 1.2.5 *Current therapies*), and is associated with correcting hyperreabsortion of sodium chloride in the proximal tubule and reinstalling a positive tubuloglomerular feedback (TGF) (Vallon V 2012). TGF is a mechanism of GFR regulation involving the macula densa, located at the end of the thick ascending limb, and the juxtaglomerular cells, located in the afferent arteriole. This regulation consists in keeping a constant filtration pressure despite variation in systemic blood pressure. If blood pressure increases, so does the filtration causing a higher sodium concentration in the tubular fluid. The macula densa senses this and releases adenosine, which provokes the vasoconstriction of the afferent arteriole and the inhibition of renin release from juxtaglomerular cells. The afferent vasoconstriction together with the efferent vasodilation, due to decreased Angiotensin II (ANGII), reduces the glomerular pressure and thus the single nephron GFR (SNGFR). In the opposite scenario, the decreased concentration of sodium in the macula densa activates renin release, leading to vasoconstriction of the efferent arteriole and therefore to a higher glomerular pressure and SNGFR (Vallon V 2010).

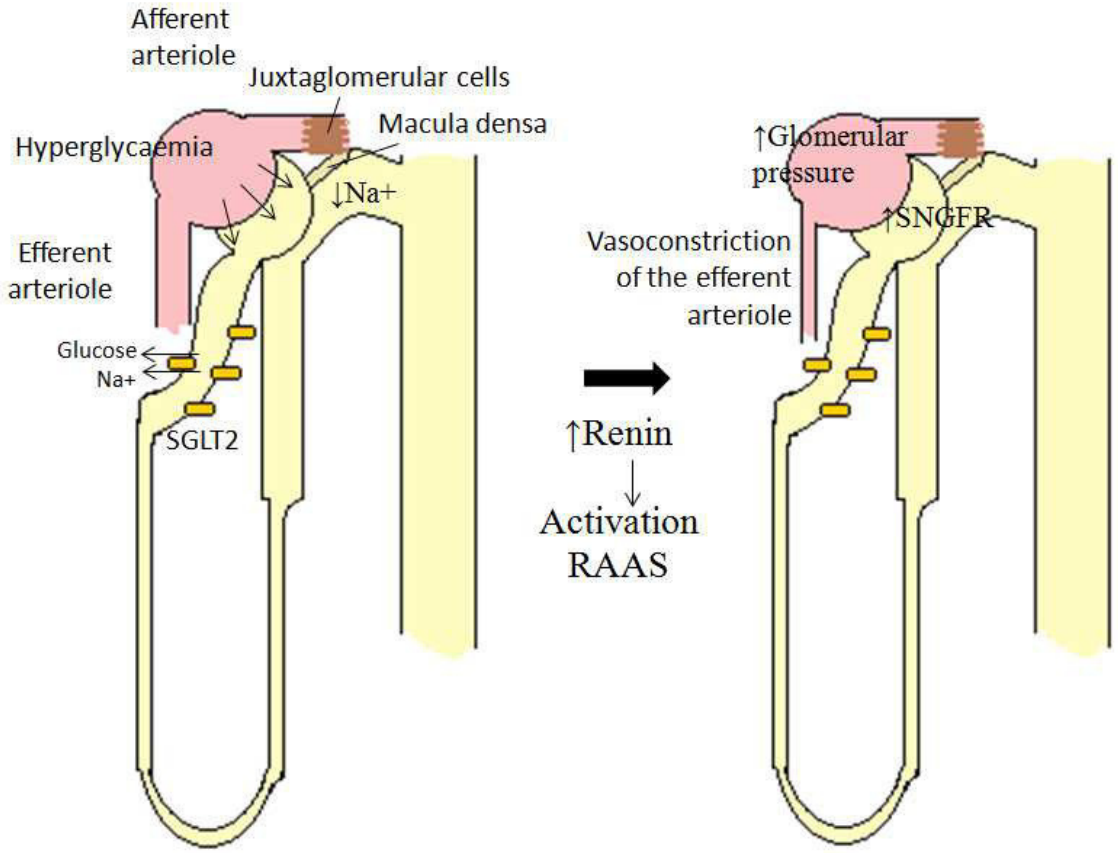

Figure 2. Hyperglycaemia and deactivation of the tubuloglomerular feedback (TGF). The increased reabsorption of glucose in the proximal tubule under hyperglycaemic conditions implies an increased reabsorption of sodium and therefore a reduced concentration of sodium in the distal tubule and the macula densa. This causes a release of renin from juxtaglomerular cells and a consequent activation of RAAS, which provokes efferent vasoconstriction and a higher glomerular pressure as well as higher SNGFR. *SGLT2 = sodium glucose cotransporter-2*, *RAAS = Renin Angiotensin Aldosterone System, SNGFR= Single-Nephron glomerular filtration rate.*

The decreased sodium concentration in the macula densa can also be caused by an augmented reabsortion of sodium in the proximal tubule, like in diabetes. Sodium is cotransported with glucose in the proximal tubule trough SGLT2 and in the distal tubule trough SGLT1. Most of glucose reabsortion, around 97%, takes place in the proximal tubule (Vallon V 2015). In hyperglycaemic conditions the reabsortion of glucose increases up to two- to three-fold (Vallon V 2015) and implies for that reason a higher reabsortion of sodium, decreasing its concentration in the macula densa and deactivating the TGF (figure 2). The higher reabsortion of glucose is not only linked to higher filtered glucose concentration but also to an upregulation of *Sglt1* and *Sglt2* genes and an overexpression of these cotransporters, as shown in Zucker rats and in in-vitro cultures of human exfoliated

proximal epithelial cells collected from T2D patients urine (Vestri S 2001, Vidotti DB 2008, Tabatabai NM 2009, Rahmoune H 2005).

Hyperreabsortion of NaCl is additionally a consequence of the tubular growth observed in diabetic kidneys. The tubular growth involves in an early phase hyperplasia and later on hypertrophy (Vallon V 2012). Growth factors such as insulin-growth-factor 1 (IGF-1), vascular endothelial growth factor (VEGF) and epidermal growth factor (EGF) contribute greatly to the early tubular hyperplasia (Chiarelli F 2009). The overexpression of genes related to proliferation, like ornithine decarboxylase (ODC) (Satriano J 2006) or mammalian target of rapamycin complex 1 (mTORC1) (Lee MJ 2007), plays also a role. The upregulation of OCD follows the activation of protein kinase C (PKC), due to high glucose concentrations, and the activation of the JAK/STAT pathway through the generation of reactive oxygen species (ROS) in a diabetic milieu (Satriano J 2006).

In a later stage, the kidney growth occurs through hypertrophy. This shift is mediated by TGF-β (Han DC 2000), induced also by the activated JAK/STAT pathway and PKC. At the same time the upregulation of the CKD inhibitors p21 and p27, promoted by TGF-β, ROS, PKC and JAK/STAT pathway, provokes a switch from proliferation to hypertrophy and eventually cell senescence (Huang JS 2007, Satriano J 2010, Vallon V 2012).

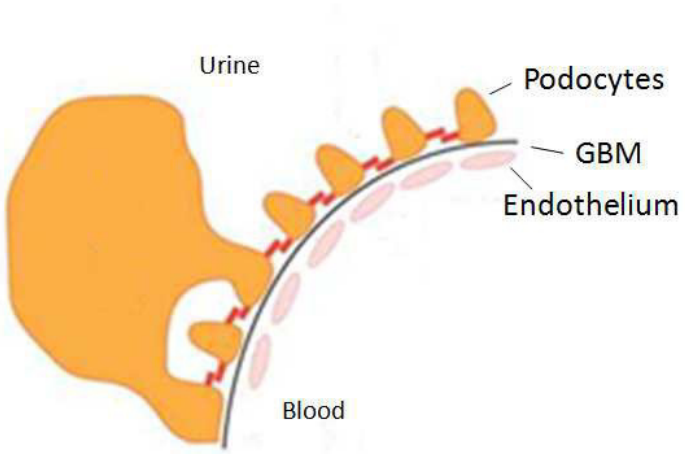

Figure 3. Schematic drawing of the glomerular filtration barrier, composed of podocytes and its pseudopods, the glomerular basement membrane (GBM) and the endothelium. Adapted from (Haraldsson B. 2008).

Another important event in the natural history of DKD is the impairment of the glomerular filtration barrier (GFB) function and the leakage of plasma proteins, resulting in intermittent microalbuminuria at the beginning and permanent macroalbuminuria in later stages. Three layers compose the glomerular filtration barrier: fenestrated glomerular endothelium, a glomerular basement membrane (GBM) and a highly specialised epithelium: the podocytes (figure 3) (Haraldsson B. 2008). Despite many factors may contribute to the development of proteinuria, such as hemodynamic changes and mesangial expansion, many studies point at podocyte injury as the main causative event (Wolf G 2008). The loss of podocytes has been demonstrated to correlate with later development of proteinuria in normoalbuminuric diabetic patients (Dalla Vestra M 2003) and with the magnitude of proteinuria in those with DKD (White KE 2004). Accordingly, many studies presented that loss of nephrin, an important structural protein from the podocyte slit diaphragm, occurs in DKD patients (Pätäri A 2003, Benigni A 2004). The detailed molecular mechanisms leading to podocytopenia and loss of nephrin are not completely understood, but many studies using rodent models point towards ANGII as an important mediator, along with the vascular endothelial growth factor (VEGF) (Sung SH 2006, Ziyadeh FN 2008). Additionally, proteinuria itself could amplify podocyte injury further by a positive feedback cycle, since albumin, like hyperglycemia, induces the overexpression of TGFβ1 in podocytes (Ziyadeh 2004, Shankland 2006, Wolf G 2007).

The albumin that is filtrated in the glomerulus can in the proximal tubule be reabsorbed by endocytosis (Birn H 2006), stimulated by ANGII (Caruso-Neves C 2005), which is synthesized not only in juxtaglomerular cells but also in tubular cells in high ambient glucose (Wei CC 2006). An increase in tubular albumin reabsorption will then activate the tubular RAAS leading to a vicious cycle (Wolf G 2004). Furthermore, tubular reuptake of albumin induces pro-inflammatory and profibrogenic cytokines (Ruiz-Ortega M 2006) and the recruitment of inflammatory cells in the glomerular and interstitial compartments (Navarro-González JF 2011). Together these processes contribute to inflammation, perpetuation of renal abnormalities, glomerulosclerosis and nephron loss.

Inflammation is also a major driving force in the development of DKD. The activation of polyol and PKC pathway due to hyperglycaemia as well as the formation of advanced glycation end-products (AGE) and reactive oxygen species (ROS) trigger a cascade of

signalling events that promote and enhance inflammation (Yashpal S 2011). An example of it is the activation of the transcription factor NF-κB, which activates the release of proinflammatory cytokines such as TGF-β1, CCL2 (chemokine ligand 2) or ICAM1 (intercellular adhesion molecule 1) (Ziyadeh FN 2008, Yang B 2008, Wada J 2013). Other cytokines critically involved in the diabetic nephropathy are IL-1, IL-6-and IL-18 (Navarro-González JF 2011).

In summary, hyperglycaemia activates a variety of pathways that promote hemodynamic changes, structural modifications, and inflammation (Wada J 2013), which further trigger the same or other pathways reinforcing this cycle and aggravating the disease. Still many other factors not yet well known play a role in the development of DKD, such as microRNAs (Hagiwara S 2013) or genetic predisposition. In fact, observational studies have shown that DKD occurs in familiar clustering and that there are important ethnical factors involved (García-García PM 2014).

1.2.4 Mouse models of diabetes

Many mouse models have been used to resemble the human pathology of diabetic nephropathy as a consequence of hyperglycaemia, but these models do not mimic the actual pathophysiology of the disease (Anders HJ 2016). For that reason, human translation is often difficult since a complex disease like diabetes, determined by multiple factors, involving both genetics and environment, is extremely difficult to imitate. The animal models so far developed can be broadly classified into spontaneous/congenital, diet-induced, chemical-induced, surgical and transgenic diabetic models (Wang B. 2014). The first ones are the most widely used and include the leptin and leptin receptor deficient models, which disrupt the leptin signaling pathway leading mainly to obesity and other metabolic disturbances. Leptin is produced mostly in the adipocytes and in a small proportion in the brown adipose tissue, skeletal muscle, placenta, ovaries, bone marrow and stomach. In the hypothalamus, leptin modulates food intake and energy expenditure. In peripheral tissues leptin also plays different roles involving energy homeostasis, skeletal growth, neuroprotection and oncogenesis (Moran O. 2003). While leptin deficient mice (ob/ob) carry a nonsense mutation on the obese gene (i.e. leptin encoding gene) that truncates the biologically active protein, leptin receptor deficient mice (db/db), on the other hand, have an

abnormal mRNA splicing of the Ob-Rb protein (i.e. leptin receptor isoform expressed mainly in the central nervous system) (Rees D.A. 2005). As a result of this spontaneous mutation, ob/ob mice develop early and severe obesity and hyperglycaemia, though mild and transient, until they are 3 months of age, when the glycemia goes back to normality, probably due to hyperinsulinemia. This compensatory hyperinsulinemia is a result of βcell hypertrophy and contributes to the obese phenotype. They display as well insulin resistance but do not develop (or they do poorly) macrovascular or microvascular complications. Contrasting with this phenotype, db/db mice do develop severe hyperglycaemia together with obesity, hyperinsulinemia, insulin resistance and eventually βcell dysfunction with no amyloid deposition. This scheme resembles a bit more the features of T2DM, albeit not mimic completely. Dyslipidemia is also present in this model but with high levels of HDL and low LDL, as opposed to humans. Macrovascular complications are generally not developed and in fact, arterial blood pressure and heart rates are reduced. Microvascular complications do faintly develop after some months, but incompletely (Wang B. 2014) (table 3).

Table 3 **Manifestations of the db/db mouse model and its similarities and differences with human T2DM features**.

Human T2DM-like features	Differences with human features
Obesity	Early-onset. Severe
Hyperglycaemia	Severe
Insulin resistance	
Hyperinsulinemia and eventual βcell destruction	No amyloid deposition
Hyperlipidemia with ↑LDL and ↓HDL	↑HDL
Development of microvascular complications	Incomplete phenotype
Normal or high blood pressure	Reduced systemic arterial blood pressure
	Depressed heart rate and basal systolic contraction

Adapted from (Wang B. 2014).

1.2.5 Current therapies

The basics of the DKD therapy is based on three pillars: a strict glycaemic control to stop changes triggered by a diabetic milieu, control of blood pressure to halt hemodynamic remodelling, and reduction of lipidemia to shrink inflammation (Gentile G 2014). First, a strict glycaemic control has been proved beneficial in many trials for both development and progression of DKD in T1D (DCCT 1993, EDIC 2003, DCCT/EDIC 2011) and T2D (UKPDS 1998, ADVANCE 2008, Ismail-Beigi F 2010), although clinical benefits are weaker when complications are already present (Fullerton B 2014). In fact, a tight control entails a cardiovascular risk for subjects with long-standing diabetes (ACCORD 2008, Dluhy RG 2008, Lachin 2010, Riddle 2010).

Empagliflozin, an inhibitor of sodium-glucose transporter (SGLT)-2, is a new oral antidiabetic (OAD) that offers promising perspectives in the treatment of DKD, not only due to the glycaemic control, but also in the correction of the deactivation of tubuloglomerular feedback (TGF) that occurs in diabetes (*see section 1.2.3 Pathophysiology of diabetic nephropathy*). By inhibiting SGLT-2, Empagliflozin decreases the reabsortion of glucose in the proximal tubule and promotes glucosuria and reduction of hyperglycaemia in an insulin-independent manner (unlike other OAD) (Wanner C 2016). At the same time, thanks to the inhibition of glucose reabsortion in the proximal tubule, the cotransport of sodium is also inhibited, being then the tubular fluid sodium concentration in the macula densa higher. This reactivates the TGF and reduces the glomerular pression and SNGFR, thus contributing to reduce hyperfiltration and its deleterious effects in diabetic kidney disease (Vallon V 2015). Additionally, the inhibition of SGLT2 inhibits renal gluconeogenesis and by means of inducing glucosuria promotes weight loss and lower blood pressure, offering a lower rate of death from cardiovascular and death from any cause (Zinman B 2015).

Second, lowering high blood pressure reduces CKD progression independently of proteinuria (Klag MJ 1996, Tozawa M 2003); therefore any drug that reduces blood pressure to less than 140/90 mmHg in non-proteinuric diabetic patient and less than 130/80 in diabetic patients with DKD is recommended (NKF 2012). The recent SPRINT trial published in 2015 may even lower the target to less than 120, since it could be shown that in those patients with systolic blood pressure (SBP) <120mmH the primary outcome in terms of myocardial infarction, acute coronary syndrome, stroke, heart failure or death from

cardiovascular disease was less reported than in those with SBP < 140mmHg (SPRINT 2015). However, the study did not include diabetic patients or patients at high risk of cardiovascular disease, reason why the study has raised some controversy (Grassi G 2016). Nonetheless among all the antihypertensive drugs the ACE inhibitors have shown to have major benefit in DKD over the others. The reason: the inhibition of RAAS does not only control blood pressure but decreases also intraglomerular pressure and hyperfiltration, translating into reduced proteinuria (Ruggenenti P 2010). Moreover, the role of ANGII as mediator of pro-inflammatory pathways could also be inhibited (Ruiz-Ortega M 2006), thus contributing further to overall renoprotection.

Third, lipid abnormalities, often found in diabetic patients (Jenkins AJ 2003), contribute to increase cardiovascular risk, albuminuria and CKD progression (Tolonen N 2009). Hence, treatment of hyperlipaedemia with statins has an important role in preventing cardiovascular outcomes. This could be shown in the SHARP trial, a randomised study comparing treatment with simvastatin plus ezetimibe and placebo, where the reduction of LDL cholesterol in patients with advanced chronic kidney disease reduced major atherosclerotic events (Baigent C 2011); however the intervention did not slow kidney disease progression in patients with chronic kidney disease (Haynes R 2014). Tonolo et al. nonetheless showed a slowed GFR decline in patients treated with simvastatine compared with cholestyramine, despite similar hypocholesterolemic effects (Tonolo G 2006), probably via attenuation of inflammatory effects and of oxidative stress.

Meanwhile, novel drugs for DKD developed after the study of its pathophysiology have been tested: inhibitors of PKC, AGE/RAGE, NF-κB and JAK/STAT, antagonists of CCR2/CCR5 or endothelin receptor or neutralizers of ICAM-1 (Gentile G 2014). An example of it is emapticap pegol, a RNA aptamer that aims to treat DKD by directly inhibiting CCL2 and reducing the activation and number of M2 macrophages, thus reducing tissue inflammation. In a phase IIa trial it improved the glycaemic control and significantly reduced the abumin/creatinin ratio, being safe and well tolerated. Moreover, those changes were maintained after cessation of the treatment, suggesting that emapticap pegol interferes with the underlying pathophisiology of DKD (Menne J 2016). Another promising drug targeting inflammation is CCX140-B, a CCR2 inhibitor that showed renoprotective effects in a phase III trial (de Zeeuw D 2015). Baricitinib is an inhibitor of JAK1/JAK2 that has been proved to

be effective in the treatment of rheumatoid arthritis and it is now being tested in a phase II randomized trial for DKD (Brosius FC 2015, O'Shea JJ 2013). CTP-499, a phosphodiesterase inhibitor, has been likewise recently tested in a phase IIA trial (Sabounjian L 2016, Perez-Gomez 2016). Another example is the compound Bardoxolone methyl, an activator of the Nrf2 pathway and inhibitor of the NF-κB pathway that reduces oxidative stress and inflammation. In the phase II clinical trial BEAM 227 patients with advanced CKD (eGFR between 20 and 45 ml/min/1,73cm^2) were included and followed for 24 weeks after Bardoxolone methyl or placebo administration. The first one showed an average increase of eGFR of 10ml/min/1,73cm^2, whereas no changes were observed in the placebo group. In October 2011 the BEACON study (phase III trial) was started with 1600 patients with CKD Stadium 4 and DKD. The study however had to be stopped after one year due to the higher cardiovascular events and overall mortality compared with the placebo line, probably due to fluid retention (de Zeeuw D 2013). For this work, Nutlin-3a, also an inhibitor of NF-κB pathway, has been proposed as a drug for DKD due to its anti-inflammatory effect and to its protective role in stressed podocytes.

1.3 Mdm2 blockade with Nutlin-3a and its potential as cancer therapy

Nutlin-3a is a cis-imadazolin that competitively inhibits Mdm2 and prevents its interaction with the tumour suppressor p53, thus stabilizing its levels and blocking tumour growth in several animal models (Shangary S 2009). Therefore, Nutlin-3a has emerged as a promising therapy for cancer and a clinical trial in humans with advanced malignancies except for leukaemia has already been completed and a new one with leukaemia is currently ongoing[1].

1.3.1 Mdm2 and p53

The gene *Mdm2* was first identified in 1987 at the Howard Hughes Medical Institute in Pennsylvenia among two other genes, *Mdm1* and *Mdm3*, in a spontaneously transformed mouse BALB/c cell line (3T3DM). The name *Mdm* stands for *Murine double minute*, as these three genes were located in small, acentromeric, extrachromosomal nuclear bodies called 'double minutes' , which have been stably maintained during long term growth of the 3T3DM cells because it provides them with growth advantage (Cahilly-Snyder L 1987). In a

[1] www.clinicaltrials.gov RO5503781.

posterior work, the tumorigenic nature of *Mdm2* and its product was proved by injecting non-transformed NIH3T3[2] cells transfected with *Mdm2* in nude mice[3], which caused the development of tumours at the site of injection (Fakharzadeh SS 1991).

Simultaneously the group of Arnold Levine in Princeton worked on the same topic with the tumour suppressor p53. They observed in different cell lines and with different antibodies that p53 always coprecipitates with a protein with a molecular weight of 90kDa – they named it p90. Subsequently, they identified p90 as the product of *Mdm2* (Momand J 1992) and its role as negative regulator of the tumour suppressor p53.

The regulation of Mdm2 upon p53 was further disclosed with *Mdm2* and *Mdm2/p53* knock-out mice germlines. The homozygous deletion of *Mdm2* resulted in lethality at an early stage in embryonic development due to enhanced cell death. This phenotype was completely rescued using double *Mdm2/p53* knock-out mice (Jones SN 1995, Montes de Oca Luna R 1995). Hence it was proved that Mdm2 negatively regulates p53 and prevents p53-dependent cell death.

1.3.2 The p53-MDM2 regulatory loop

Mdm2 is the main regulator of p53. Although p53 can be degraded in a Mdm2-independent manner, via MDMX and probably through other E3 ubiquitin ligases, like Cop1, Pirh2, ARF-BP1, Topors, CAPPs or Synoviolin, the low efficiency of this process shows the importance of Mdm2 for such purpose (Clegg HV 2008, Marine JC 2010).

[2] NIH 3T3 mouse embryonic fibroblast cells come from a cell line isolated and initiated in 1962 at the New York University School of Medicine Department of Pathology. 3T3 refers to the cell transfer and inoculation protocol for the line, and means "3-day transfer, inoculum 3 x 10^5 cells." Using this protocol, the immortal cell line begins to thrive and stabilize in cell culture after about 20-30 generations of in vitro growth. George Todaro and Howard Green, the scientists who first cultured this cell line, obtained the cells from desegregated NIH Swiss mouse embryo fibroblasts. The cell line has since become a standard fibroblast cell line.

[3] Athymic mice.

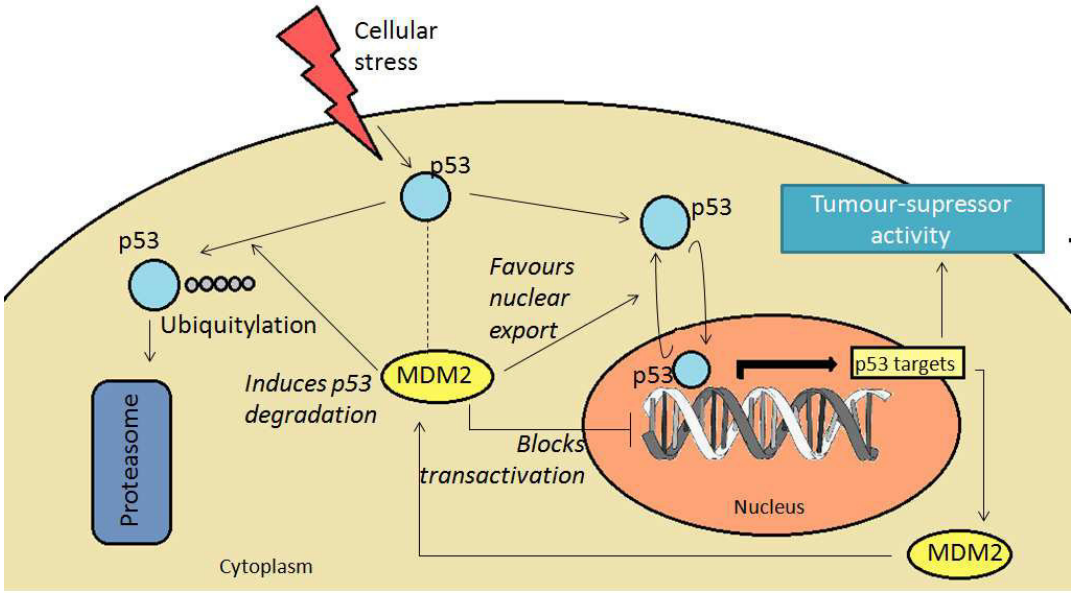

Figure 4. Autorregulatory feedback loop. In conditions of no stress, Mdm2 inhibits p53 in three ways: 1) blocks transactivation of p53, 2) favours nuclear export, and 3) induces p53 degradation. However, upon DNA damage, p53 levels increase and transactivation of p53 targets takes place. Among p53 target genes, there is Mdm2. If the DNA damage is repaired, the increasing levels of Mdm2 will again inhibit p53 and restore its levels. Adapted from (Chène 2003).

Mdm2 negative p53 regulation is achieved through three mechanisms (figure 4). First, Mdm2 hinders p53 to promote transcription by competing with its transcriptional machinery (Momand J 1992, Chen J 1993, Oliner JD 1993, Haupt Y 1997). Second, Mdm2 exports p53 from the nucleus to the cytoplasm, hence hampering further p53-dependent transcription (Roth J 1998). Third, by means of E3 ligase activity Mdm2 mediates ubiquitination of p53 promoting its proteasomal degradation (Haupt Y 1997, Honda R 1997, Kubbutat MH 1997). At the same time, p53 induces among other genes the transcription of *Mdm2,* establishing a negative feedback loop that further regulates levels of both proteins (Barak Y 1993, Perry ME 1993).

Interestingly, Mdm2 can also promote p53 translation by interacting with *p53* mRNA, while Mdm2 E3 ligase activity would be inhibited. Once the p53-Mdm2 protein complex is released from the polysome, Mdm2 ubiquitin ligase activity is released (Yin Y 2002, Candeias MM 2008, Naski N 2009). That proves further how the equilibrium of these two proteins is tightly regulated through several mechanisms that have evolved over time.

1.3.3 Mdm2 protein domains

Mdm2 has several domains that are conserved among species (figure 5). The first of these domains in the aminoterminal region is the binding site of p53, which binds to the aminoterminal region of p53 (Chène 2003, Iwakuma T 2003, Zhao Y 2014). In this domain, Mdm2 forms a deep hydrophobic cleft, where p53 fits with mainly three side chains: Phe19, Trp23 and Leu26 (Chène 2003, Vassilev LT 2004). Mdm2 also possesses a conserved nuclear localization sequence (NLS) and a conserved nuclear export signal (NES) that mediate its ability to shuttle between the nucleus and the cytoplasm (Roth J 1998, D. A. Freedman 1999). This ability to commute between nucleus and cytoplasm was thought to be the means with which Mdm2 carries p53 out of the nucleus. However, Stommel et al asserted that the nuclear export of p53 was independent of Mdm2's NES (Stommel JM 1999). Yet Mdm2 may still contribute to the nuclear export with another conserved domain: the RING finger domain with E3 ubiquitin ligase activity (Geyer RK 2000).

In addition, the RING finger domain promotes p53 proteasomal degradation (Haupt Y 1997, Honda R 1997, Kubbutat MH 1997). This domain in the carboxi-terminus of Mdm2 can catalyse p53 monoubiquitinitation, and thereby promote nuclear export, or p53 polyubiquitination, and with it trigger proteasomal degradation. Whether the action is one or the other depends on p53 levels: in nonstressed cells, where p53 levels are low, E3 ligase induces monoubiquitination to keep the transcription factor out of the site of action and thus controls its response. But in stressed cells, where p53 levels are increased, the RING finger domain drives polyubiquitination to better control overexpression of the tumour suppressor (Li M 2003). Moreover, via the RING finger domain, Mdm2 can also ubiquitin itself and induce its own degradation, further commanding the regulatory mechanism that titrates precisely the levels of Mdm2 and p53 (Fang S 2000, Honda R 2000). Other authors however discuss that Mdm2 does not drive its own degradation, but other E3 ubiquitin ligases such us PCAF do (p300-CBP-associated factor) (Linares LK 2007, Clegg HV 2008).

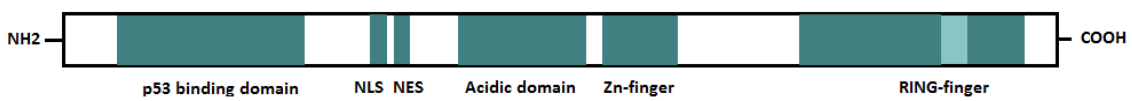

Figure 5. Mdm2 protein domains. The conserved domains of Mdm2 are the p53 interaction domain in the aminoterminus, the nuclear localization signal (NLS) and the nuclear export signal (NES), the acidic domain and Zinc finger, which interact with ribosomal proteins, and in the carboxiterminus the RING finger domain with E3 ubiquitin ligase activity. Adapted from (Iwakuma T 2003).

In brief, the ability of Mdm2 to promote p53 degradation depends on the integrity of the amino-terminal p53-binding domain, the central acidic domain, also largely preserved among species, and the RING-finger domain (Marine JC 2010). Therefore, any mutation, post-translational modification or functional inhibition of any of them can lead to a disruption of p53-Mdm2 homeostasis and precipitate on one side an uncontrolled proliferation or on the other side cell death.

1.3.4 Mdm2 and p53 homeostasis and cell cycle

The homeostatic equilibrium between p53 and Mdm2 ensures a proper progression of the cell cycle. In response to DNA damage or other stress signals, such as hypoxia, lack of nutrients, ribosomal stress or oncogene activation, p53 is stabilized and hinders cell cycle progression (Chène 2003, Kruiswijk F 2015). Here, the function of p53 is the surveillance of the genome; if the DNA is somehow modified, p53 prevents these changes to be transmitted via mitosis. First, by inducing the cyclin kinase inhibitor p21, p53 induces cell cycle arrest at the G1/S and G2/M restriction points and allows the cell to repair DNA damage (Bunz F 1998, Taylor WR 2001, Foijer F 2006). When the damage can however not be repaired, p53 drives the cell out of the cell cycle inducing senescence or cell death (figure 6) (Zhang XP 2009, Mirzayans R 2012). Consequently, a disrupted balance between Mdm2 and p53, that favours p53 inactivation, can cause uncontrolled cell proliferation. This occurs with:

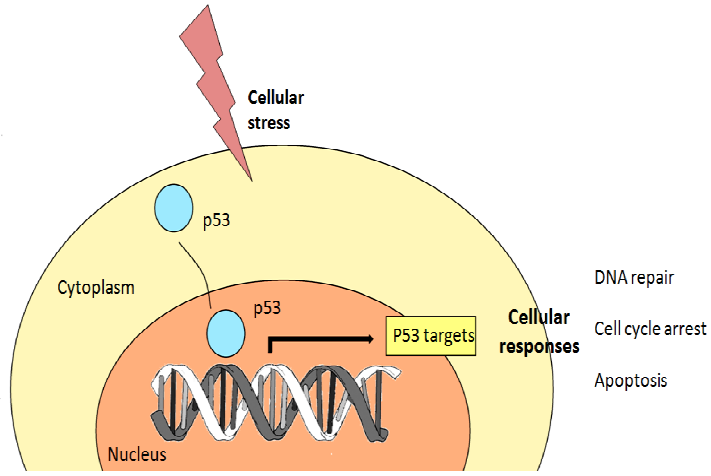

Figure 6. p53 stabilization and response. In non-stressed cells, p53 exists in very low concentrations. Under cellular stress, the levels of p53 raise and p53 mediates the transcription of genes involved in apoptosis, cell cycle arrest, and DNA repair. Adapted from (Chène 2003).

1. p53 mutation or loss of function. This is seen in almost 50% of all tumours (Hainaut P 2000), highlighting the importance of p53 as guardian of the genome.
2. Gain of function of Mdm2 via amplification of the gene, increase transcription or overexpression. This process is found in numerous types of tumors, such us sarcomas, glioblastomas, leukaemias, lymphomas and breast carcinoma and malignant melanomas, as well as in cancer-prone family syndromes (Reifenberger G 1993, Watanabe T 1994, Bueso-Ramos CE 1995, Poremba C 1995, Bueso-Ramos CE 1996, Picksley SM 1996).
3. Mdm2 gain of function coupled with p53 loss-of-function (Watanabe T 1994). This apparent redundancy suggests that Mdm2 has other oncogenic properties, independent of p53. (Jones SN 1998, Iwakuma T 2003).

For this reason, to restore p53 wild type levels is a promising strategy in the treatment of several tumours (Li Q 2014).

1.3.5 Mdm2 inhibitors and Nutlin-3a

Two classes of Mdm2 inhibitors have been developed: peptide inhibitors and low molecular weight compounds. While the first inhibitors mimic p53 structure, the second compounds were developed with computational tools (Chène 2003, Shangary S. 2009). Among this last group cis-imadazolines, benzodiazepins and spiro-oxindoles have been studied. The cis-imadazolines, named Nutlin, are the first reported inhibitors with a good interaction with p53 (Patel S 2008). Among them, Nutlin-3, a racemic mixture of Nutlin-3a (active enantiomer) and Nutlin-3b (inactive enantiomer), has shown excellent pharmacokinetic properties: rapid absorption, high bioavailabitlity and saturable elimination kinetics (Vassilev LT 2004, Zhang F 2011).

The interaction between Mdm2 and p53 can also be inhibited with HLI98, a compound that binds Mdm2 non-competitive and inhibits the E3 ligase activity, and RITA (**r**eactivation of p53 and **i**nduction of **t**umour cell **a**poptosis), which binds p53 instead of Mdm2, thus inhibiting the interaction between these two partners as well (Marine JC 2010) (figure 7).

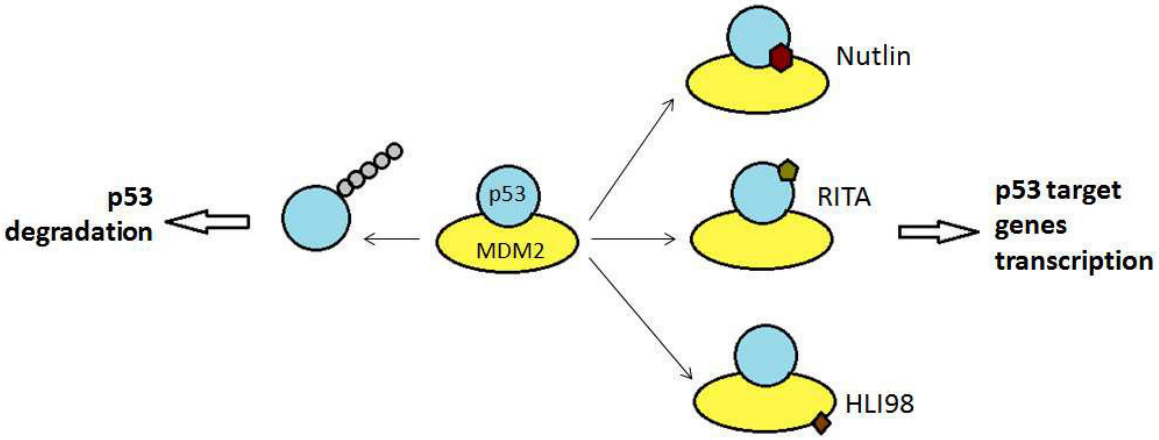

Figure 8. Inhibitors of the Mdm2-p53 interaction. Schematic representation of the Mdm2 and p53 proteins. Nutlin binds Mdm2 in the p53 binding domain in the aminoterminus, HLI98 binds Mdm2 in the RING domain, and RITA binds p53 in the transactivation domain. Adapted from (Marine JC 2010).

Despite sharing the same goal, all these inhibitors differ on the target, which might bestow each of them with particular features. For example, small molecules binding Mdm2 might inhibit not only p53-dependent but also p53-independent activities (Marine JC 2010), as it has already been shown with Nutlin-3a (see section below *1.4.2 P53-independent roles of Mdm2*). And the other way around: inhibiting the interaction of p53 and Mdm2 by binding p53, stabilizes Mdm2 and promotes p53-independent activities, like the ubiquitination of hnRNPk. This promotes proteasomal degradation and prevents this protein to induce p21 transactivation. The result of this is an induction of proapoptotic genes and cell death instead of cell cycle arrest (Eischen CM 2009). These differences might be therefore of advantage when treating different pathologies and aiming different goals.

1.4 Nutlin-3a in previous studies of kidney disease

1.4.1 Nutlin-3a in acute kidney injury (AKI)

The role of Nutlin-3a in blocking Mdm2 and interfering with proliferation raised rapidly concern over a negative effect of this drug upon tissue regeneration. Mulay *et al.* approached this question with a murine model of acute kidney injury (AKI). They observed that in the kidney, Mdm2 is mainly expressed in tubular cells and that Mdm2 levels in these cells raise after 5 days of ischemia-reperfusion injury (Mulay SR 2012), coinciding with the regeneration phase. In an earlier phase of damage, however, p53 levels are elevated in

parenchymal cells (Kelly KJ 2003, Molitoris BA 2009). Surely, these observations were to be expected. After injury, damaged cells initiate a program through p53 of either repair or death depending on the severity. In a later phase, Mdm2 levels augment induced by high levels of p53 and inhibit further cell death whilst proliferation and regeneration are promoted.

For that reason, Mulay et al revealed that inhibiting Mdm2 after renal ischemia-reperfusion injury leads to a worse outcome 5 days post-AKI, with increased TUNEL positive tubular cells compared to control (Mulay SR 2012). These results were consistent with other studies, such as the work of Gannon et al, where Mdm2 deletion in skin epithelium resulted in increased cellular senescence and impaired wound healing (Gannon HS 2011).

Nonetheless, in this study a positive effect of Nutllin-3a was observed during an early phase, one day after AKI. This unexpected result could be reproduced in p53 knock-out mice, revealing a p53-independent effect of Mdm2.

In this regard, Mulay et al performed another study about rapidly progressive glomerulonephritis (RPGN). Here the pre-emptive and delayed onset blockade of Mdm2 with Nutlin-3a ameliorated the outcome of mice with crescentic glomerulonephritis 7 days after sheep GBM antiserum injection in terms of serum creatinine levels, blood urea nitrogen (BUN), albuminuria and neutrophil and macrophage recruitment. This effect was shown to be mostly p53-independent, since the same results were observed in p53-knockout mice. The inhibition of parietal epithelial cells (PEC) hyperplasia was however p53-dependent. Together, it could be shown that Mdm2 drives inflammation in glomerulonephritis in a p53-independent way and PEC proliferation in a p53-dependent way; being its inhibition with Nutlin-3a a promising therapeutic strategy (Mulay SR 2016).

1.4.2 P53-independent roles of Mdm2

As introduced above, the work by Mulay and colleagues revealed a p53-independent role of Mdm2 on tissue inflammation that was later confirmed *in vitro*: Mdm2 facilitates the binding of nuclear factor κB (NFκB) to DNA (McNicholas BA 2012, Mulay SR 2012, Thomasova D. 2012). This finding was consistent with the report of Hashimoto et al. showing that Mdm2

inhibition with Nutlin-3a suppressed NFκB dependent inflammation in vascular smooth muscle cells (Hashimoto T 2011). Similarly, Nutlin-3a attenuated LPS-induced lung inflammation in mice via NFκB regulation, though in this case the effect was dependent on the presence of p53 (Liu G 2009).

In addition, Mdm2 might have other p53-independent roles related with carcinogenesis. Data showing that some tumours have not only an overexpression of Mdm2 but also mutations in p53 suggests that Mdm2 on its own may provide growth advantages independent of p53 (Watanabe T 1994). Jones et al. demonstrated that mice overexpressing Mdm2 and lacking p53 were more prone to tumour formation than those retaining wild type p53 (Jones SN 1998). An example of this independent contribution to cell proliferation is the Mdm2-dependent ubiquitilation of the transcription factor and tumour suppressor Forkhead box O 3a (FOXO3a), which contributes to Ras-ERK-mediated degradation and hence to the promotion of cell proliferation (Yang JY 2008). Furthermore, Mdm2 can interact with proteins that play a key role in the control of cell proliferation, including Rb, E2F1 and Smads (Marine JC 2010).

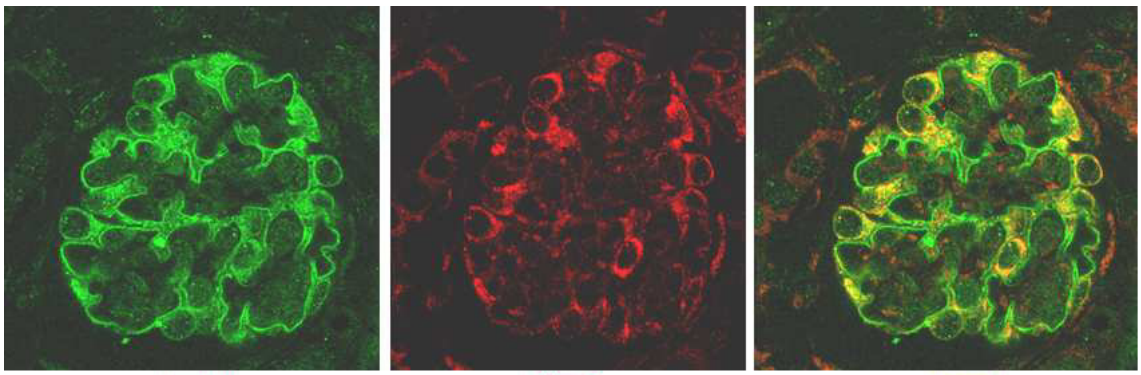

Figure 8. **Immunofluorescence staining for Nephrin and Mdm2 of a glomerulus**. In the first picture on the left, nephrin stains in green the cytoplasm of podocytes. In the second one, expression of Mdm2 inside the glomerulus is stained in red. In the last picture, on the right, merged colours show how the localisation of nephrin coincide with that of Mdm2. Picture ceded by Dr. Thomasova.

1.4.3 Nutlin-3a administration in mouse chronic kidney disease (CKD) models

The antiinflammatory effect of Nutlin-3a was also observed in a CKD model of lupus nephritis (Allam R 2011). In this study the administration of Nutlin-3a to MRL-Fas(lpr) mice (a mouse model of lupus) showed a beneficial effect on preventing nephritis and lung disease by reducing systemic inflammation and abnormal proliferation of T-cells (Allam R 2011).

The role of Mdm2 and its blockade with Nultin-3a has been also studied in a mouse adriamycin model that causes progressive glomerulosclerosis, a process that accounts for the vast majority of chronic kidney disease (CKD) cases. It was expected, that administration of Nutlin-3a would worsen CKD by enhancing podocyte cell death, since Mdm2 is strongly expressed in podocytes inside the glomerulus (figure 8). Interestingly, renal function and podocyte survival improved significantly after blockade of Mdm2 owing to less mitotic catastrophe (Mulay SR 2013). Mitotic catastrophe is a type of cell death characterized by an aberrant chromosome segregation that leads to death immediately after mitosis or shortly after via programmed cell death or necrosis (Castedo M 2004). In differentiated podocytes, such aberrant chromosome segregation occurs because mitosis requires a complete reorganization of the actin cytoskeleton, which is not compatible with maintaining secondary foot processes and the slit membrane (L Lasagni 2013). Mdm2 inhibits the p53 dependent cell cycle arrest and allows podocytes to override the cell cycle restriction point and complete aberrant mitosis leading to cell death (figure 9) (L Lasagni 2013, Mulay SR 2013).

In DKD, podocyte injury is also a major event in the progression of the disease, although the mechanisms of injury are not well known (see section *1.2.3 Pathophysiology of diabetic nephropathy*). Nutlin-3a could be a novel approach to hamper podocyte injury and to diminish inflammation, thus protecting the kidney from disease progression.

1.4.4 Toxicity of Nutlin-3a in kidney tissue

Although sufficient evidence exists suggesting that transformed cells are more sensitive to p53-induced apoptosis than their normal counterparts, the observed p53-dependent pathologies after Mdm2 loss raise concern of the toxicity of small molecule inhibitors of Mdm2-p53 upon healthy tissues (Marine JC 2010).

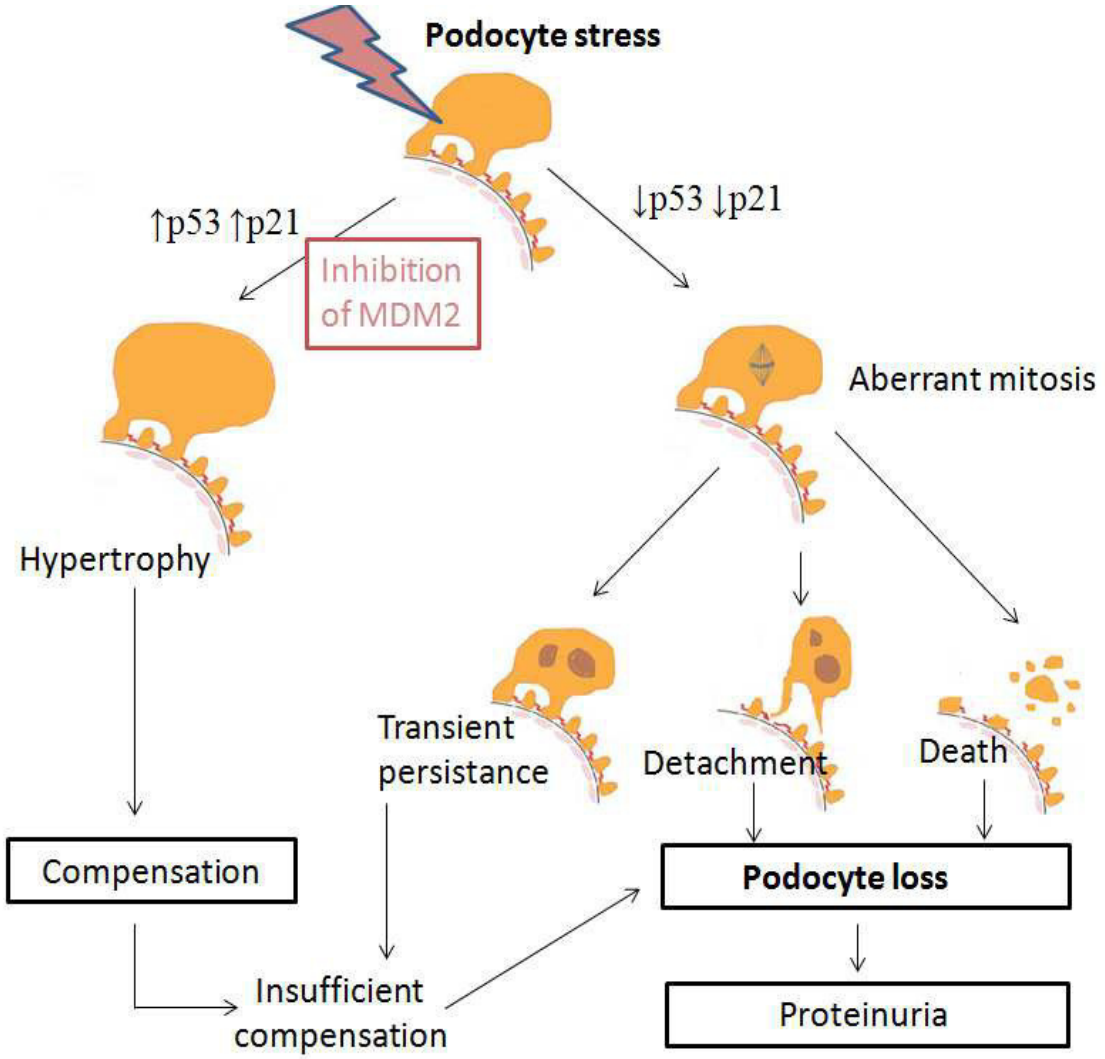

Figure 9. Schematic diaphragm of podocytopathies and mitotic catastrophe. Podocyte stress activates podocytes to undergo hypertrophy to compensate podocytopenia. Hypertrophy takes place because of p53-mediated induction of cyclin kinases such as p21, which arrest cell cycle in the G1 restriction point. Mdm2 inactivates p53 and its targets and drives the podocyte to complete (aberrant) mitosis, resulting in bi- or multinucleated podocytes. As a consequence, aneuploid podocytes undergo immediately cell death and detach from the GFB or remain for some time in the GFB and then die. Adapted from (L Lasagni 2013).

To illustrate this, in mice lacking Mdm2 and p53 the restoration of p53 for only ~24 hours initiated an ineluctable pathology leading to death within 5-6 days (Ringshausen I 2006). Profound body weight, diarrhoea and severe aplastic anaemia were observed, ascribed to death of radiosensitive organs such as bone marrow and intestine. Other tissues also displayed overexpression of p53 and exhibited cell proliferation inhibition, but in low-replicating tissues, the effects of p53-mediated growth arrest would take a long time to be manifested. However, specific deletion of Mdm2 can show individual outcomes in each

tissue. For instance, selective deletion of Mdm2 in cardiomyocytes resulted in heart failure at E13.5 (Grier JD 2006), or selective deletion of Mdm2 in osteoblasts engendered mice that died at birth with multiple skeletal defects (Lengner CJ 2006).

In renal tissue, the relevance of Mdm2 in podocyte homeostasis was highlighted by Thomasova *et al.* in resting podocytes both *in vitro* and *in vivo*. *In vitro*, deletion of Mdm2 with siRNA caused an overexpression of p53 and cell death (Thomasova D. 2015). So far, **p**53 **o**verexpression-**d**ependent cell death – a process named by Thomasova et al as "**pod**optosis"- was assumed to be apoptosis in the literature, since p53 induces numerous apoptosis-related genes (Aylon Y 2007, Valentin-Vega YA 2008). Yet, in this study they observed that podoptosis does not imply caspase activation, therefore podocytes die not via apoptotic cell death. Other types of cell death including pyroptosis, pyronecrosis, necroptosis, ferroptosis and parthanatos were also excluded as modes of cell death (Ebrahim M 2015, Thomasova D. 2015).

Accordingly, Mdm2 knockdown caused podocyte loss and proteinuria in a zebrafish model and in a podocyte-specific *Mdm2*-knockout mouse model, where the same abnormalities were observed along with progressive glomerulosclerosis. The phenotype of both animals was rescued with co-deletion of p53, further revealing the role of Mdm2 in maintaining homeostasis and long-term survival in podocytes (Thomasova D. 2015).

These studies remark the risk of inhibiting Mdm2 in healthy tissues. Nonetheless, the use of small molecules to inhibit Mdm2 cannot be compared to genetic ablation, as they have a limited half-time. Hence it might be possible to find a therapeutic window.

2. HYPOTHESES

Based on the above literature, the two following hypothesis were formulated:

- **Inhibition of Mdm2 with the small molecule Nutlin-3a damages renal function by promoting p53-overexpression dependent cell death (podoptosis) in podocytes and tubular cells.**

Previous work in our laboratory has shown that specific deletion of Mdm2 in both podocytes (Thomasova D. 2015) and tubular cells (data not yet published) triggers overexpression of p53 and cell death. In both cases, the structural and functional changes of these compartments led to CKD. Consistently, we hypothesized that the administration of Nutlin-3a, a small molecule that inhibits the interaction of p53 and Mdm2, damages both podocytes and tubular cells *in vitro* and *in vivo* in a similar manner.

- **Inhibition of Mdm2 with Nutlin-3a ameliorates diabetic kidney disease via attenuation of inflammation and prevention of podocyte mitotic catastrophe.**

In a CKD mouse model with adriamycin and FSGS (focal segmental glomerulosclerosis) was revealed that rather than promoting cell death, inhibition of Mdm2 with Nutlin-3a in a context of podocyte stress protected them from mitotic catastrophe and improved the outcome (Mulay SR 2013) In addition, Nutlin-3a displayed beneficial effects in an inflammatory milieu after acute kidney injury (AKI) by inhibiting the transcription factor NFκB in a p53-independent manner (Mulay SR 2012).

For that reason, we hypothesized that inhibition of Mdm2 with Nutlin-3a in diabetic kidney injury slows down the progression of the disease protecting podocytes from death via mitotic catastrophe and decreasing inflammation.

3. MATERIALS AND METHODS

3.1 Materials

3.1.1 Instruments

Anaesthesia

Isofluorane anaesthesia chamber	Harvard Anaesthesia system, UK

Balances

Analytic balance, BP110S	Sartorius, Göttingen, Germany
Mettler PJ 300	Mettler-Toeldo, Greifensee, Switzerland

Cell culture incubators

Type B5060 EC-CO_2	Heraeus Sepatech, München, Germany

Centrifuges

Heraeus, Minifuge T	VWR International, Darmstadt, Germany
Heraeus, Biofuge primo	Kendro Laboratory Products, Hanau, Germany
Heraeus, Sepatech Biofuge A	Heraeus Sepatech, München, Germany

ELISA Reader

Tecan, GENious Plus	Tecan, Crailsheim, Germany

Microscopes

Olympus DC 300F	Leica Microsystems, Cambridge, UK
Leica DC 300F	Leica Mycrosystems, Cambridge, UK

Real time PCR

Light cycler 480	Roche, Germany

Other equipment

Glucometer accu check sensor	Roche, Manheim, Germany
Homogenizer ULTRA-TURRAX T25	IKA GmbH, Staufen, Germany
Nanodrop	PEQLAB Biotechnology, Erlangen, Germany

pH meter WTW	WTW GmbH, Weilheim, Germany
Vortex Genie 2^{TM}	Bender&Hobein AG, Zurich, Switzerland
Water nath HI 1210	Leica Mycrosystems, Bensheim, Germany
Neddles	BD Drogheda, Ireland
Pipette's tips 1-100ul	Eppendorf, Hamburg, Germany
Plastic histocasettes	NeoLab, Heidelberg, Germany
Syringes	Becton Dickinson GmbH, Heidelberg, Germany
Tissue culture dishes 100x20mm	TPP, Trasadingen, Switzerland
Tissue culture 96 well-plates	TPP, Trasadingen, Switzerland
Tissue culture 6-well plates	TPP, Trasadingen, Switzerland
Tubes 1.5, 2, 15, 50ml	TPP, Trasadingen, Switzerland
Water bath HI 1210	Leica microsystems, Bensheim, Germany
Pure Link RNA mini kit Ambion	LifeTechnologies, Carlsbad, CA, USA
RT-PCR primers	Metabion, Martinsried, Germany

Cell culture

RPMI-1640 medium	GIBCO/Invitrogen, Paisley, Scotland, UK
DMEM-medium	Biochron KG, Berlin, Germany
Dulbecco's PBS (1x)	PAA Laboratories GmbH, Cölbe, Germany
FSC	Biochrom KG, Berlin, Germany
Penicillin/Streptomycin (100x)	PAA Laboratories GmbH, Cölbe, Germany
Trypsin/EDTA (1x)	PAA Laboratories GmbH, Cölbe, Germany

3.1.2 Reagents

Antibodies

Mac2	Cederlane, Ontario, Canada
TNFα	Abcam, Cambridge, UK
Col 1	Abcam, Cambridge, UK
p53	Santa Cruz Biotechnology, Santa Cruz, CA
Wt1	Santa Cruz Biotechnologies, Santa Cruz, CA
Nephrin	Acris Antibodies GmbH, Herford, Germany

ELISA and colorimetric assays

Albumin	Bethyl Laboratories, TX, USA
Creatinine FS	Diasys Diagnostic System, Holzheim, Germany
Urea FS	Diasys Diagnostic System, Holzheim, Germany
Cholesterol FS	Diasys Diagnostic System, Holzheim, Germany
Triglycerides FS	Diasys Diagnostic System, Holzheim, Germany
Cytotoxicity Detection Kit (LDH)	Roche, Basel, Switzerland
Cell Titer Proliferation Assay	Promega, Madison, WI, USA

3.1.3 Chemicals

Acrylamide 30%	Carl Roth GmbH, Karlsruhe, Germany
Beta-mercapto ethanol	Roth, Karlsruhe, Germany
Bovine Serum Albumin	Roche Diagnostics, Manheim, Germany
DMSO	Merck, Darmstadt, Germany
Eosin	Sigma, Deisenhofen, Germany
Ethanol	Merck, Darmstadt, Germany
Formalin	Merck, Darmstadt, Germany
Hcl (5N)	Merck, Darmstadt, Germany
Isopraponolol	Merck, Darmstadt, Germany
Sodium chloride	Merck, Darmstadt, Germany
Sodium citrate	Merck, Darmstadt, Germany

3.2 Methods

3.2.1 Animal studies

Male wild type C57BL/6J mice from Charles River (Sulzeld, Germany) and male diabetic C57BLKS db/db mice from Taconic (Ry, Denmark) were purchased and housed in filter top cages with a 12 hours dark/light cycle. All animals had unlimited access to food and water throughout the study duration, except for the four hours previous to glucose measurement (see below in *Glucose measurement*). All animal experiments were approved by the local government authorities.

Study design

Wild type mice (C57B/6J) were purchased at the age of 15 weeks, except 5 mice that were purchased at an age of 6 weeks-old, as baseline (control). All mice were treated with Nutlin-3a on alternative days from week 16th until week 19th for a total of 4 weeks and sacrificed at the end of the treatment (week 20). Nutlin-3a (Selleckchen, USA) was administered in alternative days intraperitoneally (i.p.) at a dose of 20mg/kg diluted in 50% Dimethyl-sulfoxide (DMSO). For the vehicle group, DMSO was injected i.p. with an equal concentration and amount (figure 10). A control group was kept separately with no intervention to rule out any independent renal or systemic effect of DMSO.

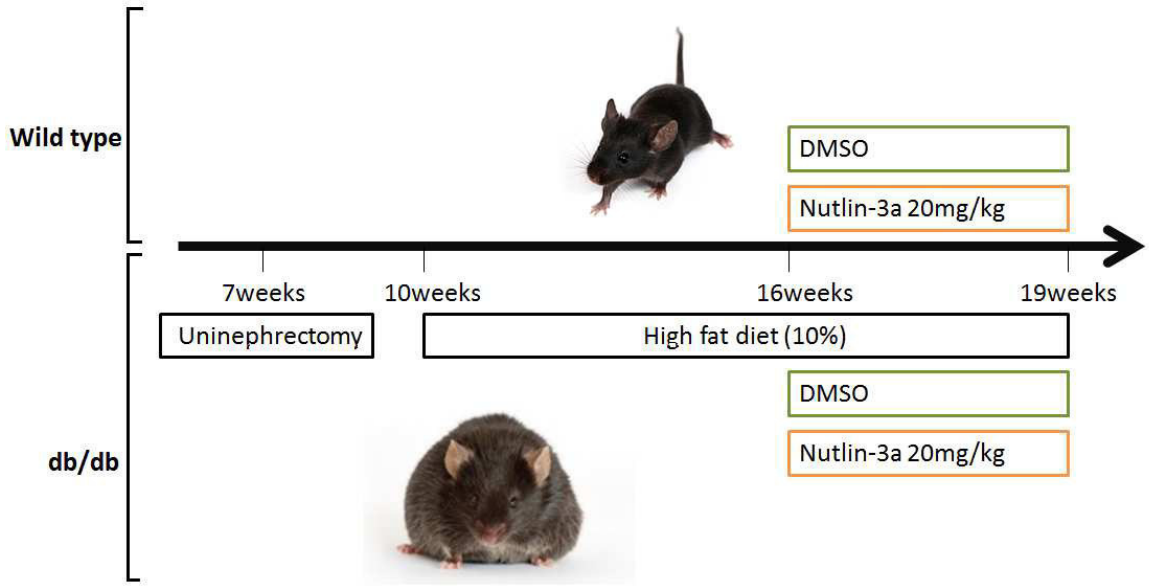

Figure 10 Experimental time line of the animal study.

Diabetic mice (BKS.Cg-m+/+Lepr^{db}/BomTac) were purchased at the age of six weeks and uninephrectomy was performed one week after, as described below in *Surgical procedure of uninephrectomy and post-surgical care*. When mice reached 10 weeks of age, chow diet was shifted to high fat diet till the end of the study to aggravate the phenotype (table 4 and 5). Nutlin-3a at a concentration of 20mg/kg (diluted in 50% DMSO) or 50% DMSO only was administered i.p. for four weeks, starting from week 16 until 19 on alternative days (figure 10).

Table 4. High fat diet composition. Composition of the high fat diet (%), which was used to feed mice within the study.

High fat diet	
Casein	24,00%
Corn starch, pre-gelatinized	43,42%
Maltodextrin	4,00%
Sucrose	5,00%
Cellulose powder	6,00%
L-Cystine	0,30%
Vitamins	1,00%
Mineral & trace elements	6,00%
Choline Cl	0,28%
Pork lard	9,00%
Soybean oil	1,00%
Cholesterol	~67mg/kg
Σ	100,00%

Table 5. Comparison between regular and high fat diet.

	Unit	Regular feed (chow diet)	High fat diet
Crude protein	%	22,0	21,1
Crude fat	%	4,5	10,1
Crude fiber	%	3,9	5,7
Crude ash	%	6,8	5,3
Starch	%	34,0	41,7
Sugar	%	5,0	6,0
Dextrins	%	-	4,0
ME (Atwater)	%	13,6	16,2
Fat	Kcal%	11	23

ME = metabolizable energy

Surgical procedure of uninephrectomy and post-surgical care

Uninephrectomy was performed under general anaesthesia in a sterile environment. All instruments were sterilized through high temperatures (121ºC). Anaesthesia was administered intraperitoneally. Anaesthetised mice with no pain reflexes were positioned in right lateral decubitus on a sterile operation bed. Shaving of the surgical area was performed followed by disinfection of the skin with povidone iodide. To minimize surgical site contamination, the mouse was then covered with a sterile sheet –without obstructing breathing- leaving only exposed the area to operate. The incision was done on the left medial lateral line using the silhouette of the spleen as a reference, visible through the skin, and the triangle formed by the end of the rib cage and the vertebral column (figure 11). Access to the peritoneal cavity allowed the localization of the left kidney, caudal and medial from the spleen. Perirrenal fat was moved apart and the kidney gently pulled out of the abdominal cavity. After that, a knot was tied around the renal hilus and the kidney was excised. The peritoneum was sutured with

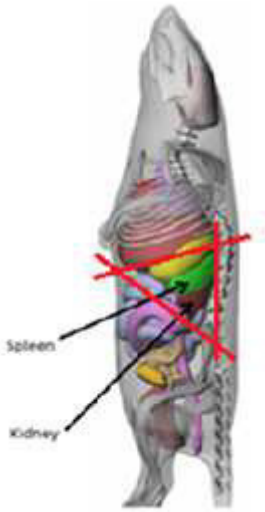

Figure 11 Incision site. Left kidney is localized slightly medial and caudal from the spleen. The triangle delimited by the end of the rib cage and the vertebral column defines the area to operate.

absorbable thread 5-0 (Vycril) and the skin with non-absorbable thread 5-0 (Ethibond). After surgery, a first dose of analgesia with buprenorphine was administered subcutaneous, followed by three days of treatment every 12 hours.

Mice were kept in single cages for at least one month after surgery to avoid bites in the wound and to facilitate good healing. Since wound healing is impaired in db/db mice (SG Keswani 2004, J Michaels 2007), mice were monitored at least twice a day for follow-up and wounds were cleaned and disinfected with povidone iodide.

Plasma, urine and tissue collection

Plasma was collected before starting the treatment, after two weeks and at the end of the treatment, before sacrifice. Small blood samples were collected under isoflurane anaesthesia in micro centrifuge tubes containing EDTA (5µl of 0.5M solution per 100µl of blood) and plasma was separated by centrifugation at 10.000 rpm for 5 minutes and stored at -20°C until analysis for creatinine and blood urea nitrogen estimation levels.

Spot urine samples were collected at the same time points as plasma and stored at -20°C for albuminuria analysis.

Kidney tissue was collected after cervical dislocation and stored in mRNA later at -20°C for mRNA isolation and gene expression analysis. The central part of the kidney was harvested for histology.

Glucose measurement

Glucose was measured every two weeks after 4 hours of fasting with a portable glucometer (Accu-Check®). For that purpose, a small incision at the end of the tail was performed to obtain approximately 10µl; that amount was enough for the measurement and not harmful for the mouse. This was considered the best option for the measurement, since multiple factors can influence the labile glucose levels: stress, anaesthesia, time of the day and fasting.

Stress causes a prompt raise of catecholamine in the mouse followed by cortisol after few hours. These stress hormones increase contraregulatory hormones such as glucagon,

which increase glycaemia. For this reason, any manipulation of the mouse in any manner can augment glucose values and overestimate them. A rapid cut in the tail with little bleeding minimized the stress of the mouse (JE Ayala 2006). A stresless bleeding under anaesthesia was for that purpose rejected, since it has been shown that anaesthesia can induce hyperglycemia in rodents (ET Brown 2005, Zuurbier CJ 2008). Due to the circadian rhythm of cortisol secretion and its influence in glycaemia (Ayala JE1 2010), glucose measurement was always performed at the same time, at noon. Additionally, in order to minimize interindividual variability ascribed to postpandrial or fasting status, glucose levels were measured in all mice after 4 hours of fasting.

Plasma creatinine and plasma BUN

Plasma creatinine levels were measured using Jaffe's enzymatic reaction using a Creatinine FS kit (DiaSys Diagnostic system, GmBH, Holzheim, Germany). Plasma samples were used undiluted and different dilutions of standard were prepared using the stock provided with the kit. Working monoreagent was prepared by mixing 4 parts of reagent 1 (R1) and 1 part of reagent 2 (R2) provided with the kit. Then, 10 µl of each of the diluted samples and standards were added to a 96 well plate with flat bottom (Nunc maxisorb plate). The monoreagent (200µl) was added to each well and the reaction mixture was incubated for one minute before measuring the absorbance at 492 nm immediately after 1 (A1) and 2 (A2) min of addition using an ELISA plate reader. The change in absorbance (ΔA) was calculated as:

$$\Delta A = [(A2 - A1)sample\ or\ standard] - [(A2 - A1)Blanck]$$

And creatinine content of samples was calculated as:

$$Creatinine\ \left(\frac{mg}{dl}\right) = \frac{\Delta Asample}{\Delta Astandard}\ x\ Concentration\ of\ standard\ (\frac{mg}{dl})$$

Plasma BUN levels were measured using an enzymatic reaction using a Urea FS kit (DiaSys Diagnotic System, GmBH, Holzheim, Germany). Different solutions of the standard were prepared using the stock provided with the kit. Working monoreagent was prepared by mixing 4 parts of reagent 1 (R1) and 1 part of reagent 2 (R2) provided with the kit. Then, 2µl of each of the sample and standards were added to a 96 well plate with flat bottom (Nunc maxisorb plate). The monoreagent (200 µl) was added to each well and the reaction mixture

was incubated for one minute before measuring the absorbance at 360 nm immediately after 1 (A1) and 2 (A2) min of addition using an ELISA plate reader. The change in absorbance (ΔA) was calculated as:

$$\Delta A = [(A2 - A1)sample\ or\ standard] - [(A2 - A1)Blanck]$$

And BUN content of samples was calculated as:

$$BUN\ \left(\frac{mg}{dl}\right) = \frac{\Delta Asample}{\Delta Astandard}\ x\ Concentration\ of\ standard\ \left(\frac{mg}{dl}\right) x\ 0{,}467$$

Urine albumin/creatinine ratio

Urin albumin levels were determined using an albumin ELISA kit from Bethyl laboratories following manufacturer's instructions. In general the albumin levels in urine samples from diabetic mice were quite high, so urine samples were diluted 100 to 1500 times with water before estimation. Briefly, a polyethylene flat bottom 96 well plates (Nunc plates) was coated with the capture antibody (Anti-Mouse albumin, 1:100 dilution) using 0.05M carbonate-bicarbonate (pH 9.6) coating buffer at 4ºC overnight. After incubation, the plate was washed 3 times with wash buffer (50 mM Tris, 0,14 M NaCl with 0.05% Tween 20, pH 8.0) and blocked with blocking solution (50 mM Tris, 0,14 M NaCl with 1% BSA, pH 8.0) at room temperature for 1 hour. Following blocking, the plate was washed 5 times with wash buffer and the diluted samples/standards added into the respective wells and incubated for 1 hour. After incubation, the plate was washed 5 times with wash buffer and HRP-conjugated detection antibody (dilution 1:100.000) was added and incubated in the dark for 1 hour. Prior to the addition of the TMB reagent (freshly prepared by mixing equal volumes of two substrate reagents) the plate was washed 5 times and then incubated in the dark until the colour reaction was completed followed by addition of the stop solution (2 M H_2SO_4). The absorbance was read at 450 nm within 10 minutes after the addition of the stop solution. The albumin content in each sample was determined using the equation of regression line generated by plotting the absorbance of different standards against their known concentrations.

Urinary creatinine levels were determined, like the plasma creatinine levels using the Jaffe's enzymatic reaction and diluting the samples 10 times (see above *Plasma creatinine and plasma BUN*).

Urinary albumin to creatinine ratio was calculated after converting the values for albumin and creatinine to the same unit (mg/dl). Albumin content for each sample (mg/dl) was divided by the creatinine content (mg/dl) for the same sample.

Plasma cholesterol and triacylglycerides

Plasma cholesterol levels were measured using an enzymatic photometric test with a Cholesterol FS kit from Diasys following manufacterer's instructions. Briefly, plasma samples were used undiluted and different dilutions of the standard were prepared using the stock provided with the kit. Then, 2µl of each sample and standard were added to a 96 well flat bottom plate (Nunc maxisorb plate). The working reagent (200µl) provided with the kit was added to each well and the reaction mixture was incubated in the dark for 20 minutes at room temperature and subsequently absorbance was measured at 500 nm with the ELISA reader.

The amount of cholesterol was calculated as:

$$Cholesterol\ \left(\frac{mg}{dl}\right) = \frac{A\ Sample - A\ blanck}{A\ standard - A\ blanck}\ x\ Concentration\ standard$$

Plasma trigyceride levels were tested with a colorimetric enzymatic assay from Dyasis following manufactere's instructions, being the procedure identical to the one described above, with less time of incubation (10minutes).

Plasma triglyceride concentration was then calculated as:

$$Tryglyceride\ \left(\frac{mg}{dl}\right) = \frac{A\ Sample - A\ blanck}{A\ standard - A\ blanck}\ x\ Concentration\ standard$$

Posteriorly, to correct values for free glycerol, 10mg/dl was substracted from the concentration calculated with the formula above.

Periodic acid Schiff staining

Formalin-fixed tissue was processed using tissue processors (Leica). For that paraffin blocks were prepared and 2 µm thick paraffin-embedded sections were cut. De-paraffinization was carried out using xylene (3 times for 5 minutes) followed by re-hydration incubating the sections in 100% absolute ethanol (3 times for 3 minutes), 95% ethanol (2 times for 3 minutes), 70% ethanol (once for 3 minutes) and a final wash with distilled water during 5 minutes. Re-hydrated sections were incubated with Periodic acid (2% in distilled water) for 5 minutes followed by washing with distilled water for 5 minutes. Then sections were incubated with Schiff solution for 2 minutes at room temperature, washed with tap water for 7 minutes and counter stained with Hematoxylin solution for 2 minutes. Finally, sections were dipped in alcohol 90%, dried and closed with cover slips.

Immunostaining and confocal Imaging

For immunohistological studies the middle part of the kidney was fixed in 4% formalin overnight, processed using tissue processors (Leica) and prepared in paraffin blocks. 2 µm thick paraffin-embedded sections were cut. Deparaffinization was done using xylene (3 times or 5 minutes) followed by re-hydration, which was carried out by incubating the sections in 100% absolute ethanol (3 times for 3 minutes), 95% ethanol (2 times for 3 minutes) and 70% ethanol (once for 3 minutes) followed by washing with PBS (2 times for 5 minutes). Blocking endogenous peroxidase was carried out by incubating sections in H_2O_2 and methanol mixture (20ml of 30% H_2O_2 in 180 ml of methanol) for 20 minutes in dark followed by washing in PBS (twice for 5minutes). Sections were then dipped in antigen unmasking solution (3ml of antigen unmasking solution + 300ml of distilled water) and cooked in the microwave for a total of 10 minutes (4 times for 2.5 minutes; every 2-5 minutes water level was checked and made up if necessary to the initial level with distilled water). After microwave cooking sections were cooled to room temperature for 20 minutes and washed with PBS. Blocking endogenous biotin was carried out by incubating sections with one drop of Avidin (Vector) for 15 minutes followed by incubation with Biotin (Vector) for further 15 minutes. After the incubation, sections were washed with PBS (twice for 5 minutes).

Sections were incubated with different primary antibodies either for 1 hour at room temperature or overnight at 4ºC in a wet chamber followed by a wash step with PBS (twice

for 5 minutes). After washing sections were incubated with biotinylated secondary antibodies (1:300, dilution in PBS) for 30 minutes followed by wash with PBS for 5 minutes and Tris for another 5 minutes. Subsequently sections were stained with DAB and counterstained with methyl green (Fluka). Later sections were washed with 96% alcohol to remove excess of antibody and xylene.

The primary antibodies used in this study are mentioned above. For each immunostaining a negative control was used consisting of an isotype control antibody. For confocal imaging, sections were labeled with the following primary antibodies: pig anti-mouse nephrin (1:100, Acris Antibodies, Herford, Germany) and rabbit anti-mouse WT1 (1:25, Santa Cruz Biotechnology, Santa Cruz, CA) and incubated 1 hour in 0.1% milk solution in room temperature. After washing, the sections were incubated with the following secondary antibodies: guinea pig Alexa Fluor 488 (1:100, Invitrogen, Carlsbad, CA) or rabbit Cy3 (1:200, Jackson ImmunoResearch Laboratories, West Grove, PA) for 30 minutes at room temperature. Stainings were evaluated using confocal microscopy with a LSM 510 microscope and LSM software (Carl Zeiss AG).

Histopathological evaluations

PAS staining

Diabetic nephropathy was evaluated by assessing the severity of glomerular damage. The following criterion in table 6 was used. For each section 20 glomeruli were evaluated and the score was expressed as mean±SEM.

Table 6. PAS glomerular score criterion.

Score	Description
0	Normal glomerulus
1	Mild mesangial matrix expansion
2	Mesangial matrix expansion
3	Severe mesangial matrix expansion, some closed capillars and/or areas of sclerosis
4	Severe mesangial matrix expansion, capillars completely closed and/or severe sclerosis.

Mac2 staining

The number of infiltrated macrophages were counted manually in 20 glomeruli per section stained with Mac2 (pan marker for macrophage) antibody. Values are expressed as mean ± SEM for each group.

Collagen and p53 staining

In order to evaluate tissue fibrosis, collagen staining was employed. The software Image J was used to quantify the percentage of collagen positive area from each section. The data are presented as mean ± SEM per group. This quantification method was also used to evaluate the expression of p53 in the kidney.

Wt1/Nephrin staining

The number of podocytes per glomerulus was quantified by Wt1/Nephrin staining. For each section 20 glomeruli were evaluated. Only a clear Wt1 staining surrounded by nephrin staining was quantified as a podocyte. Two nuclei that appeared too close together were counted as one, as they could belong to the same cell.

RNA isolation, cDNA preparation and real-time PCR

One part of the kidney from each mouse was preserved in RNA-later immediately after kidney harvest and stored at -20ºC until processed for RNA isolation. RNA isolation was carried out using the RNA isolation kit from Ambion (Ambion, CA, USA). Briefly, tissues (~30mg) preserved in RNA-later were homogenized using a blade homogenizer for 30 seconds in lysis buffer (600 µl) containing 1% β-mercaptothanol. The homogenate was centrifuged at 600 rpm for 5 minutes and 350 µl of 70% ethanol was added and mixed gently. This whole mixture was then loaded on a RNA column and processed for RNA isolation as per manufacturer's instruction.

The isolated RNA samples were quantified using a Nano drop (PEQLAB Biotechnology GmbH, Erlangen, Germany). The ratio of optical densities at 260 nm and 280 nm was an indicator for RNA purity (indicative of protein contamination in the RNA samples). Only samples with a ratio of 1.8 or more were considered to be of acceptable quality.

The isolated RNA samples were quantified and processed for cDNA using reverse transcriptase II (Invitrogen, Karlsruhe, Germany). RNA samples were diluted with water to get a final concentration of 2µg/20µl, to this diluted RNA samples 13.9 µl of master mix was added. The master mix was prepared by mixing 9µl of 5x buffer (Invitrogen, Karlsruhe, Germany), 1µl of 25 mM dNTP mixture (Amersham Pharmacia Biotech, Freiburg, Germany), 2 µl of 0,1M DTT (Invitrogen, Karlsruhe Germany), 1µl of 40U/µl RNAsin (romega, Mannheim, Germany), 0,5µl of Hexanucleotide (Roche, Mannheim, Germany) and 1µl of Superscript (Invitrogen, Karlsruhe, Germany). The tubes were incubated at 42ºC for 1 hour and 30 minutes on a thermal shaker followed by 5 minutes heating at 90ºC. Upon completion of incubation cDNA samples were stored at -20ºC until used for RT-PCR analysis using SYBR green. The cDNA samples prepared as described above were diluted 1:10 and 2 µl of diluted cDNA samples were mixed with SYBR green master mix (10µl), forward primer specific for gene of interest (0,6 µl), reverse primer specific for gene of interest (0,6 µl), Taq polymerase (0,16µl) and distilled water (6,64µl).

The RT-PCR was performed using a Light Cycler 480. Pre-incubation was carried out for 5 minutes at 95ºC so as to activate the polymerase and complete de-naturation of cDNA samples. Then the cDNA was amplified for 40 cycles, each comprising of 15 seconds incubation at 95ºC and 45 seconds incubation at 60ºC. For melting curve initially 95ºC for 5 seconds followed by 65ºC for 1 minute with continuous heating was used. The RT-PCR for the reference genes (18s rRNA) was carried out under same conditions. The CT[1] (cycle threshold) values were calculated using the Light Cycler 480 and the results were normalized with respective reference gene expression for each sample. In all cases controls consisting of ddH_2O were negative for target or reference genes. All designed SYBR green primers for all genes evaluated were obtained from Metabion (Metabion, Martinsried, Germany). The oligonucleotide primers in table 7 were used in this study.

[1] The cycle threshold (CT) is the number of cycles required for the fluorescent signal to cross the threshold (i.e. exceeds background level).

Table 7. Primer sequences used in this study.

Gene	Sequence	
18s	Forward	GCAATTATTCCCCATGAACG
	Reverse	AGGGCCTCACTAAACCATCC
Mdm2	Forward	TGTGAAGGAGCACAGGAAAA
	Reverse	TCCTTCAGATCACTCCCACC
P53	Forward	TCCGACTGTGACTCCTCCAT
	Reverse	CTAGCATTCAGGCCCTCATC
Bcl-2	Forward	GGTCTTCAGAGACAGCCAGG
	Reverse	GATCCAGGATAACGGAGGCT
Bax	Forward	GATCAGCTCGGGCACTTTAG
	Reverse	TTGCTGATGGCAACTTCAAC
PUMA	Forward	CACCTAGTTGGGCTCCATTT
	Reverse	ACCTCAACGCGCAGTACG
P21	Forward	CGGTGTCAGAGTCTAGGGGA
	Reverse	ATCACCAGGATTGGACATGG
Nephrin	Forward	TTAGCAGACACGGACACAGG
	Reverse	CTCTTTCTACCGCCTCAACG
Wt1	Forward	GGTTTTCTCGCTCAGACCAGCT
	Reverse	ATGAGTCCTGGTGTGGGTCTTC
Synaptopodin	Forward	TCCTTCTCCACCCGGAATGCTG
	Reverse	AGCCGTCCAGGCTGCTAGGAG
Podocin	Forward	TGACGTTCCCTTTTTCCATC
	Reverse	CAGGAAGCAGATGTCCCAGT
Podocalyxin	Forward	ATAACCAGGCGGTGGCAGTGAA
	Reverse	CCAGCTTCATGTCACTGACTCC
CD2AP	Forward	TCCAAAGCCTGACCTGTCAGCT
	Reverse	CTTTTTGGGCGGGACTTGAGGA
P50 (NFκB1)	Forward	GCTGCCAAAGAAGGACACGACA
	Reverse	GGCAGGCTATTGCTCATCACAG
P65 (RELA)	Forward	TCCTGTTCGAGTCTCCATGCAG
	Reverse	GGTCTCATAGGTCCTTTTGCGC
CCL5	Forward	CCTGCTGCTTTGCCTACCTCTC
	Reverse	ACACACTTGGCGGTTCCTTCGA

CCL2	Forward	CCTGCTGTTCACAGTTGCC
	Reverse	ATTGGGATCATCTTGCTGGT
IL-1β	Forward	ACACACTTGGCGGTTCCTTCGA
	Reverse	GTTCATCTCGGAGCCTGTAGTG
TNFα	Forward	CCACCACGCTCTTCTGTCTAC
	Reverse	AGGGTCTGGGCCATAGAACT
iNOS	Forward	TTCTGTGCTGTCCCAGTGAG
	Reverse	TGAAGAAAACCCCTTGTGCT
IL-12α	Forward	GTTCATCTCGGAGCCTGTAGTG
	Reverse	CCTCATAGATGCTACCAAGGCAC
IL6	Forward	TGATGCACTTGCAGAAAACA
	Reverse	ACCAGAGGAAATTTTCAATAGGC
Fibronectin	Forward	CCCTATCTCTGATACCGTTGTCC
	Reverse	TGCCGCAACTACTGTGATTCGG
aSMA (ACTA1)	Forward	ACCATCGGCAATGAGCGTTTCC
	Reverse	GCTGTTGTAGGTGGTCTCATGG
Col1a1	Forward	CCTCAGGGTATTGCTGGACAAC
	Reverse	CAGAAGGACCTTGTTTGCCAGG
Col4a1	Forward	ATGGCTTGCCTGGAGAGATAGG
	Reverse	TGGTTGCCCTTTGAGTCCTGGA
Laminin	Forward	TGTCTGCAAGCCAGGAGCTACA
	Reverse	GAGACAGAACGGCATCACCAAC
TGFβ	Forward	GGTCTGGAGAATCTTCAGGAACC
	Reverse	CACCACTGGAAGAGGAGAATGG

Abbreviations: *Bcl-2 = B-Cell lymphoma 2, PUMA = p53 upregulator of apoptosis, Wt1 = wilms tumour protein 1, CD2AP = CD2 associated protein, TNFα = tumour necrosis factor α, iNOS = inducible nitric oxide synthase, aSMA = actin, alpha skeletal muscle, ACTA1 = actin alpha 1, Col1/4 = collagen type 1/4, TGFβ = transforming growth factor beta.*

3.2.2 *In-vitro* methods

Podocyte cell culture

A conditionally immortalized mouse podocyte cell line was used for the *in vitro* experiments. This cell line is highly proliferative under permissive conditions and undergoes growth arrest within 6 days when those conditions are removed. During growth arrest, the cells differentiate into mature podocytes, in a similar way as podocytes *in vivo* (P Mundel 1997).

Both non differentiated and differentiated podocytes express Wt1, and as the cytoskeleton is rearranged and foot processes are formed, proteins such as synaptopodin, nephrin and podocalyxin, among others, are expressed (SJ Shankland 2007).

Cells were cultured in RPMI 1640 with glutamine (Gibco) medium containing 5% HEPES, 5% Bicarbonate, 5% Pyruvate, 5% fetal bovine serum and 1% penicillin/streptomycin. Cells were expanded under permissive conditions – 33ºC and 50U/ml INFγ- and then seeded in 96 well flat bottom plates (12.000 cells/well). To allow for a complete differentiation into podocytes, cells were kept under nonpermissive conditions for 15 days at 37ºC without INFγ and then stimulated.

Mouse tubular cells culture

Moue tubular cells were cultured in DMEM medium (Biochron) containing 10% fetal bovine serum and 1% penicillin/streptomycin and kept at 37ºC.

Cell freezing and thawing

At earlier passages large amounts of cells were grown first under standard culture conditions and then frozen for future cell culture experiments. For freezing, detached cells from the culture plates were collected and centrifuged under sterile conditions for 3 minutes at 100 rpm. The cell pellet was maintained on ice and carefully re-suspended in cold freezing medium (90% respective culture medium and 10% DMSO) by pipetting the suspension repeatedly up and down. 1,5 ml aliquots were quickly dispensed into freezing vials (4ºC). The cells were slowly frozen at -20°C for 1 hour and then at -80^C overnight. The next day, all aliquots were transferred into the liquid nitrogen for long-term storage.
For thawing frozen cells, a vial was removed from the liquid nitrogen and put in to the water bath at 37°C. The cells were then dispensed in 5ml of warm complete growth medium and centrifuged at 100 rpm for 5-7 minutes to remove the old media and DMSO. After centrifugation, cells were resuspended in fresh medium and transferred into a new culture plate. The medium was changed one more time after 24 hours.

In-vitro assessment of cell death

To analyze cytotoxicity, lactate dehydrogenase (LDH) release was measured via a colorimetric assay (Cytotoxicity Detection Kit (LDH), Roche). Podocytes were seeded in a

collagen-coated 96 well plate (12.000 cells/well) and differentiated for 15 days under non-permissive conditions. After 15 days, serum was removed – except for the survival control group - and cells were either cultured in normal glucose media (11mM) or high glucose media (45mM). After 24 hours, cells were stimulated with different concentrations of Nutlin-3a or with vehicle alone, dymethil sulfoxide (DMSO), as a control. Triton X was additionally administered as positive control. The same protocol was used for mouse tubular cells, although no differentiation of these cells was needed, nor a coated plate. The density of cells per well was for MTC 8.000 cells/well.

After 6 and 24 hours, 100 µl of the supernatant was collected and transferred into a NUNC 96 well plate. 100 µl of freshly prepared reagent, containing 11,25 ml of catalyst and 250 µl of dye solution, was added and after 20 minutes the absorbance was measured with an ELISA reader at 492 nm. A background control was employed for each group.

The average absorbance values of each group were calculated and then the value of the background control was substracted. The percentage of cytotoxicity was then calculated as:

$$Cytotoxicity\ (\%) = \frac{Av.value - background}{Positive\ control}\ x\ 100$$

In vitro viability assessment

Cell viability was tested to complement cytotoxicity assessment with an MTT assay. This assay measures via absorbance the amount of tetrazolium dye MTT (3-(4,5-dimethylthiazol-2-yl)-2,5-diphenyltetrazolium) that has been reduced to its insoluble form formazan by NAD(P)H-dependent cellular oxidoreductase enzymes, which reflect the number of metabolically active and viable cells.

Cells were seeded as described above (*In-vitro assessment of cell death)* and after 6 and 20 hours, the MTT dye solution was added to the cells at a volume of 15 µl. After 4 hours, the reaction was stopped with MTT stop solution and the plate left overnight covered in aluminum foil. The following day, absorbance was measured with the ELISA reader at 570 nm.

3.2.3 Statistical analysis

Data are presented as mean ± SEM. For multiple comparison of groups one way ANOVA was used followed by Tukey's Multiple Comparison Test. Student's T-test or Mann Whitney test (when normality could not be assumed) were used for the comparison of single groups and 2-Way-ANOVA when two groups were compared over different time-points. Statistical analysis was conducted with GraphPrism. A value of $p<0,05$ was considered of statistical significance.

4. RESULTS

4.1 Mdm2 blockade with Nutlin-3a in mouse podocytes and mouse tubular cells

To test whether blockade of Mdm2 with Nutlin-3a in podocytes can also increase cell death similar to that seen in siRNA studies (Thomasova D 2015), mouse podocytes were cultured under normal glucose conditions and stimulated after complete differentiation (see section above *3.2.2 In vitro methods, Podocyte cell culture*) with different doses of the drug -10, 15 and 20µM- and, as a control, with its vehicle (DMSO) in a concentration comparable to the group with the highest dose of Nutlin-3a. Using a MTT assay, the viability of cells, in terms of their capacity of reducing MTT into formazan –a reaction that is proportional to the measured absorbance at 570nm- was assessed (see section above *3.2.2 In vitro methods, In vitro viability assessment*). As shown in figure 12A, treatment of podocytes with Nutlin-3a decreased the absorbance in a dose-dependent manner after 12 hours, although not significantly. However, after 24 hours (figure 12B) the decreased absorbance, illustrating reduced viability, becomes significant in comparison to the not stimulated group (NG) and to the vehicle group (NG+DMSO). To confirm this data, we further performed an LDH assay to determine the cytotoxic effect of Nutlin-3a on podocytes. After 6 and 24 hours, the cytotoxicity significantly increased when cells were treated with a higher dosage of Nutlin-3a compared to control groups (figure 12C and 12D).

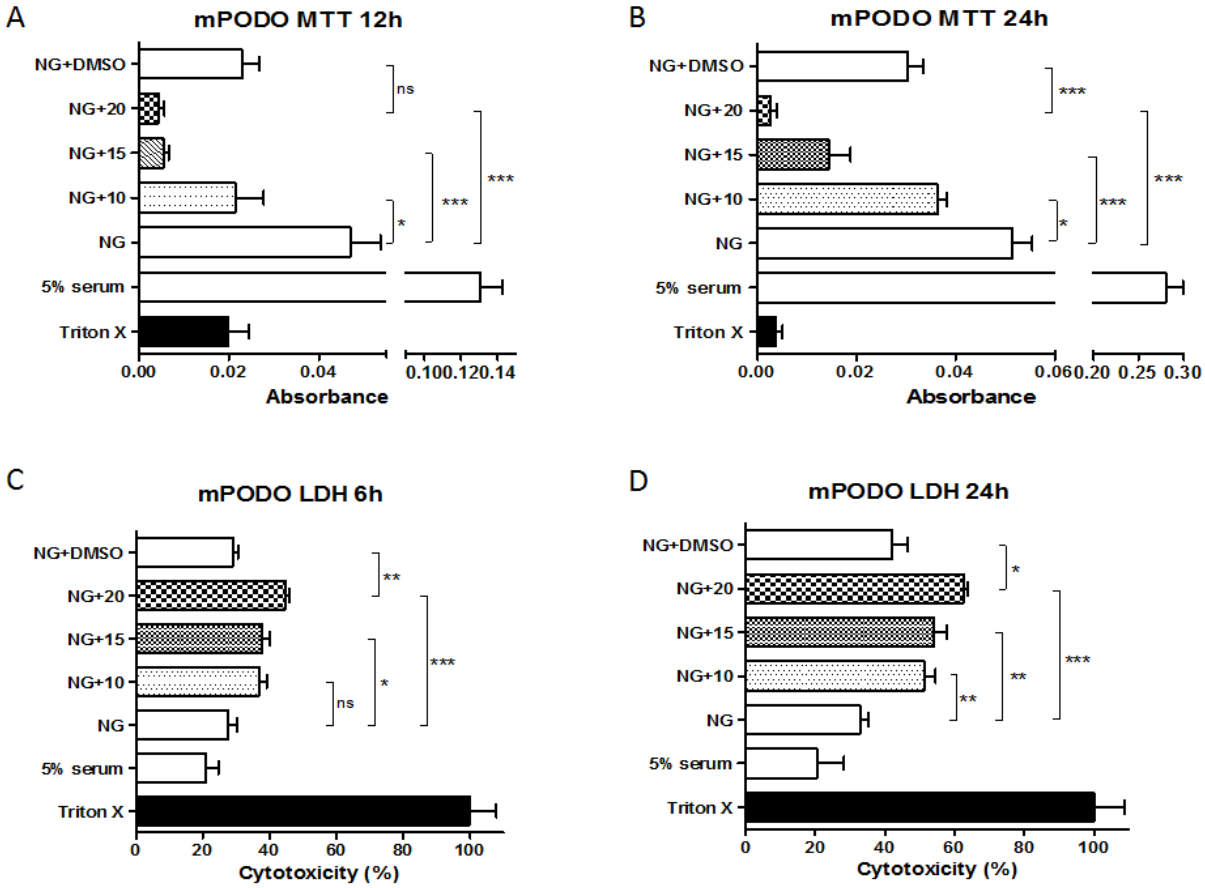

Figure 12. Viability (MTT assay) and cytotoxicity (LDH assay) in mouse podocytes. A) Stimulation with Nutlin-3a significantly reduced podocyte viability after 12 hours of stimulation compared to control. The difference with the vehicle however showed no significance. **B)** After 24 hours, this difference between Nutlin3a and vehicle becomes statistically significant (p<0,0005). **C-D)** Cytotoxicity also increased significantly with Nutlin-3a compared to control and vehicle in a dose-dependent manner. Triton X was used as negative control in the viability assay and as positive control and reference for the cytotoxicity assay. On the other hand, podocytes cultured in media with 5% serum represented the survival control. n=5 for each group. Data was analysed using 1-way ANOVA with Tukey's Multiple Comparison Test. *NG = normal glucose media (11mM); NG+10 = normal glucose media with 10µM of Nutlin-3a; NG+15 = normal glucose media with 15µM of Nutlin-3a; NG+20 = normal glucose media with 20µM of Nutlin-3a; NG+DMSO = normal glucose with 20µl/ml of DMSO. * = p<0,05; ** = p<0,005; *** = p<0,0005.*

Next, we wanted to investigate the effect of Nutlin-3a on the viability (MTT assay) and cytotoxicity (LDH assay) of mouse tubular cells (MTCs) under normal glucose conditions. As represented in figure 13A and 13B, treatment of MTCs with Nutlin-3a resulted in a decreased absorbance in the MTT assay after 12 and 24 hours in a dose-dependent manner, indicating that Nutlin-3a reduces the viability of MTCs. Next, an LDH assay was performed to determine the cytotoxic effect of Nutlin-3a. Like in podocytes, Nutlin3a was also cytotoxic to MTCs as indicated by a significant increase in the percentage of cytotoxicity after 6 and 24 hours (figure 13C and 13D, respectively).

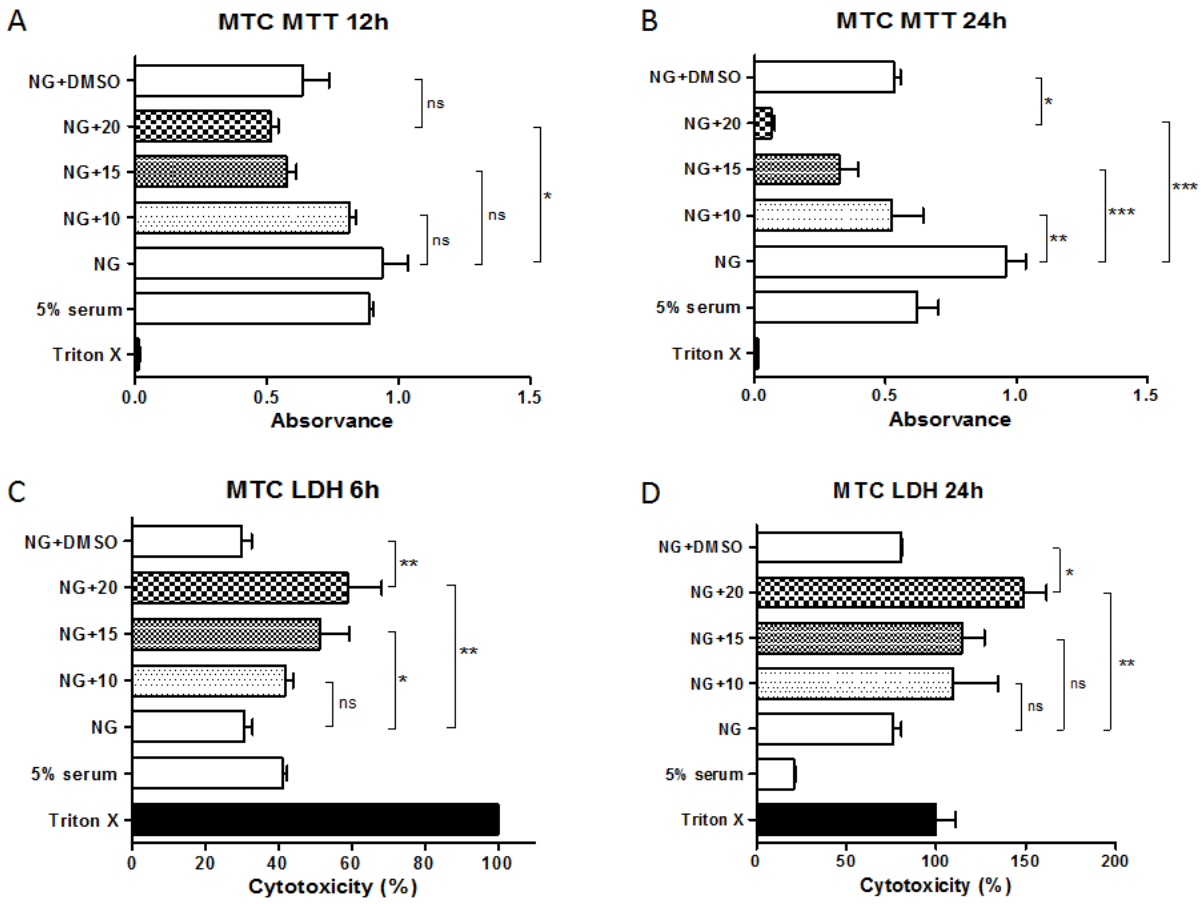

Figure 13. A-B) Viability (MTT assay) and C-D) cytotoxicity (LDH assay) in mouse tubular cells. A) Stimulation with Nutlin-3a reduced tubular cell viability after 12 hours and **B)** after 24 hours post-stimulation compared to control and vehicle, being statistically significant at the later time point. **C-D)** Nutlin-3a stimulation increased significantly cytotoxicity in a dose-dependent manner after 6 and 24 hours. Triton X was used as negative control for the MTT assay and as positive control and reference for the cytotoxicity assay. Podocytes cultured in media with 5% serum served as survival control. n = 5 for each group. *NG = normal glucose media (5,5mM); NG+10 = normal glucose media with 10µM of Nutlin-3a; NG+15 = normal glucose media with 15µM of Nutlin-3a; NG+20 = normal glucose media with 20µM of Nutlin-3a; NG+DMSO = normal glucose with 20µl/ml of DMSO*. Data was analyzed using 1-way ANOVA with Tukey's Multiple Comparison Test. * = p<0,05; ** = p<0,005; *** = p<0,0005.

To look whether a diabetic environment had an impact on the viability and cytotoxicity of podocytes and MTCs, stimulation with high glucose was carried out. Podocytes were cultured in high glucose serum-free media (25mM) for 24 hours and then MTT and LDH assays were performed 30/36 hours and 48 hours later. As shown in figure 14A, the viability of podocytes exposed to high glucose media was significantly higher than those to normal glucose media (11mM). Accordingly, cytotoxicity was significantly lower under diabetic conditions than normal glucose conditions after 24 hours. The culture of MTCs with high glucose media did not cause any difference in terms of viability compared to normal

glucose media (figure 14B) but the cytotoxicity after 48 hours was significantly higher in normal glucose than in high glucose conditions (p<0,0005), similar to that seen in podocytes.

To further investigate the effect of Nutlin-3a in diabetic conditions, the same viability and cytotoxicity assays were performed in podocytes cultured in a high glucose environment (45mM). Again, stimulation of podocytes stimulated with Nutlin-3a present a decreased viability after 12 hours (figure 15A) with a significant reduction of cell viability observed after 24 hours compared to vehicle (figure 15B). Cytotoxicity assessed using an LDH assay showed that stimulation with Nutlin-3a caused a significant increase in podocyte cytotoxicity compared to control and vehicle in a dose-dependent manner after 6 and 24 hours (figure 15C and 15D), as observed under normal glucose conditions.

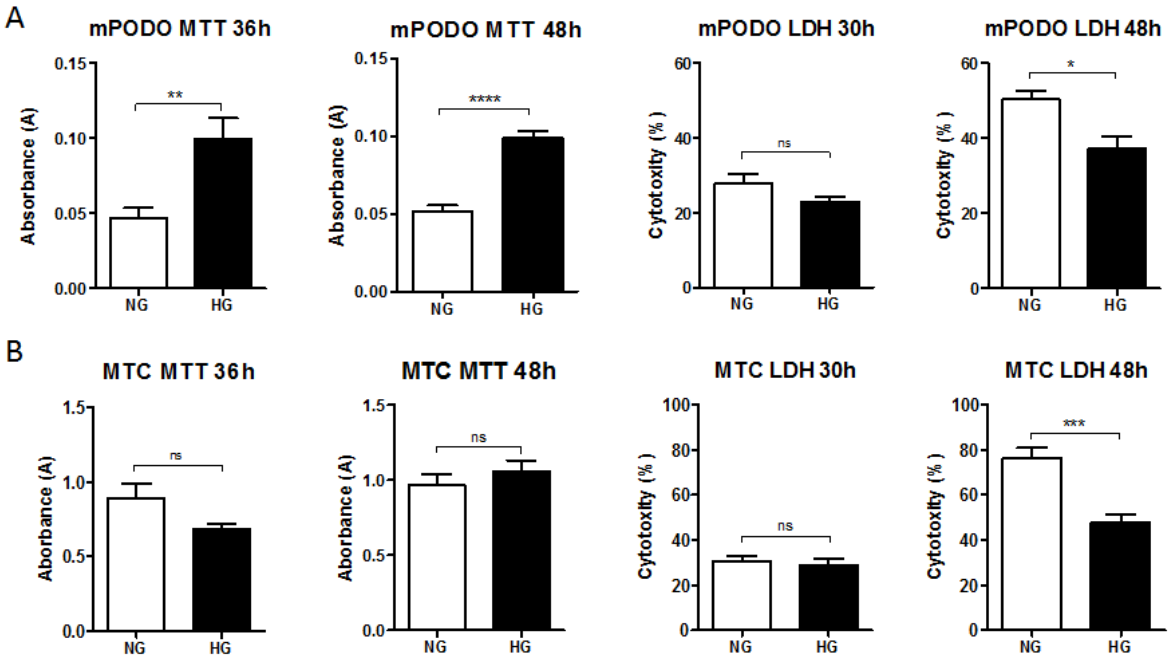

Figure 14. **Viability (MTT assay) and cytotoxicity (LDH assay) in mouse podocytes and mouse tubular cells exposed to normal (5,5-11mM) or high glucose media (45mM). A)** An environment rich in glucose increases mouse podocyte viability and reduces significantly cell death after 48 hours. **B)** Mouse tubular cells presented by contrast no statistical difference in viability but again they did in cytotoxicity in the later time point, being significantly greater in a normal glucose than in high glucose media. Data was analyzed with t-test.n = 10 in each group. *NG = normal glucose media (5-10mM)*; *HG = high glucose media (25mM)*. * = p<0,05; ** = p<0,005; *** = p<0,0005.

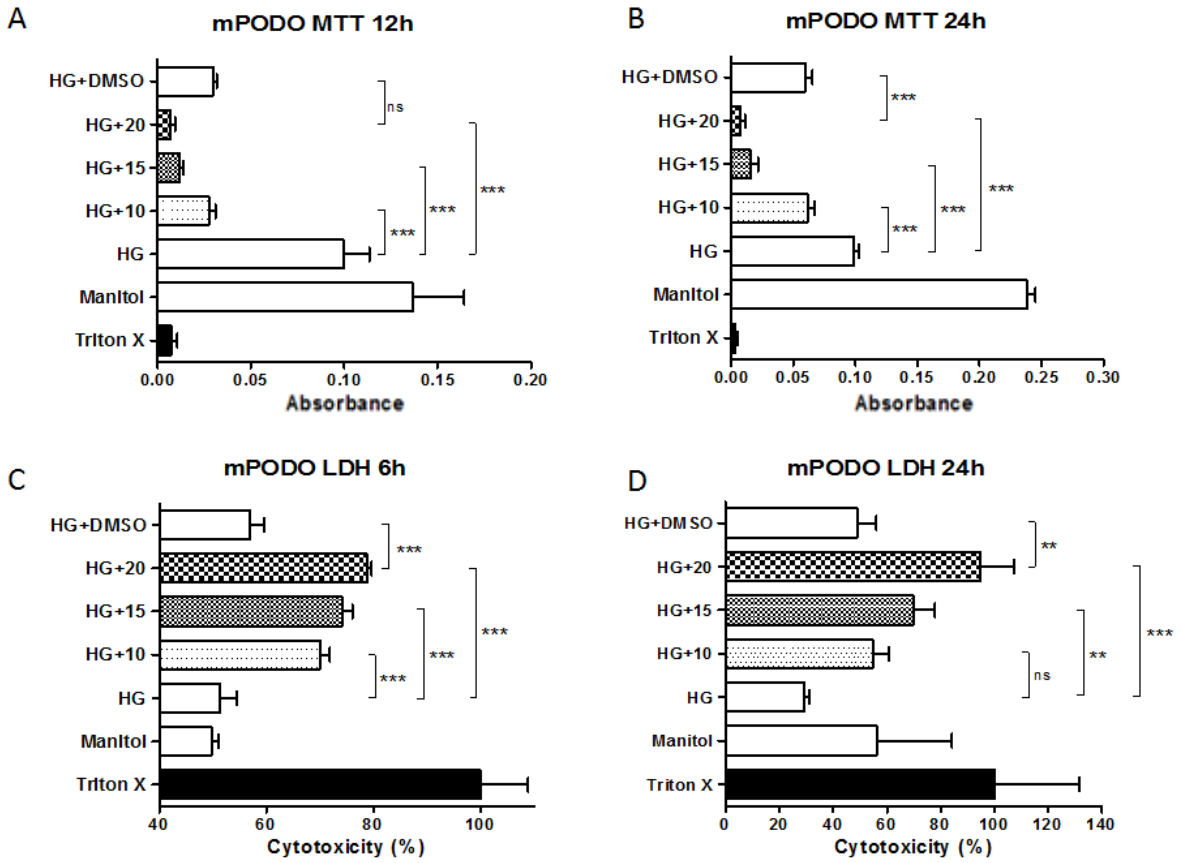

Figure 15. **Viability (MTT assay) and cytotoxicity (LDH assay) in mouse podocytes cultured in high glucose media (45mM). A)** Podocyte stimulation with Nutlin-3a in a high glucose media reduces significantly cell viability in a dose-dependent manner compared to control after 12 hours and **B)** after 24 hours, which was significantly different compared to vehicle. **C-D)** Nutlin-3a stimulation in podocytes exposed to high glucose media increases significantly the cytotoxicity in a dose-dependent manner compared to control and vehicle after 6 and 24 hours. Triton X was used as negative control in the viability assay and as positive control and reference for the cytotoxicity assay. Manitol (25mM) was used as control of osmolarity for the high glucose environment. No statistical differences were found between manitol and high glucose that could suggest a negative effect of high glucose media in cell osmolarity. Data was analyzed with 1 way ANOVA withTukey's Multiple Comparison Test. n = 5 per group. *HG = high glucose media; HG+10 = high glucose media with 10µM of Nutlin-3a; HG+15 = high glucose media with 15µM of Nutlin-3a; HG+20 = high glucose media with 20µM of Nutlin-3a; HG+DMSO = high glucose with 20µl/ml of DMSO.* * = p<0,05; ** = p<0,005; *** = p<0,0005.

In the same way, the effect of Nutlin-3a on MTCs exposed to high glucose levels was determined regarding viability and cytotoxicity. The viability after 12 and 24 hours of stimulation with Nutlin-3a significantly decreased compared to control, but not to vehicle (figure 16A and 16B). The percentage of cytotoxicity was not significantly higher following Nutlin-3a treatment compared to vehicle after 6 hours (figure 16C) and 24 hours (figure 16D).

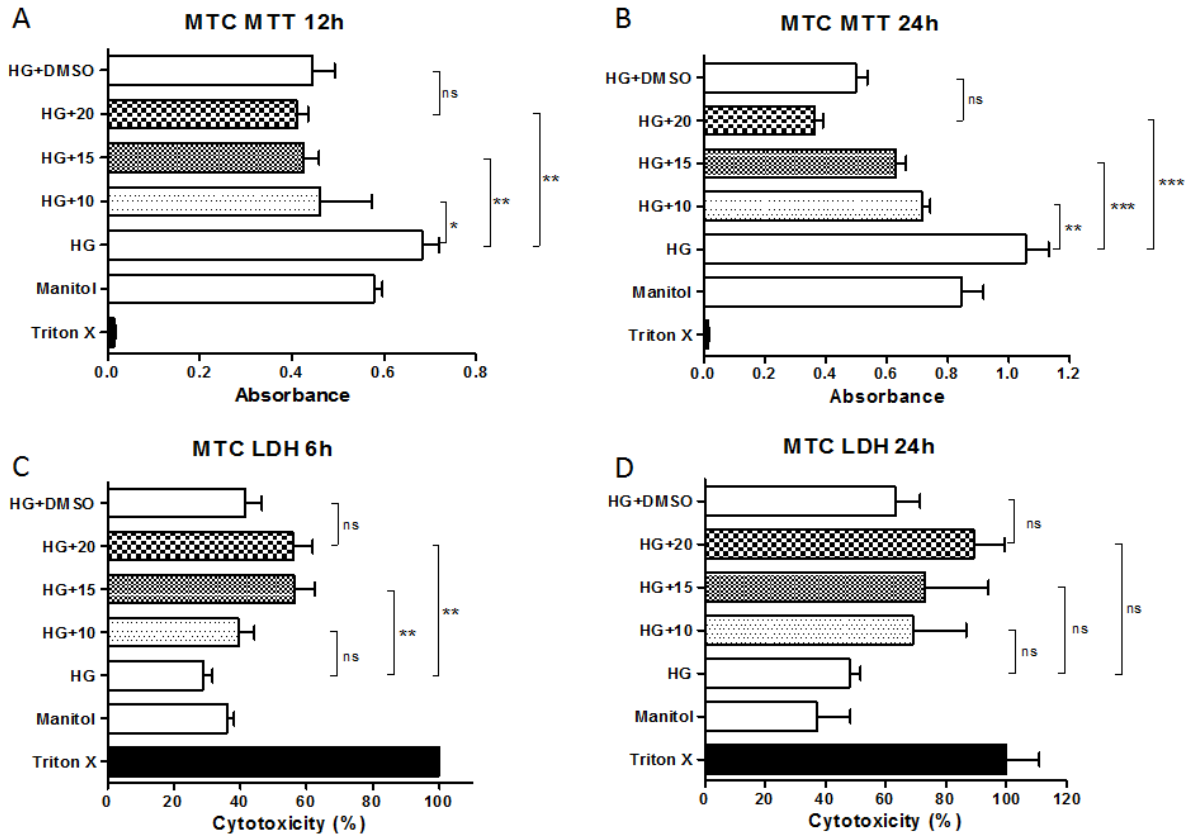

Figure 16. **Viability (MTT assay) and cytotoxicity (LDH assay) in mouse tubular cells cultured in high glucose media (45mM). A)** Stimulation of mouse tubular cells with Nutlin-3a of exposed to high glucose media reduced significantly the cell viability in a dose-dependent manner compared to control after 12 hours. **B)** After 24 hours, viability was also significantly reduced after Nutlin-3a stimulation compared to control but not to vehicle. **C)** Cytotoxicity in MTCs exposed to high glucose media increased in the Nutlin-3a-treated groups compared to control after 6 hours, but the difference was not significant compared to vehicle. **D)** After 24 hours of stimulation with Nutlin-3a no significant differences were seen among the groups. Triton X was used as negative control in the viability assay, and as positive control and reference for the cytotoxicity assay. Manitol (25mM) was used as control of osmolarity for the high glucose environment. No statistical differences were found between manitol and high glucose that could suggest a negative effect of high glucose meda in cell osmolarity. Data was analyzed with 1-way ANOVA with Tukey's Multiple Comparison Test. n = 5 per group. *HG = high glucose media; HG+10 = high glucose media with 10µM of Nutlin-3a; HG+15 = high glucose media with 15µM of Nutlin-3a; HG+20 = high glucose media with 20µM of Nutlin-3a; HG+DMSO = high glucose with 20µl/ml of DMSO.* * = p<0,05; ** = p<0,005; *** = p<0,0005.

Taken together, Mdm2 blockade with Nutlin-3a increased the cytotoxicity and decreased the viability of mouse podocytes and tubular cells under normal glucose condition (11 and 5,5mM, respectively). In mouse podocytes under high glucose concentration the cytotoxicity also increased and the viability decreased following Nutlin-3a treatment. In mouse tubular cells in a hyperglycaemic milieu however a significant difference compared to vehicle was not observed.

4.2 Pharmacological blockade of Mdm2 with Nutlin-3a in healthy mice

After Nutlin-3a showed to induce cell death in mouse podocytes and tubular cells *in vitro*, we further wanted to test whether Nutlin-3a could have deleterious effects *in vivo.* Therefore, wild type C57B/6J mice were randomly divided into three groups: one group was injected with 20 mg/kg Nutlin-3a for four weeks every two days, the second group was injected with vehicle for four weeks every two days, and a third group received no intervention and served as a control to exclude any effects of the vehicle treatment.

4.2.1 Nutlin-3a-treated mice present higher mortality and lower body weight

During the treatment, three mice died in the Nutlin-3a-treated group (72% survival), while all vehicle and control mice reached the end point of the study (figure 17C). Although a necropsy was performed on these mice, no macroscopic cause of death was found. A systemic toxic effect of the drug or a renal failure could hence not be excluded. Along the treatment, the body weight and blood glucose levels were monitored. After the first week of treatment, the body weight of Nutlin-3a-treated mice decreased, whereas in the vehicle and control mice the body weight continued to increase progressively (figure 17A). At the end of the study, the body weight of Nutlin-3a-treated mice (24,62 ± 0,36 g) was significantly lower compared to both the vehicle (28,78 ± 0,84 g; $p<0,0005$) and the control (27,23 ± 0,66 g; $p<0,05$) group (figure 17B).

As the effect of Nutlin-3a in the kidney might resemble some molecular features of diabetic nephropathy, glycaemia was also monitored during the treatment to exclude that high blood glucose levels could be the reason for such similarity in the kidney outcome. At the end of the study, we observed a significant difference in glycaemia as demonstrated by a significant decrease of plasma glucose levels in Nutlin-3a-treated mice (141,8 ± 7,3 mg/ml) compared to vehicle-treated mice (170,7 ± 7,5 mg/ml; $p<0,05$), indicating that Nutlin-3a had no diabetogenic effect (figure 17D).

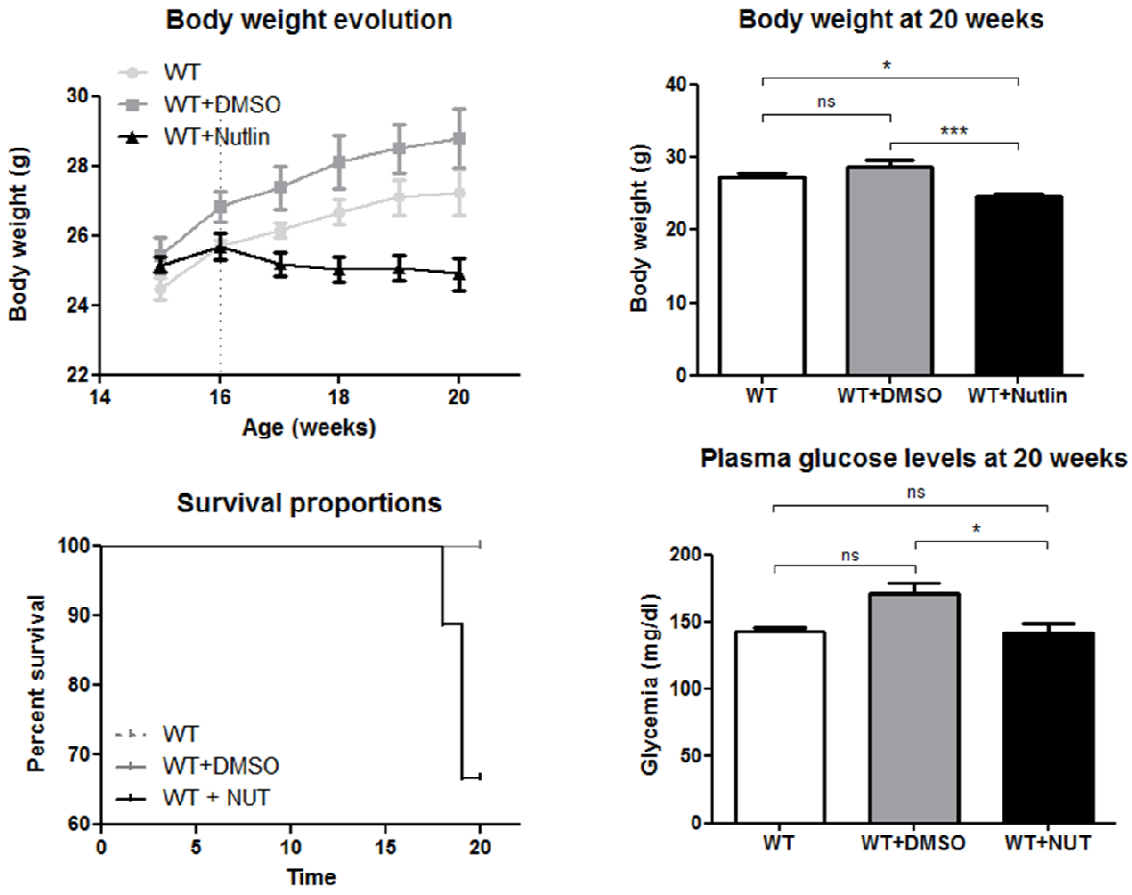

Figure 17 **Body weight, blood glucose levels and survival percentage. A)** Body weight monitoring during treatment with Nutlin-3a. While body weight in vehicle and control mice increased progressively with age, Nutlin-3a-treated mice lost weight from the moment that the treatment was established. **B)** At the end of the study, the body weight of Nutlin-3a-treated mice was significantly lower compared to control and vehicle ($p<0.0005$). **C)** 100% of control (n=3) and vehicle (n=6) mice survived until the end of the study while only 72% of Nutlin-3a-treated mice did (n=11). The difference is however no significant ($p=0.2$). Survival curves were compared with Mantel-Cox test. **D)** Glycaemia at the end of the study was significantly lower in Nutlin-3a-treated mice compared to vehicle ($p<0.05$) but not compared to control mice ($p>0.05$).

4.2.2 *Nutlin-3a induces albuminuria and aggravates renal function*

To further evaluate global renal function, blood urea nitrogen (BUN) levels together with plasma creatinine were evaluated. As shown in figure 18A, plasma creatinine levels were elevated in Nutlin-3a mice (2,8 ± 1,4 mg/dl) compared to vehicle and control mice (1,8 ± 0,7 and 1,7 ± 0,6 mg/dl, respectively; $p > 0,05$), but no statistically significances were observed. However, the BUN levels were significantly increased in Nutlin-3a-treated mice (36,2 ± 3,6 mg/dl) compared to vehicle (23,9 ± 3,2 mg/dl; $p<0,05$) (figure 18B).

Albuminuria, measured as albumin/creatinine ratio, was evaluated in spot urine samples collected before starting the Nutlin-3a treatment, then two weeks after and at the end of the study. As expected, control (0,4 ± 0,16) and vehicle mice (0,3 ± 0,04) displayed a normal range of albumin creatinine ratio, indicating a competent glomerular filtration barrier. However, following Nutlin-3a treatment, albuminuria significantly increased compared to control and vehicle mice three weeks after the start of the treatment (1,66 ± 0,3) and at the end of the study (2,0 ± 0,6; $p<0.05$) (figure 18C and D).

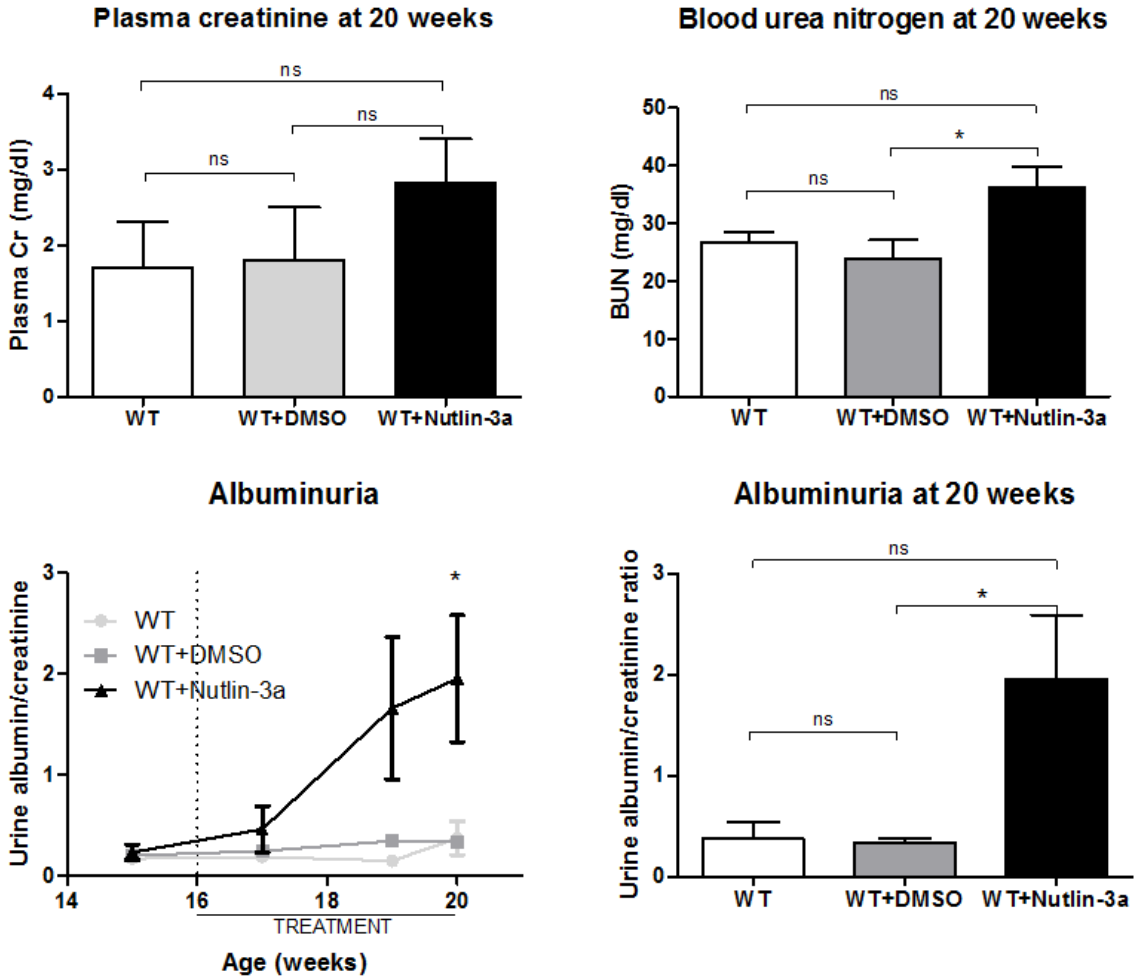

Figure 18 Renal functional parameters. A) Plasma creatinine levels increased in the Nutlin-3a group (2.8 ± 1.4 mg/dl) compared to vehicle and control (1.8 ± 0.7 and 1.7 ± 0.6 mg/dl, respectively), but not significantly. **B)** Blood urea nitrogen (BUN) levels at the end of the study significantly increased in Nutlin-3a-treated group (36.2 ± 3.6 mg/dl) compared to vehicle (23.9 ± 3.2 mg/dl) ($p<0,05$), but not to control (26.7 ± 1.7 mg/dl). **C-D)** Albumin/creatinine ratio increased slightly after the first week of treatment and strikingly at the end of the treatment, being significantly higher compared to vehicle and control ($p<0.05$). Data were analysed with 1-way ANOVA with Tukey's Multiple Comparison Test. n(Control) = 3; n(Vehicle) = 6; n(Nutlin-3a) = 5. *ns = statistically not significant; * = p<0,05.*

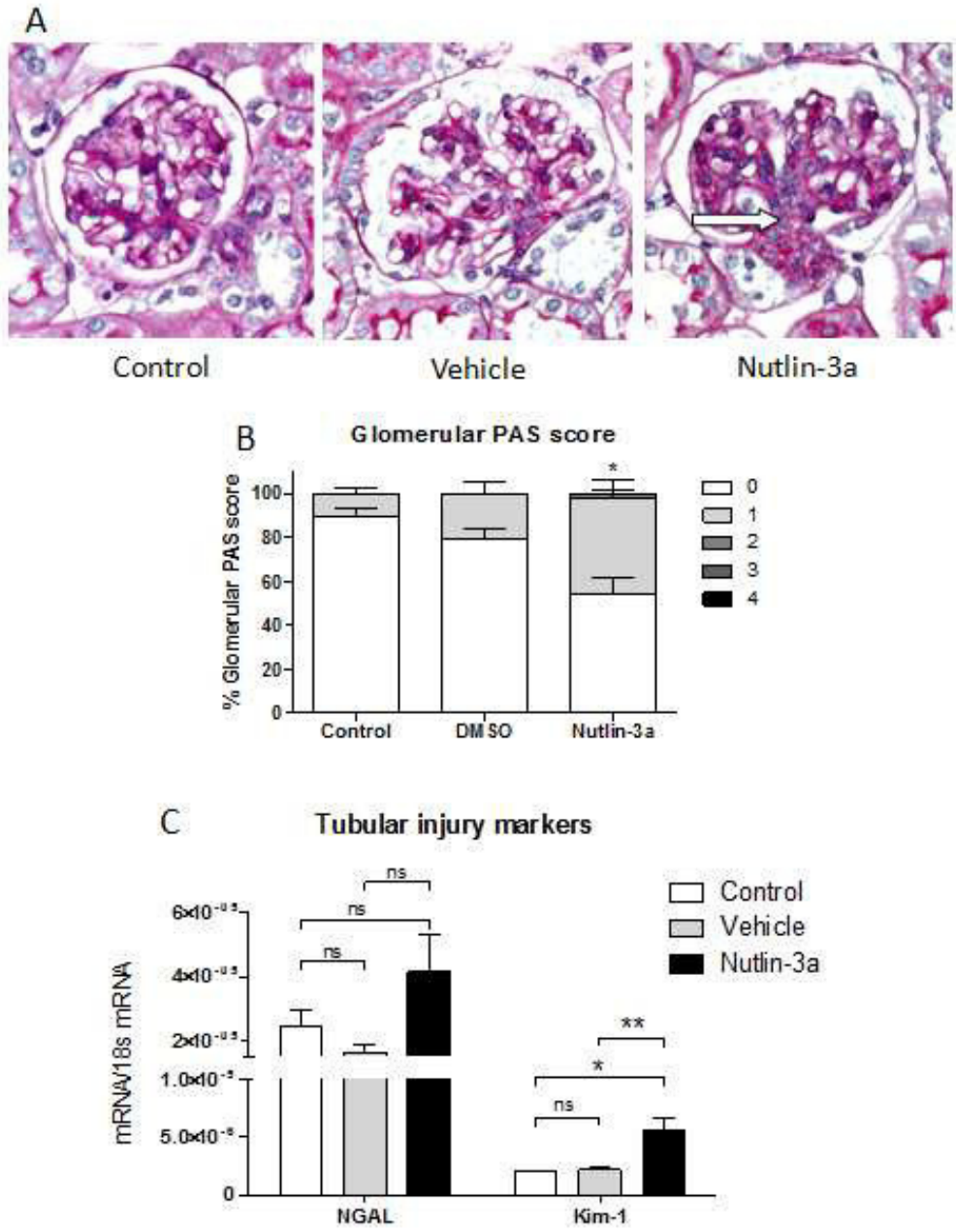

Figure 19 Glomerular PAS score and mRNA expression. A) Representative pictures of each group. Original magnification 40x. (Arrow: mild mesangial expansion). **B)** Semiquantification of glomerular damage in PAS stained slides of paraffin-fixed kidney tissue. While control and vehicle mice have an average of 0.11±0.05 and 0.20±0.13, being 0 considered as normal and 1 as mild mesangial proliferation, Nutlin-3a-treated mice present a significant higher score with an average of 0.50±0.14. **C)** Gene expression of tubular injury markers appear upregulated in Nutlin-3a mice. Data was analysed with 1 way ANOVA with Tukey's Multiple Comparison Test. n(Control) = 3; n(Vehicle) = 6; n(Nutlin-3a) = 5. *ns = statistically not significant; * = p<0,05.*

The functional parameters have shown a significant increase in proteinuria associated with higher BUN levels in the Nutlin-3a-treated group. To analyse the glomerular morphology of the kidneys, kidneys were harvested at the end of the study and embedded in paraffin, and kidney sections stained for Periodic Acid Schiff (PAS). As illustrated in figure 19A and B, glomerular morphology was evaluated using a glomerular score (GS) in a blind manner with the following criteria: 0 for normal glomerulus, 1 for mild mesangial matrix expansion, 2 for moderate to severe mesangial matrix expansion with no sclerotic segments, 3 for severe mesangial matrix expansion, partially closed capillaries and sclerotic segments and 4 for collapsed glomerulus and total sclerosis. A minimum of 20 glomeruli were scored for each mouse. The histopathology of all mice was normal, except for a mild mesangial matrix expansion in the Nutlin-3a-treated group (GS Nutlin-3a group 0.50 ± 0.14 *versus* GS control 0.11 ± 0.05 and GS vehicle 0.20 ± 0.13) compared to vehicle and control ($p<0.005$) (figure 19A). Although no tubular damage was observed via histopathology, total mRNA levels of neutrophil gelatinase-associated lipocalin (NGAL)[1] ($p=0,07$) and kidney injury molecule-1 (Kim-1)[2] ($p<0,05$) were upregulated in kidneys of Nutlin-3a-treated mice compared to the control and vehicle group, indicating an incipient tubular damage (figure 19C).

4.2.3 Nutlin-3a promotes Mdm2 and p53 gene expression and increases p53 protein levels

By binding to the N-terminal p53 binding domain, Nutlin-3a blocks the interaction between Mdm2 and p53. The direct consequence of this blockade is the elevation of p53 levels (Shangary S. 2009, Nicholson 2014), since p53 is stabilized and cannot longer be degraded in the proteasome system. As illustrated in figure 20A and B, a higher expression of p53 in Nutlin-3a-treated mice was observed compared to the vehicle and control group by immunohistochemistry (figure 22A). Further quantification of the percentage of the stained area showed significantly higher p53 levels (% of black area) in the Nutlin-3a-treated group compared to the vehicle and control group (figure 20B). Additionally, mRNA levels of *Mdm2* and *p53* in the kidney of Nutlin3a-treated mice were significantly elevated compared to the vehicle and control group (figure 20C).

[1] Neutrophil gelatinase-associated lipocalin (NGAL) is produced in the distal nephron and its synthesis is up-regulated in response to kidney injury {Devarajan P, 2008 #182}.

[2] Kidney injury molecule-1 (Kim1) is a type 1 transmembrane protein, whose expression is markedly up-regulated in the proximal tubule in the post-ischemic rat kidney (Han WK, 2002).

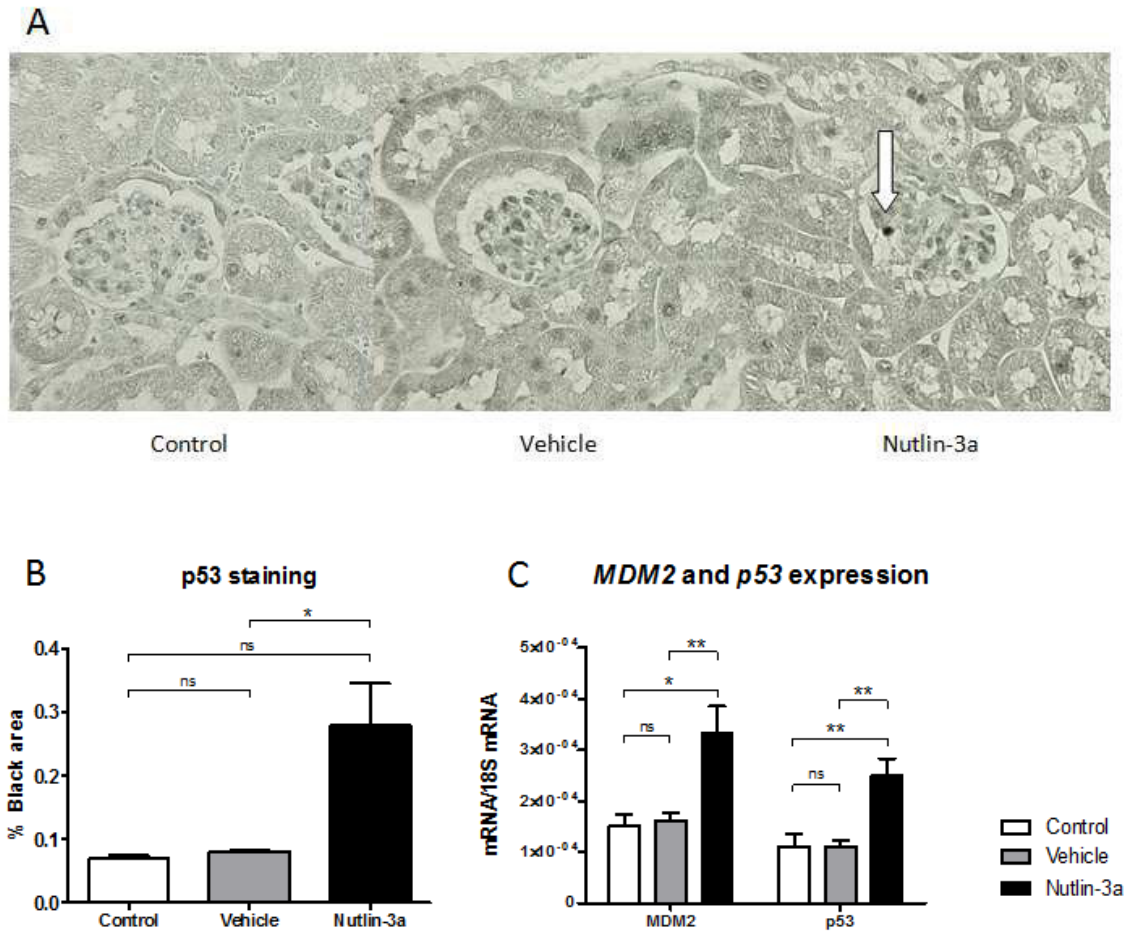

Figure 20 p53 immunostaining and gene expression of MDM2 and p53. **A)** Representative pictures of p53 immunostaining. In the Nutlin-3a group, overexpression of p53 in the periphery of the glomeruli and in some tubular cells was seen, as shown in the picture (white arrow), whereas no p53 staining was observed in vehicle and control treated mice. **B)** Quantification of the percentage of stained area that shows significantly higher p53 levels in the Nutlin-3a group compared to vehicle ($p<0,05$). **C)** Both *Mdm2* and *p53* expression is upregulated in Nutlin-3a-treated mice compared to control and vehicle ($p<0.05$). Data was analysed with 1 way ANOVA with Tukey's Multiple Comparison test. *ns = statistically not significant*; ** = p<0,05; ** = p<0,005.*

The p53 protein functions in part as a transcriptional regulator. Several genes associated with apoptotic cell death and cell cycle are mediated by p53 on a transcriptional level including the pro-apoptotic genes that belong to the Bcl-2 family, Bcl-2-associated X protein (Bax) and p53 upregulated modulator of apoptosis (PUMA), as well as the cell cycle progression regulator p21 (Chène 2003, Kruiswijk F 2015). To investigate whether Nutlin-3a had an effect on the mRNA expression levels of these particular genes, RT-PCR on the kidney was performed. As demonstrated in figure 21, Nutlin-3a treatment induced a significant upregulation of the mRNA levels of *Bcl-2*, *Bax* and *p21* in mice compared to

vehicle. However, no difference was observed in the gene expression levels of *PUMA* between all groups.

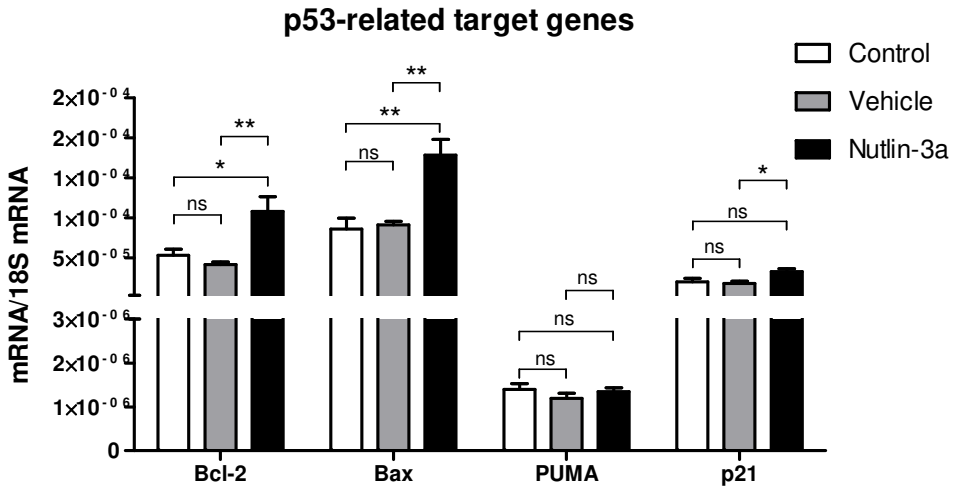

Figure 21. Gene expression of p53-related target genes. The pro-apoptotic genes Bcl-2 and Bax are upregulated in the Nutlin-3a group compared to vehicle and control ($p<0,05$), whereas mRNA levels of PUMA did not differ between groups. The gene expression of cyclin-dependent kinase inhibitor p21 is also upregulated in the Nutlin-3a-treated group compared to vehicle ($p<0,05$), but not to control. Data was analysed with 1-way ANOVA with Tukey's Multiple Comparison Test. *ns = statistically not significant*; ** = p<0,05; ** = p<0,005.*

4.2.4 Nutlin-3a-treated mice display less number of podocytes

In order to investigate the effect of Nutlin-3a on podocytes, kidneys were stained with the classical podocyte markers Wilms tumor protein 1 (Wt-1) and Nephrin. As illustrated in Figure 22A, Wt1, a transcription tumor protein important for the development of the urogenital system that locates in the nuclei of renal cells was marked in red and Nephrin, a structural component of the slit diaphragm, in green. The number of podocytes was counted in at least twenty different glomeruli for each kidney. As seen in figure 22B, while control and vehicle group showed a count of 15,87 ± 0,35 and 13,66 ± 0,68, respectively, Nutlin-3a had a significantly lower number of podocytes (11,55 ± 0,48; $p<0,05$).

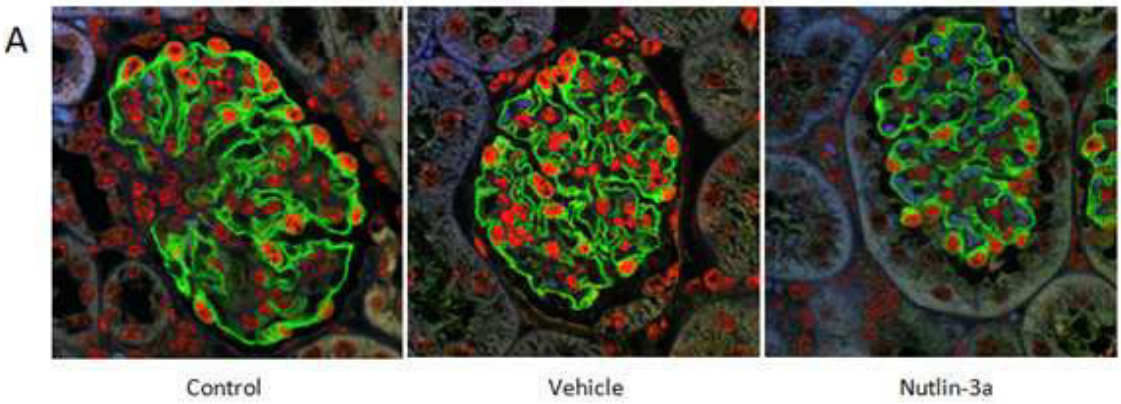

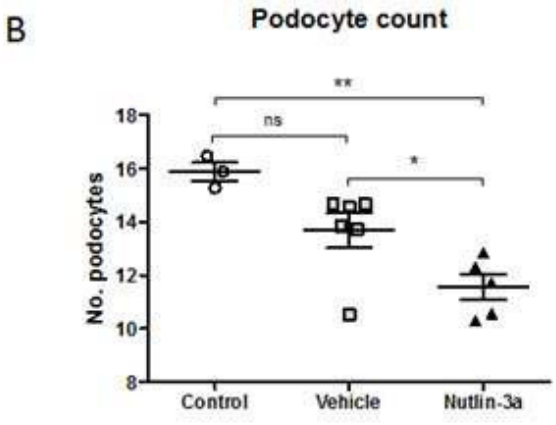

Figure 22. Wt-1/Nephrin staining and podocyte count. **A)** Representative pictures of each group. In red, Wt1; in green, Nephrin. **B)** Quantification. The number of podocytes in the Nutin-3a-treated group was significantly lower (11,55 ± 0,48) than the one in the vehicle group (13,66 ± 0,68) and control group (15,87 ± 0,35). Data was analysed with the average of podocytes per glomerulus in each kidney, involving a minimum of 20 glomeruli for each kidney. 1-way ANOVA with Tukey's Multiple Comparison Test was applied. *ns = statistically not significant*; ** = p<0,05; ** = p<0,005*.

4.2.5 Nutlin-3a promotes inflammation in healthy mice

It has been shown, that inhibition of Mdm2 with Nutlin-3a can also attenuate inflammation through inhibition of the NFκB pathway (Mulay SR 2012, Thomasova D. 2012). Therefore, we analysed the gene expression of the NFκB subunits p50 and p65 to investigate the inhibitory effect of Nutlin-3a. Surprisingly, mRNA levels of both subunits of the nuclear factor NFκB were upregulated ($p<0.05$), as shown in figure 23A. To further look into how inflammation was affected by Nutlin-3a administration, intrarenal mRNA levels of tumor necrosis factor α (TNFα), inducible nitric oxide synthase (iNOS), monocyte chemotactic protein 1 (MCP1 or CCL2), CCL5, interleukin 6 (IL-6), interleukin 12a (IL-12a) and interleukin 1β (IL-1β) were analysed by RT-PCR. As represented in figure 23B, treatment

with Nutlin-3a upregulated significantly the mRNA levels for all inflammatory markers compared to vehicle and control.

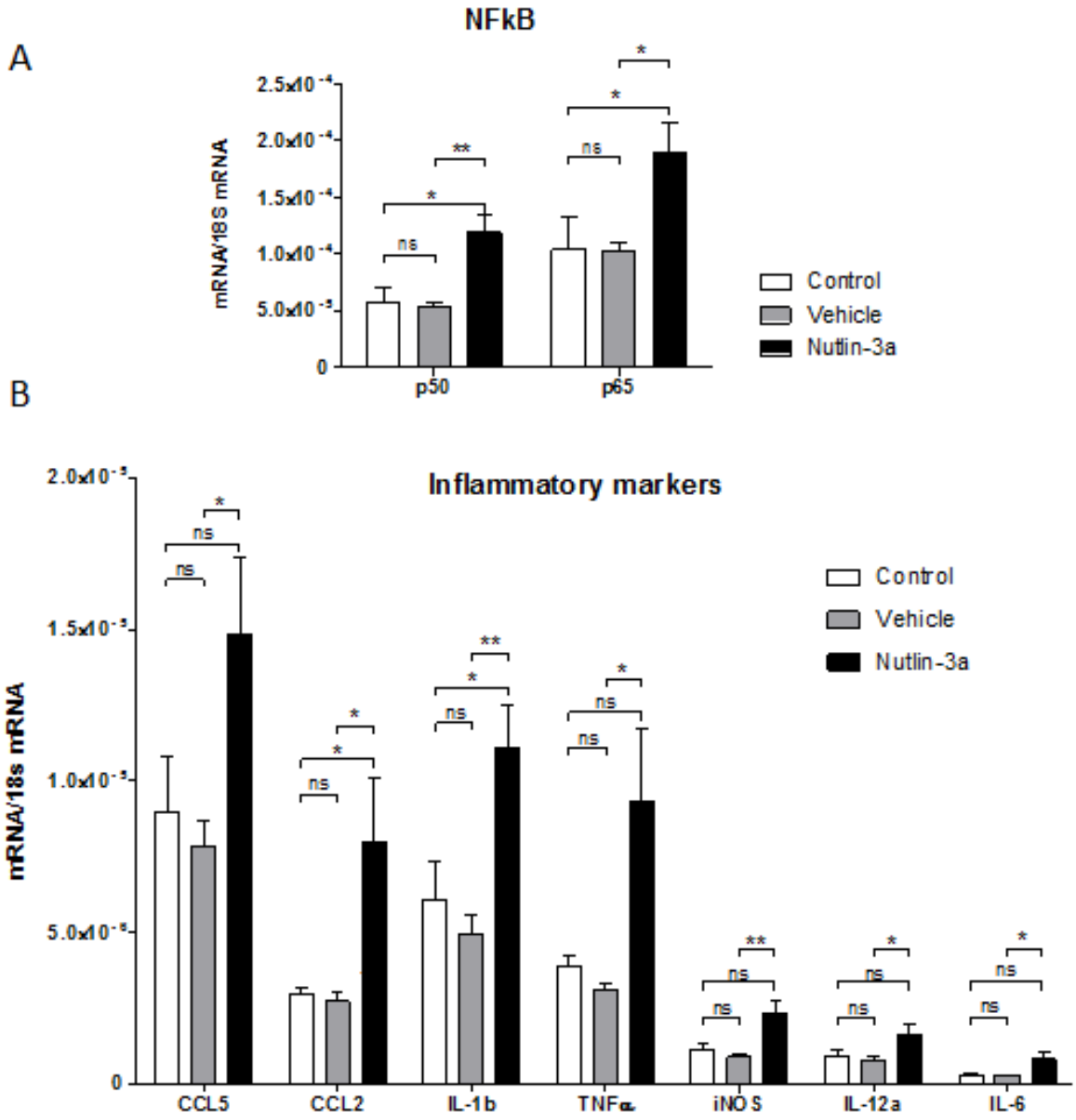

Figure 23 Gene expression of NFκB and inflammatory markers. A) mRNA levels of the NFκB subunits, p50 and p65, appear significantly upregulated in the Nutlin-3a-treated group compared to control and vehicle ($p<0,05$). **B)** mRNA levels of CCL5, CCL2, IL-1β, TNFα, iNOS, IL-12a and IL-6 are significantly upregulated in Nutlin-3a-treated mice compared to vehicle ($p<0.05$). Data was analysed with 1-way ANOVA with Tukey's Multiple Comparison Test. *ns = statistically not significant; * = p<0,05; ** = p<0,005.*

One hallmark of an inflammatory response is the infiltration of macrophages. To investigate whether the previously observed inflammatory response of Nutlin-3a was also inducing the infiltration of macrophages, kidney sections were stained with the Mac2 antibody and the number of macrophages in each glomerulus counted. Consistent with the upregulation of inflammatory markers following Nutin-3a treatment, the number of infiltrating macrophages into the glomerulus was significantly higher in this group compared to vehicle as illustrated by immunohistochemistry in figure 24A. The average number of macrophages counted in the glomeruli was 0,59 ± 0,11, whereas in the Nutlin-3a-treated group an average of 0,98 ± 0,11 was observed (figure 24B).

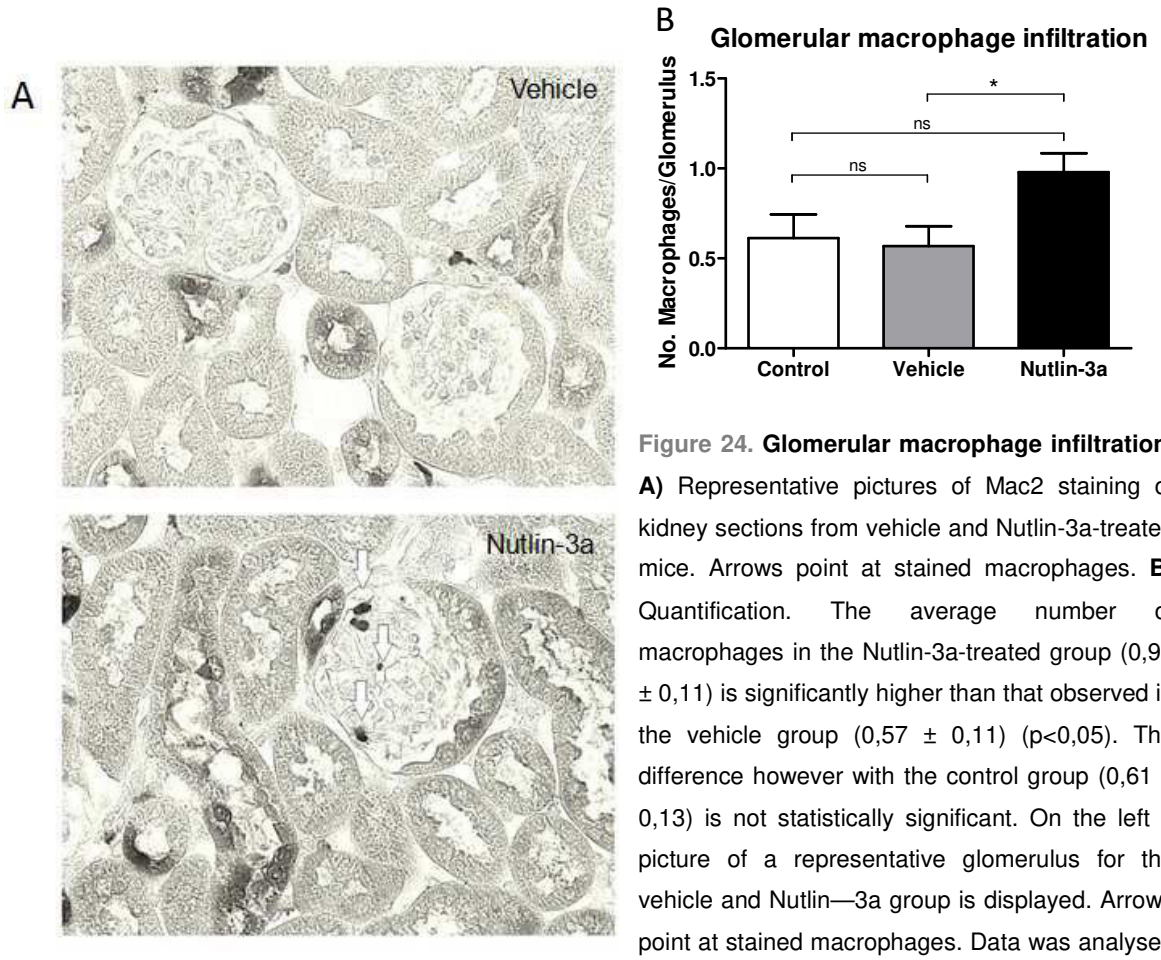

Figure 24. Glomerular macrophage infiltration. **A)** Representative pictures of Mac2 staining of kidney sections from vehicle and Nutlin-3a-treated mice. Arrows point at stained macrophages. **B)** Quantification. The average number of macrophages in the Nutlin-3a-treated group (0,98 ± 0,11) is significantly higher than that observed in the vehicle group (0,57 ± 0,11) ($p<0,05$). The difference however with the control group (0,61 ± 0,13) is not statistically significant. On the left a picture of a representative glomerulus for the vehicle and Nutlin—3a group is displayed. Arrows point at stained macrophages. Data was analysed with 1-way ANOVA with Tukey's Multiple Comparison Test. *ns = statistically not significant; * = p<0,05..*

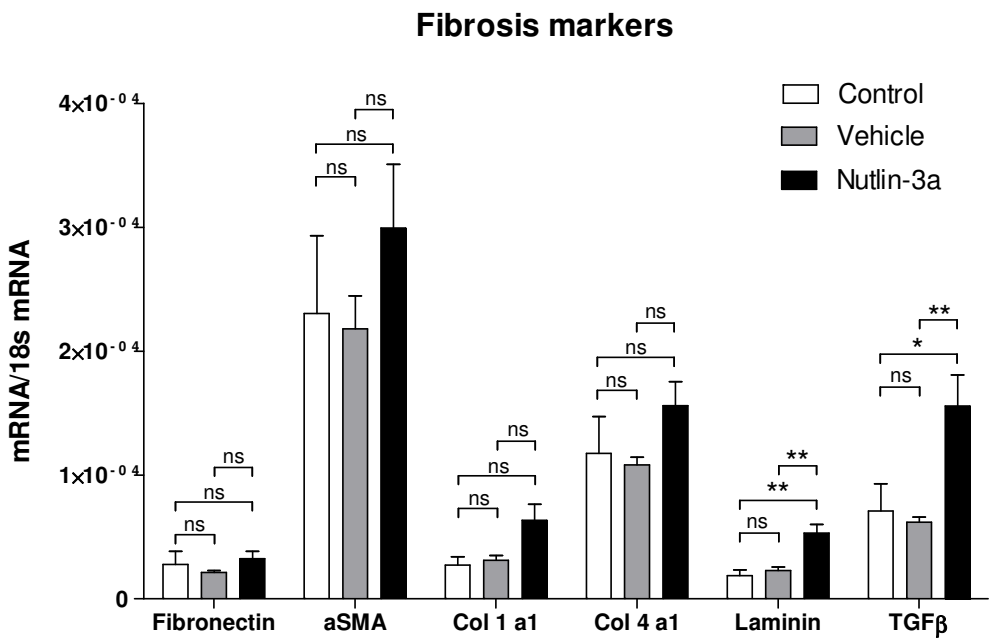

Figure 25. Gene expression of fibrosis markers. There are no significant differences between groups in the gene expression of fibrotic markers such as Fibronectin, aSMA, Col1a1 and Coll4a1. However, expression of Laminin ($p<0,05$) and TGFβ ($p<0,05$) are significantly upregulated compared to vehicle and control. Data was analysed with 1-way ANOVA with Tukey's Multiple Comparison Test. *ns = statistically not significant; * = p<0,05; ** = p<0,005*

The effect of Nutlin-3a on renal fibrosis was also investigated. As shown in figure 25, intrarenal mRNA expression levels of fibronectin, collagen and aSMA did not significantly change in Nutlin-3a-treated mice compared to the vehicle and control group. In contrast, the mRNA expression of the fibrosis markers laminin ($p<0,005$) and TGFβ ($p<0,005$) were significantly upregulated in Nutlin-3a-treated mice, indicating that Nutlin-3a induced renal fibrosis to some extent.

In addition, to look at fibrosis was further using immunohistochemistry, kidney sections were stained with collagen 1 (Col1) and the percentage of the stained area quantified via microscopy and the program Image J. As illustrated in figure 26A, kidney sections from Nutlin-3a-treated mice showed no difference in the staining quality of Col1 (black colour) compared to the vehicle and control group. That was further quantified by determining the percentage of the black stained area between the groups ($p=0,52$) (figure 26B).

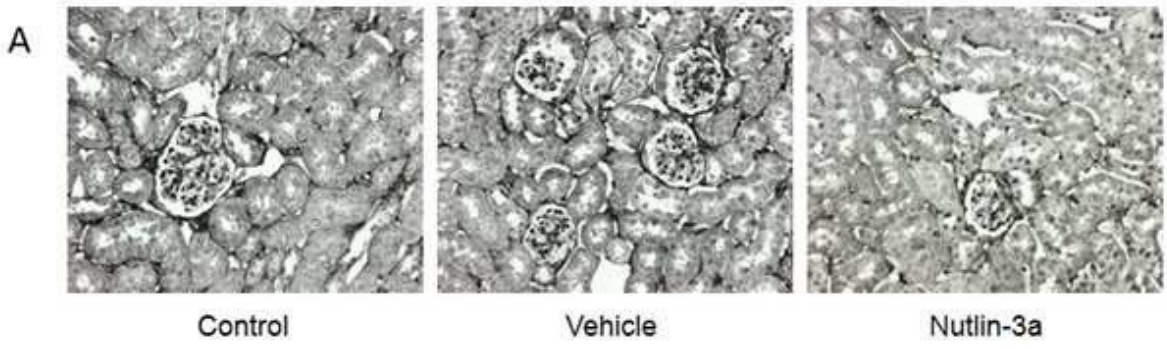

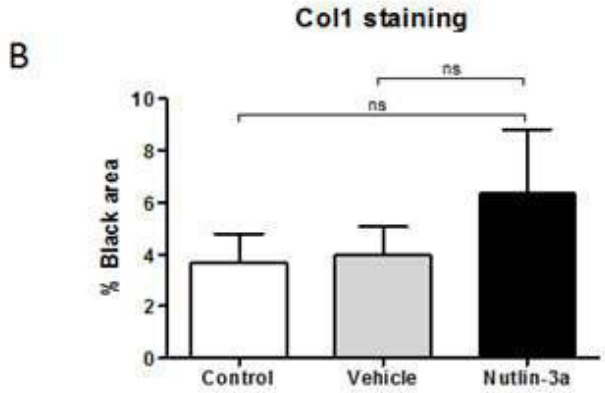

Figure 26. Collagen 1 immunohistochemistry. **A)** Representative pictures of collagen 1 staining for each group. No significant differences were observed between groups. Pictures were analysed with Image J. **B)** Quantification of the percentage of stained area. Data was analyzed using 1 way ANOVA and Tukey's Multiple Comparison Test. *ns = statistically not significant.*

4.3 Pharmacological blockade of Mdm2 with Nutlin-3a in db/db mice

4.3.1 Nutlin-3a does not affect body weight, glycaemia or mortality in db/db mice

The effects of Nutlin-3a treatment were also investigated in a diabetic nephropathy mouse model. For this, mice with a mutation in the leptin receptor (db/db) were used. To aggravate the nephropathy complications, db/db mice were fed with high fat diet and underwent a uninephrectomy (see section *3.2.1 Animal studies, Study design*) and after recovery from the surgery were randomized into two groups: one was injected with 20mg/kg Nutlin-3a for four weeks every two days and the second group was injected with vehicle for four weeks every two days.

Mice survival rate was determined throughout the whole experiment; whereby; deaths that occurred due to surgery or complications including infections were not counted because the mice at that early time point had not been yet randomized. As shown in figure 27A, the mortality rate was very high in both groups, as demonstrated by a decrease in the percentage of the survival rate. At the end of the study after 20 weeks, there was no significant difference observed between the Nutlin-3a-treated group (37,5%) and the vehicle group (57,1%) with a p = 0,2.

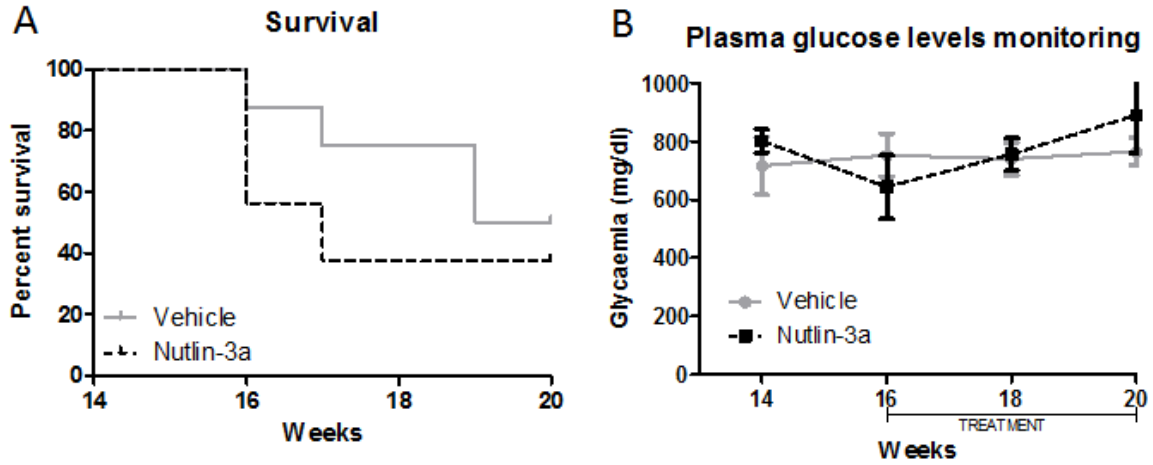

Figure 27. **Percentage of survival and glycaemia**. **A)** In both groups, mortality during the treatment was very high but no significant differences were seen between survival rates. **B)** Plasma glucose levels were steadily high in both groups, and no significant difference was observed between groups. S*urvival curves were compared with Mantel Cox Test and glycaemia was analysed with 2-Way-ANOVA.*

Glycaemia was monitored along the treatment with either Nutlin-3a or placebo in db/db mice. Throughout the experiment, there was no difference observed in glycaemia, as indicated by the plasma glucose levels after 20 weeks: 669,5 ± 142,2 mg/ml in Nutlin-3a-treated mice and 765,0 ± 46,8 mg/ml in vehicle (figure 27B).

Additionally, uninephrectomized db/db mice were either fed a control diet, a normal chow diet containing 4,5% fat, or a high fat diet containing 10% fat (9% pork lard and 1% soyabean oil) to aggravate the complications of diabetic nephropathy and to mimic closer the human features of T2D. In order to investigate whether the high fat diet had an influence on the blood lipid levels, blood was collected from uninephrectomized db/db mice that were fed a high fat or normal chow diet, and triacylglyceridemia and cholesterolemia were analysed after 12, 16 and 20 weeks.

As illustrated in figure 28A, blood levels of triacylglycerides did not change in high fat diet fed mice compared to a normal diet, except at the beginning, at week 12, when paradoxically triacylglyceride levels appeared significantly higher in mice fed with normal chow diet than in mice fed with high fat diet (157,4 ± 2,79 vs 201,2 ± 8,09 g/dl at 12 weeks, $p<0,5$; 145,7 ± 18,28 vs 161,9 ± 14,87 mg/dl at 16 weeks, $p=0,51$; 444,2 ± 42,87 vs 436,7 ± 55,19 mg/dl at 20 weeks, $p=0,92$). In contrast, cholesterol levels significantly increased in mice fed with a high fat diet compared to mice fed with a normal chow diet (176,5 ± 11,74 vs 122,7 ± 6,55mg/dl at 12 weeks, $p<0,005$, 133,4 ± 8,79 vs 86,12 ± 5,67 mg/dl at 16 weeks, $p<0,0005$, 192,2 ± 28,09 vs. 106,7 ± 10,48 mg/dl at 20 weeks, $p<0,05$), as seen in figure 28B.

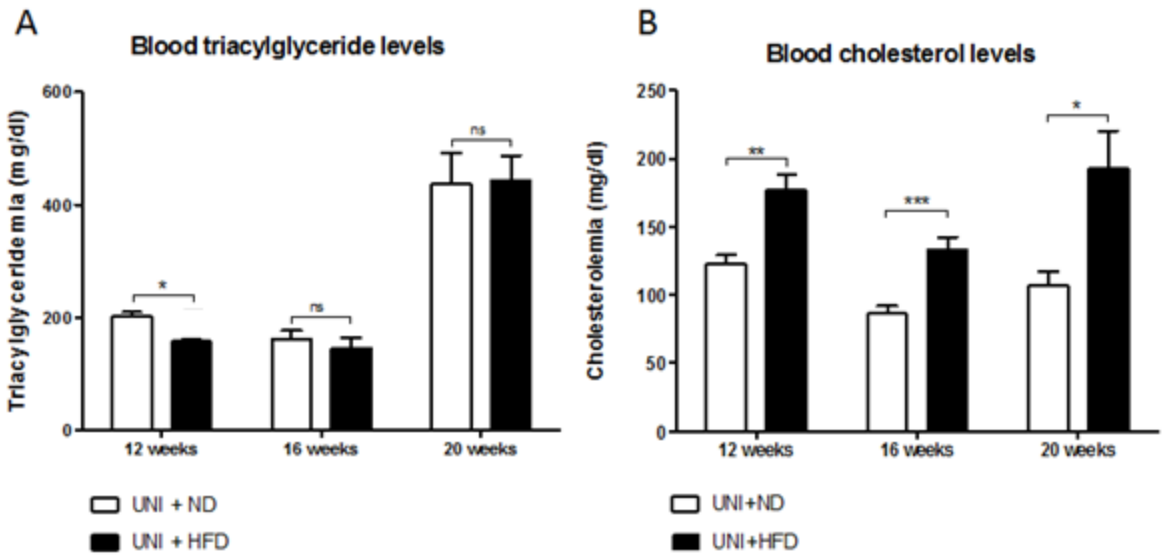

Figure 28 Cholesterolemia and triacylgliceridemia. A high fat diet (10% fat content) was employed in the study, to emulate closer the human environmental factors of diabetes type II. As a control, blood of diabetic mice with the same background and age, which also underwent uninephrectomy, was concurrently analysed with a colorimetric assay. **A)** Triacylgliceride levels increased significantly over time (p<0,0001) but were not affected by a diet richer in fat content (p=0,36); however, **B)** cholesterolemia was significantly higher in these mice than in those fed with a normal diet (p<0,0001) . Data were analysed with 2-Way-ANOVA. *UNI = uninephrectomized; ND = normal diet (4,5% fat content); HFD = high fat diet (10% fat content); ns = statistically not significant; * = p<0,05; ** = p<0,005; *** = p<0,0005.*

4.3.2 Treatment with Nutlin-3a in diabetic mice aggravates renal function

To evaluate global renal function, blood urea nitrogen (BUN) levels and plasma creatinine levels were measured in plasma samples from uninephrectomized db/db mice that were on a high fat diet with or without Nutlin-3a treatment. As shown in figure 29A, plasma creatinine levels were higher but not statistically significant in Nutlin-3a-treated db/db mice (2.10 ± 0.23 mg/dl) compared to the vehicle group (1.33 ± 0.06 mg/dl, p=0,09). Plasma BUN levels were determined after 15 weeks prior to Nutlin-3a treatment and after 17 and 20 weeks following treatment with Nutlin-3a (figure 29B). Prior to Nutlin-3a treatment, no difference in the BUN level was observed between groups, whereas treatment with Nutlin-3a increased the BUN levels in Nutlin-3a-treated mice compared to the vehicle group after 20 weeks (vehicle group 39,5 ± 7,8 mg/dl vs. Nutlin-3a group 69,1 ± 12,4 mg/dl, p<0,01, n=3). After 17 weeks, although BUN levels also increased, the difference between two groups was not statistically significant (vehicle-group 48,5 ± 2,8 mg/dl vs. Nutlin-3a group 55,5 ± 1,2 mg/dl, p>0,05 n=7).

To investigate the glomerular function, albuminuria was assessed by measuring the albumin/creatinine ratio. This was evaluated in spot urine samples collected prior to the treatment with Nutlin-3a, two weeks after and at the end of the study (20 weeks). As depicted in figure 29C, albuminuria increased as the disease progressed until week 17 and decreased after. This trend could be explained due to the high mortality rate at the end of the study, resulting in a survival bias. After 20 weeks, the difference in albuminuria between vehicle and Nutlin-3a-treated groups was not statistically significant (albumin/creatinine ratio in vehicle 5,6 ± 1,1 vs. albumin/creatinine ratio in Nutlin-3a-treated 7,1 ± 1,2, p=0,3) (figure 29D).

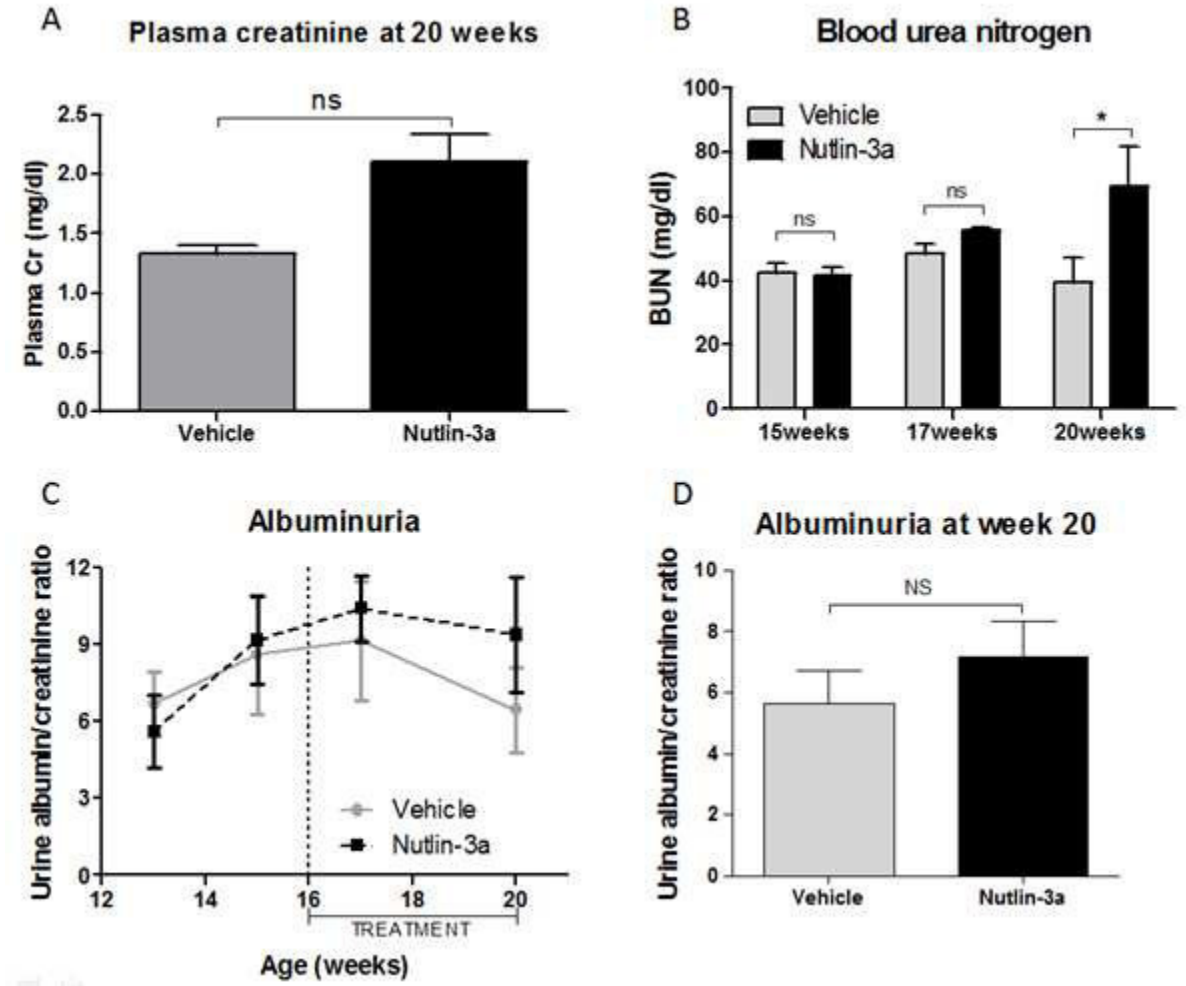

Figure 29. Renal functional parameters. **A)** Plasma creatinine levels are increased in Nutlin-3a group (2.10 ± 0.23 mg/dl) compared to vehicle (1.33 ± 0.06 mg/dl), but not significantly (p=0,09). **B)** Blood urea nitrogen (BUN) levels increased overtime, being significantly higher after four weeks of treatment with Nutlin-3a (p<0,05).. **C-D)** Albuminuria as means of albumin/creatinine ratio appeared not significantly different between groups. Data was analysed with Man Whitney Test for A and D, and with 2-Way-ANOVA for B. n(Vehicle) = 4, n(Nutlin-3a) = 6. *ns = statistically not significant; * = p<0,05*

While the renal functional parameters showed a trend towards a worse outcome in the Nutlin-3a-treated db/db mice, the renal histological architecture presented only mild glomerular sclerosis in this group compared to the vehicle group (figure 30A and B). The glomerular structure was examined in periodic-acid Schiff (PAS) stained kidney sections and scored using the following criteria: 0 for normal glomerulus, 1 for mild mesangial expansion, 2 for moderate to severe mesangial proliferation with no sclerotic segments, 3 for severe mesangial proliferation, partially closed capillaries and sclerotic segments and 4 for collapsed glomerulus and total sclerosis. A minimum of 20 glomeruli were scored for each mouse and the evaluation was made blindly.

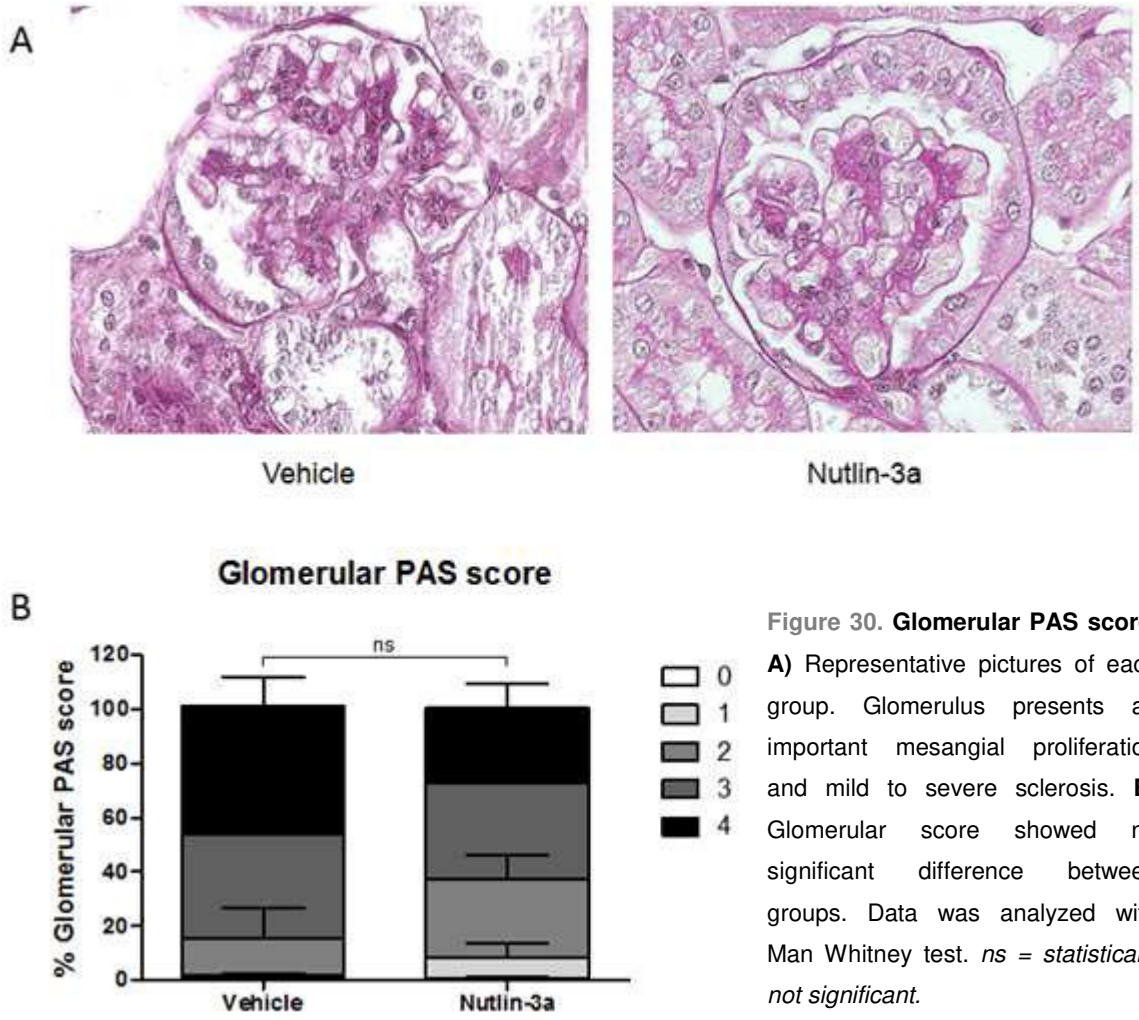

Figure 30. **Glomerular PAS score**. **A)** Representative pictures of each group. Glomerulus presents an important mesangial proliferation and mild to severe sclerosis. **B)** Glomerular score showed no significant difference between groups. Data was analyzed with Man Whitney test. *ns = statistically not significant.*

4.3.3 Expression of p53 in db/db mice after Nutlin-3a-treatment

As seen in previous studies and in healthy mice, p53 levels were expected to increase after administration of Nutlin-3a by blocking proteasomal degradation. However, in diabetic mice immunohistochemistry did not show a significant increase in p53 in terms of percentage of p53 stained area (figure 31A and B). Besides, intrarenal gene expression of *p53* showed a significant downregulation in Nutlin-3a-treated mice compared to vehicle (figure 31C), as opposed to what was observed in healthy mice (see section *4.2.3 Nutlin-3a promotes Mdm2 and p53 gene expression and increases p53 protein levels*). Consistently, Mdm2 mRNA levels were also lower in Nutlin-3a-treated mice compared to vehicle (figure 31C).

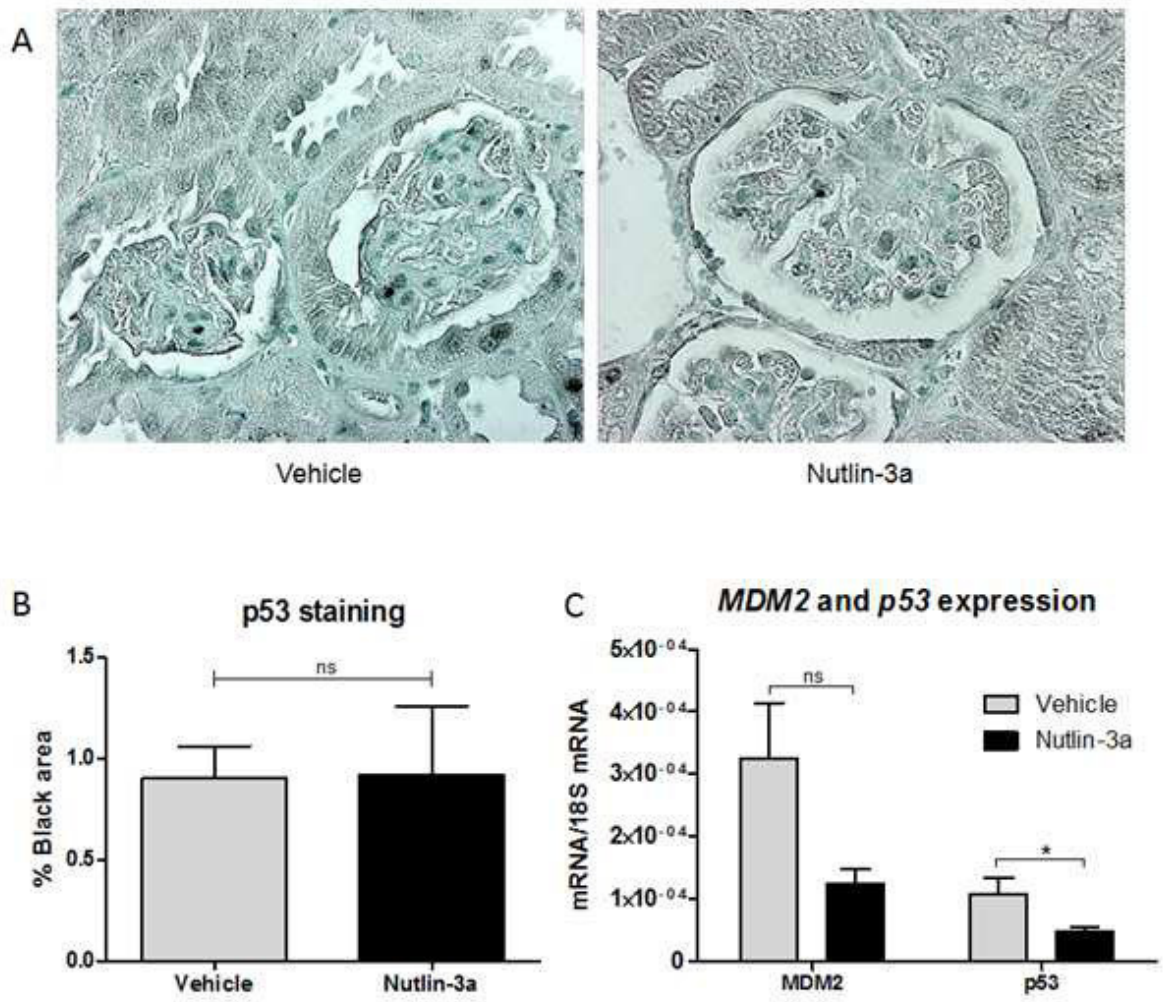

Figure 31. p53 immunostaining and gene expression of Mdm2 and p53. **A)** Representative pictures of p53 immunostaining. No significant differences were seen between groups. **B)** Quantification of the percentage of stained area that shows no significant differences between the Nutlin-3a group and vehicle group. **C)** p53 gene expression is downregulated in Nutlin-3a-treated mice compared to vehicle ($p<0.05$), without being significant for Mdm2 mRNA levels. Data was analysed with Man Whitney test. *ns = statistically not significant*; ** = p<0,05.*

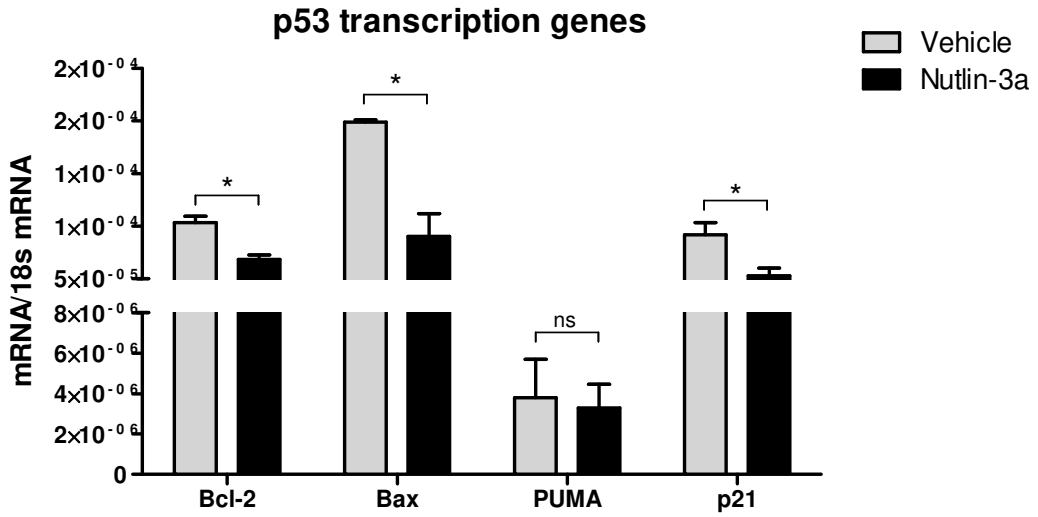

Figure 32. Gene expression of p53-tanscription dependent genes. The proapoptotic genes Bcl-2 and Bax are downregulated in the Nutlin-3a-treated group compared to vehicle ($p<0,05$) whereas mRNA levels of PUMA show no difference between groups. The gene expression of cyclin-dependent kinase inhibitor p21 is also downregulated in the Nutlin-3a-treated group compared to vehicle ($p<0,05$). Data was analysed with Mann Whitney Test. *ns = statistically not significant*; ** = p<0,05..*

Next, the expression of genes, whose transcription depends on p53, was analysed to further evaluate the impact of Nutlin-3a treatment on a transcriptional level. As shown in figure 32, the proapoptotic genes *Bax* and *Bcl-2* and the cyclin-dependent kinase inhibitor *p21* appeared consistently downregulated in the Nutlin-3a-treated group compared to vehicle, whereas *PUMA* showed no significant difference.

4.3.4 Nutlin-3a-treated mice display less number of podocytes and a downregulation of podocyte marker gene expression

In healthy mice, treatment with Nutlin-3a resulted in the damage of the glomerular filtration barrier in terms of a significant increase in proteinuria and lower podocyte count. In order to see whether Nutin-3a had the same effect in db/db mice with diabetic nephropathy, kidneys were stained for Wt1 (in red) and Nephrin (in green) (figure 33A) and the number of podocytes was counted in twenty different glomeruli for each kidney. As demonstrated in figure 33B the average of podocytes per glomerulus in Nutlin-3a-treated mice was significantly lower (5,84 ± 0,22) compared to vehicle-treated mice (6,59 ± 0,07).

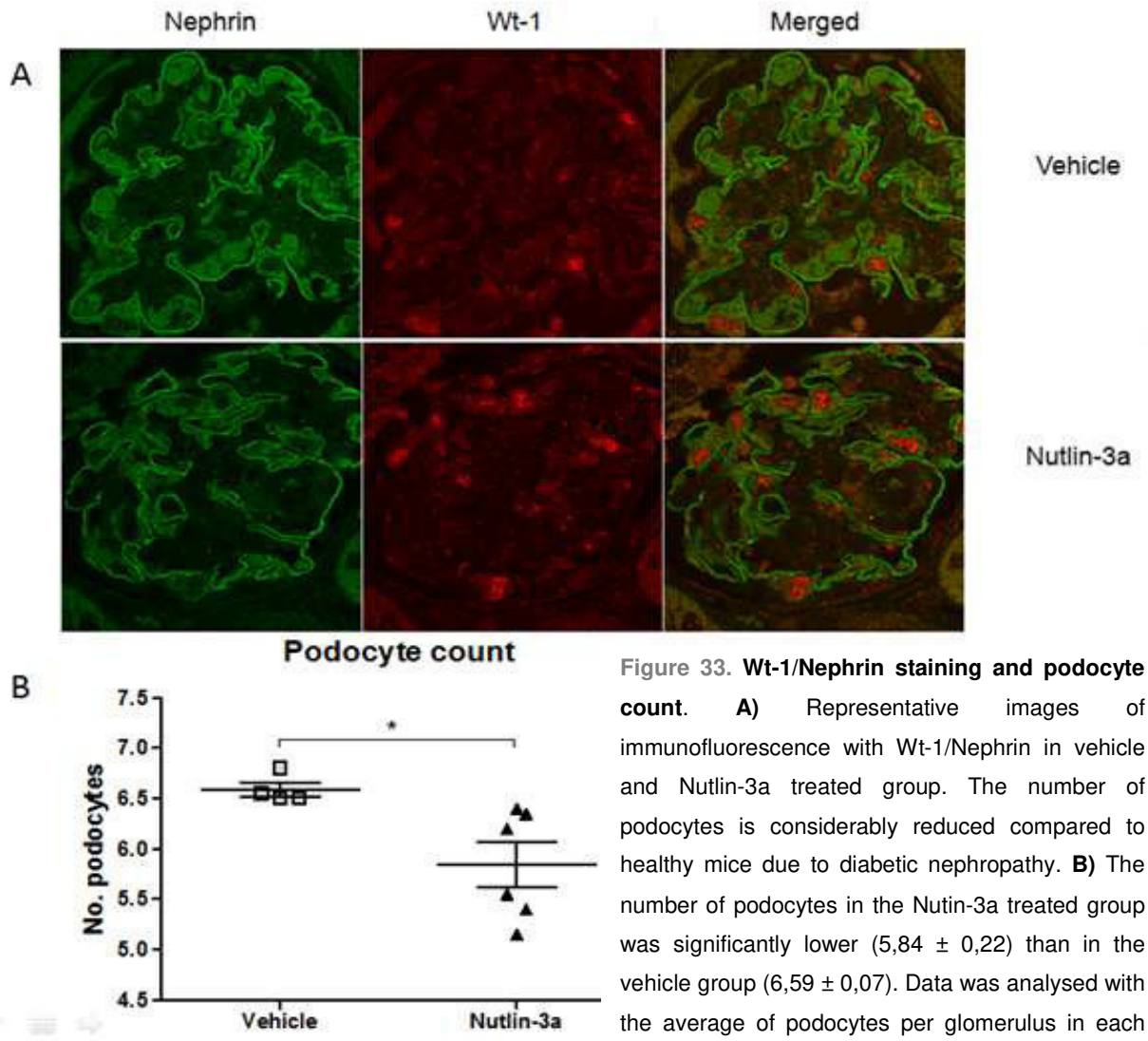

Figure 33. Wt-1/Nephrin staining and podocyte count. **A)** Representative images of immunofluorescence with Wt-1/Nephrin in vehicle and Nutlin-3a treated group. The number of podocytes is considerably reduced compared to healthy mice due to diabetic nephropathy. **B)** The number of podocytes in the Nutin-3a treated group was significantly lower (5,84 ± 0,22) than in the vehicle group (6,59 ± 0,07). Data was analysed with the average of podocytes per glomerulus in each kidney, counting a minimum of 20 glomerules for each kidney. Data was analysed with Man Whitney test. ** = p<0,05.*

To further evaluate the effect of Nutlin-3a upon podocytes in diabetic mice, mRNA levels of podocyte markers were quantified using RT-PCR. As represented in figure 34, mRNA levels of Wt-1, podocalyxin, podocin, synaptopodin, nephrin and CD2AP were significantly reduced in Nutlin-3a-treated mice compared to vehicle ($p<0,05$).

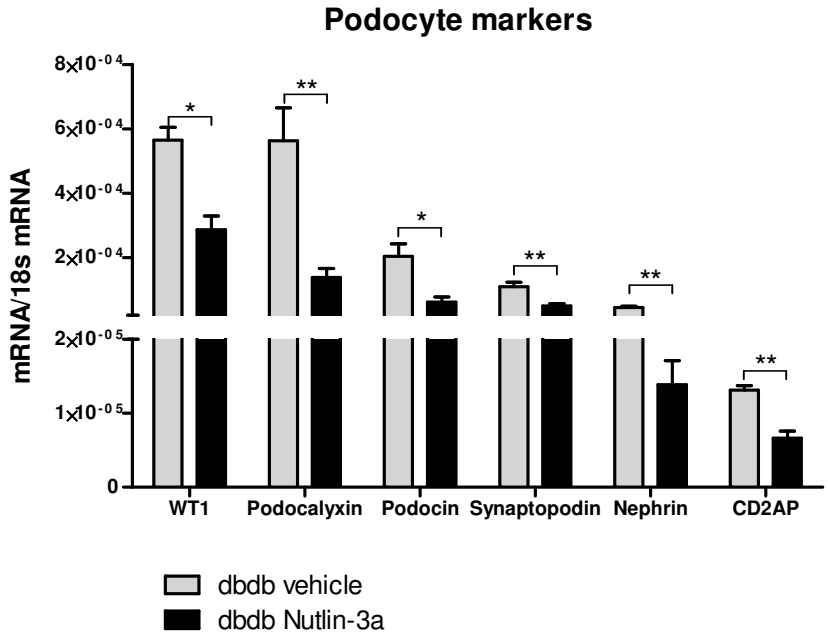

Figure 34 Gene expression of podocyte markers. mRNA levels of podocyte markers, such as nephrin, Wt-1, synaptopodin, podocin, Podocalyxin, and CD2AP are downregulated in the Nutlin-3a group compared to control and vehicle (p<0,05). Data was analysed with Mann Whitney Test. *ns = statitstically not significant*; ** = p<0,05; ** = p<0,01*.

4.3.5 Nutlin-3a attenuates renal inflammation and fibrosis diabetic mice

Mulay and colleagues have shown that Nutlin-3a has an anti-inflammatory potential associated with inhibiting the p53-independent regulatory role of Mdm2 upon NFκB activation (Mulay SR 2012). Within this study, however, Nutlin-3a treatment in healthy mice displayed the opposite effect, whereby the number of infiltrating glomerular macrophages was higher and the intrarenal inflammatory markers were upregulated in Nutlin-3a-treated mice. In order to elucidate the anti- or proinflammatory role of Nutlin-3a in diabetic mice, mRNA levels of inflammatory markers were screened in renal tissue of diabetic mice treated with Nutlin-3a or vehicle. Intrarenal mRNA expression of the NFkB subunits p50 and p65 decreased in the Nutlin-3a-treated group compared to vehicle (p= 0,07 and 0,11, respectively) (figure 35C). The intrarenal mRNA expression levels of the inflammatory markers TNFα, CCL2, CCL5 and iNOS decreased following Nutlin-3a treatment, whereas the other inflammatory markers such as IL-1β, IL-6 and IL-12a did not change (figure 35D). Macrophage infiltration was significantly lower in Nutlin-3a-treated-mice than in the placebo group (figure 35A and B). This indicated that treatment with Nutlin-3a may exert anti-inflammatory properties in db/db mice, consistent with the previous study done by Mulay et. al. (Mulay SR 2012).

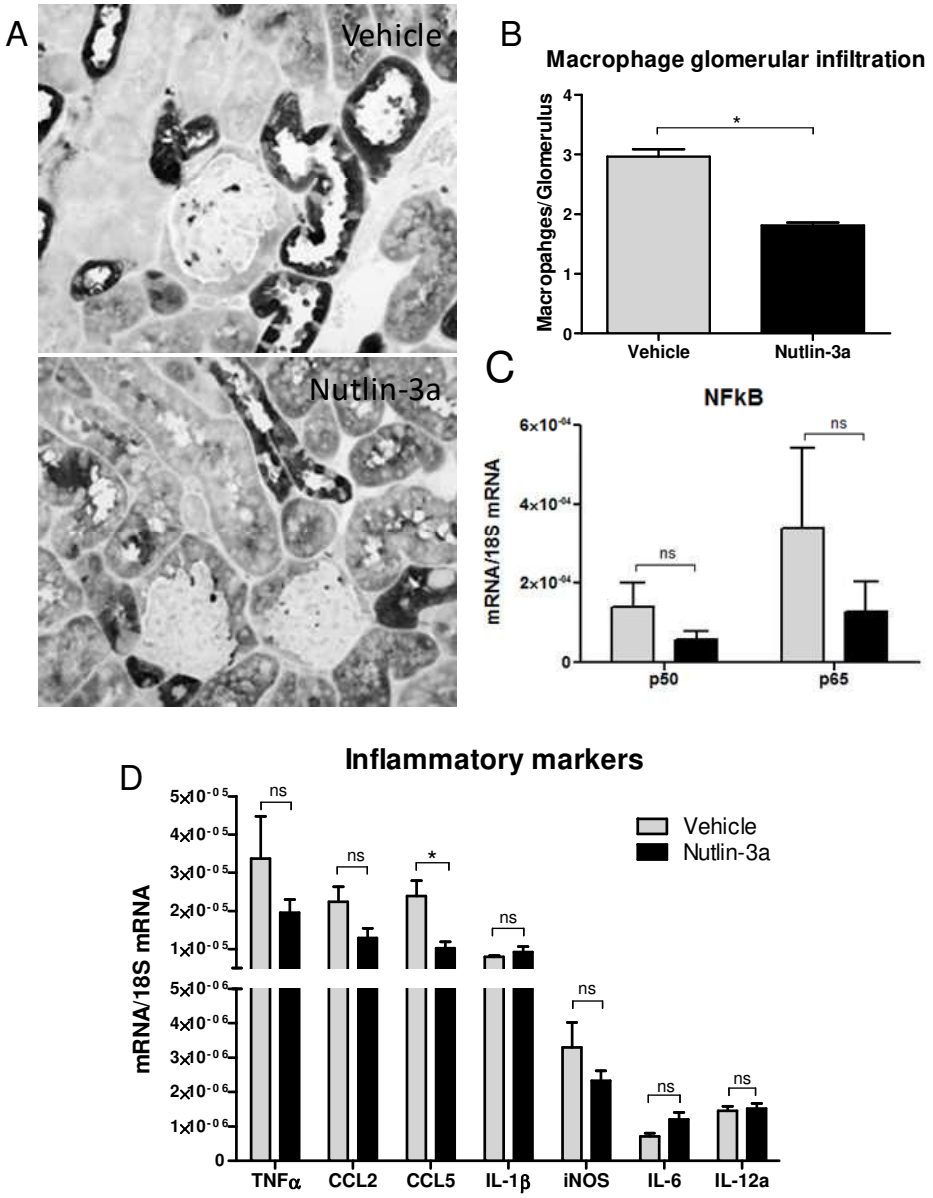

Figure 35. Glomerular macrophage infiltration and gene expression of NFκB and inflammatory markers. **A)** Representative pictures of Mac2 staining for each group. **B)** Quantification of number of macrophages per glomerulus in each group. A minimum of 20 glomerules were scored for each kidney. While vehicle group presents an average of 2,97 ± 0,12 macrophages per glomerulus, Nutlin-3a-treated group displayed 1,81 ± 0,05 ($p<0,05$). **C)** mRNA levels of the NFκB subunits p50 and p65 are downregulated in the Nutlin-3a-treated group compared to vehicle; difference is not statistically significant ($p=0,07$ and $p=0,11$, respectively). **D)** mRNA levels of inflammatory markers are not significantly reduced in the Nutlin-3a group, except for CCL5 ($p<0.05$). Data was with Mann Whitney Test. N(Vehicle) = 4; n(Nutlin-3a)=6. *ns = statistically not significant; * = p<0,05.*

In addition, renal fibrosis in diabetic mice treated with Nutlin-3a or vehicle was analysed regarding the mRNA levels of fibrotic markers and collagen 1 expression. Immunohistochemistry of kidney sections for collagen 1 (figure 36A) showed a significant

lower deposition in Nutlin-3a-treated mice than in vehicle (p<0,005) in terms of percentage of stained area (figure 36B). Intrarenal mRNA levels of fibronectin, laminin, transforming growth factor beta (TGFβ), aSMA, collagen 1 subunit a1 and collagen 4 subunit a1 were significanly downregulated in Nutlin-3a-treated mice compared to the vehicle group (p<0,05) (figure 36C).

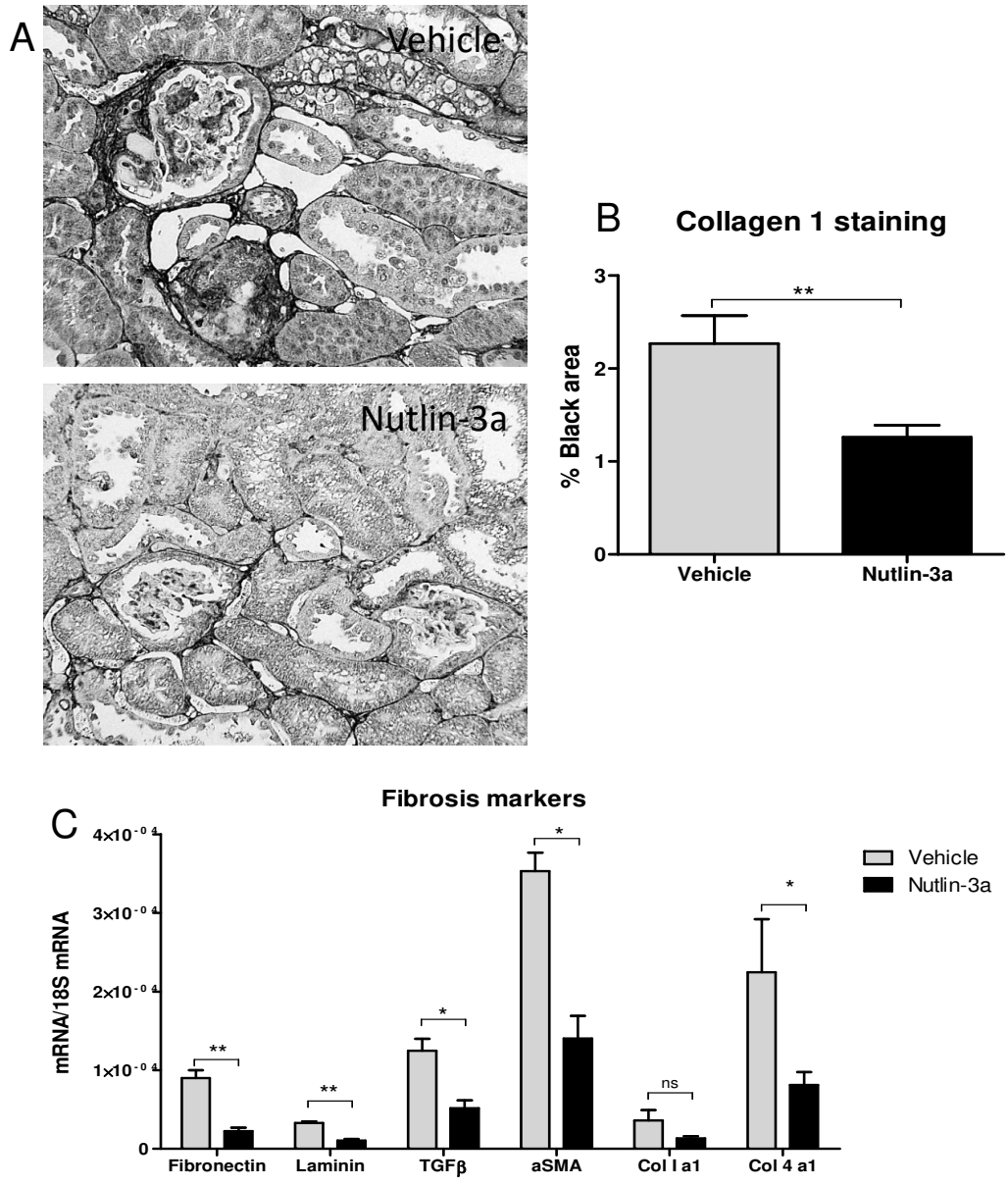

Figure 36. Collagen 1 staining and gene expression of fibrosis markers. **A)** Immunohistochemistry. Representative pictures of collagen 1 staining of kidney sections from db/db mice treated with Nutlin-3a or vehicle. **B)** Quantification of the stained area. Nutlin-3a mice displayed a significant lower expression of collagen 1 than the vehicle group (p<0,005). **C)** mRNA levels of fibronection, laminin, TGFβ, aSMA and collagen 4 a1 are downregulated in the Nutlin-3a-treated group compared to vehicle (p<0,05). Collagen 1, however, does not reach statistical significance. Data was analysed with Mann Whitney Test. *ns = statistically not significant; * = p<0,05; ** = p<0,01.*

5. DISCUSSION

5.1 Mdm2 blockade with Nutlin-3a damages healthy renal tissue

In resting cells, the right balance between Mdm2 and p53 is crucial to maintain proliferation in a controlled manner. In the kidney, where Mdm2 is mainly expressed in epithelial tubular cells and podocytes, deletion of Mdm2 in resting podocytes showed p53-overexpression dependent cell death (podoptosis) *in vitro* and the development of albuminuria and glomerulosclerosis in an *in vivo* model (Thomasova D. 2015). Similarly, tubular cells specific Mdm2 deletion in a mouse model manifested a rapid development of CKD (data not yet published). Hence, we hypothesized that inhibition of Mdm2 with Nutlin-3a damages renal function by promoting podoptosis in podocytes and tubular cells.

To test our hypothesis, cultured mouse podocytes and mouse tubular cells were stimulated with Nultin-3a in three different doses and the viability and cytotoxicity in two different time points was then measured. As hypothesized, the culture of immortalized mouse podocytes and mouse tubular cells with Nutlin-3a prompted cell death and decreased viability in a dose-dependent manner, showing that the blockade of Mdm2 with the drug can certainly affect healthy cells, as it has been previously shown in siRNA experiments (Thomasova D. 2015). This result seems to contradict the work of Jiang et al., where they showed that the administration of Nutlin-3 was not toxic to normal cultured tubular cells. However, Nutlin-3 represents a mixture of the active enantiomer 3a and the inactive 3b (Vassilev 2004); that means that the employed concentrations of Nutlin-3 might not have been sufficient to reach the efficiency of the full active Nutlin-3a. Furthermore, toxicity was evaluated in terms of apoptosis, assessing cell morphology and caspase activation (Jiang 2007). Thus, the lack of caspase activity rather than proving no toxicity, further supports an alternative caspase-independent cell death, i.e. podoptosis.

In light of the results *in vitro*, systemic injections of Nutlin-3a during one month were given to healthy mice to monitor renal function. Although the renal function, in terms of plasma creatinine levels, was not significantly affected, blood urea nitrogen levels were significantly higher and the urine albumin/creatinine ratio increased progressively in the treated group reaching significance at the end of the study. Consistently, the number of podocytes was significantly lower in this group.

In addition, body weight was observed to decrease in contrast to control groups, which progressively increased weight with age. This observation was already made by Mendrysa *et al.*, who generated mice that possessed a hypomorphic allele expressing approximately 30% of the total Mdm2 levels. These mice not only had decreased body weight, like in the present study, but displayed defects in haematopoiesis and were more radiosensitive than normal mice (Mendrysa SM 2003). This translates a lower capacity to respond to injury and to proliferate. Hence, small insults in renal tissue (and other tissues as well) might affect the kidney in a greater way when Mdm2 is blocked than under normal conditions. In fact, mice treated with Nutlin-3a not only manifested an incipient defect in the glomerular filtration barrier, but presented upregulation of tubular injury markers, inflammatory markers and increased glomerular macrophage infiltration. In the previous studies by Mulay *et al.*, Nutlin-3a attenuated inflammation during acute kidney injury and rapid progressive glomerulonephritis (Mulay SR 2012, Mulay SR 2016), whereas under healthy conditions the opposite was now observed. It is therefore possible that Mdm2 has a dual role upon NFkB activation, as described by Cheney in transformed cells (Cheney MD 2008).

The findings of the present study confirm that inhibition of Mdm2 with Nutlin-3a damages podocytes and tubular cells, hence impairing the glomerular filtration barrier and renal function. The higher expression of p53 in renal tissue and the upregulation of its target genes, such as Mdm2, p21, Bax and Bcl-2, point towards podoptosis as the mechanism of podocytopenia. It is noteworthy to mention that the gene expression of *p53 upregulated modulator of apoptosis (PUMA)*, a pro-apoptotic gene induced by p53 that belongs to the Bcl-2 family, appeared unchanged. This observation was consistent with the findings by Jiang et al. (Jiang 2007), and further supports podoptosis as a specific type of regulated cell death and not apoptosis.

5.2 Nutlin-3a affects the outcome of diabetic nephropathy in db/db mice in opposite ways

Nutlin-3a attenuates inflammation and fibrosis

Given that in an inflammatory milieu Mdm2 has been shown to promote the NFκB pathway in a p53-independent manner (Mulay SR 2012, Mulay SR 2016) and that diabetic disease is characterized by chronic inflammation, partly promoted by the activation of the NFκB

pathway (Schmid H 2006, Sanchez AP 2009), we hypothesized that Nutlin-3a would ameliorate diabetic kidney disease by attenuating chronic inflammation. Indeed, reduced inflammation was observed in Nutlin-3a-treated mice, which presented less glomerular macrophage infiltration, downregulation of fibrotic markers and less collagen deposition.

Nutlin-3a aggravates podocytopenia in db/db mice

By means of an adriamycin nephropathy model with BALB/c mice, a model for focal segmental glomerulosclerosis (FSGS), Mulay *et al*. showed how Mdm2 drives podocytes under stress into mitotic catastrophe, leading to increased cell death. Blocking Mdm2 with Nutlin-3a ameliorated the disease in this model by preventing mitotic catastrophe and allowing podocytes to remain arrested and to undergo hypertrophy (Mulay SR 2013). Given that podocyte loss is a major and early event in diabetic nephropathy and that hypertrophy of these cells has also been described in the course of the disease (Hoshi S. 2002, Petermann AT 2005), we hypothesized that blocking Mdm2 with Nutlin-3a in diabetic nephropathy would slow down the progression of the disease by protecting podocytes from mitotic catastrophe.

Cell culture of mouse podocytes in a high glucose media did however not show a protective role from Nutlin-3a. Yet these results have to be interpreted rather carefully, since hyperglycaemia *per se* did not induce podocyte death as described in the literature (Susztak K 2006, Eid AA 2009, Ma T 2013). Tubular cell death in a diabetic milieu has likewise been reported previously (Allen DA 2003, Verzola D 2004, Habib SL 2013), but was not observed in this study.

Nevertheless, the results *in vivo* supported those *in vitro*: Nutlin-3a-treated mice displayed a lower number of podocytes and lower gene expression of podocyte markers after Mdm2 inhibition. This observation revealed that Nutlin-3a induces podocytopenia in this diabetic nephropathy mouse model rather than having a protective effect. Therefore, this outcome strongly argues for mitotic catastrophe being a mechanism of podocyte death in this study. In fact, more types of cell death other than mitotic catastrophe have been described in podocytes (figure 37), including apoptosis (P Mundel 1997, Schiffer M. 2001, Ryu M 2012) and podoptosis (M Ebrahim 2015, Thomasova D. 2015). In both types of cell death, p53 is overexpressed and drives programmed cell death. The first being a caspase-dependent

type of cell death, whereas in podoptosis caspases are not involved (Thomasova D. 2015). Owing to the fact that Nutlin-3a inhibits Mdm2 negative regulation of p53 and promotes its stabilization, the idea of any of these two pathways being the cause of podocytopenia in this study is surely plausible. However, p53 immunostaining did not show an increase of p53 expression in the glomeruli in the Nutlin-3a-treated group. In addition, the transcription of genes promoted by p53 was downregulated. It remains therefore unclear, through which pathway injured podocytes died or detached from the glomerular barrier membrane (GBM) in this model of diabetic nephropathy, thus causing podocytopenia.

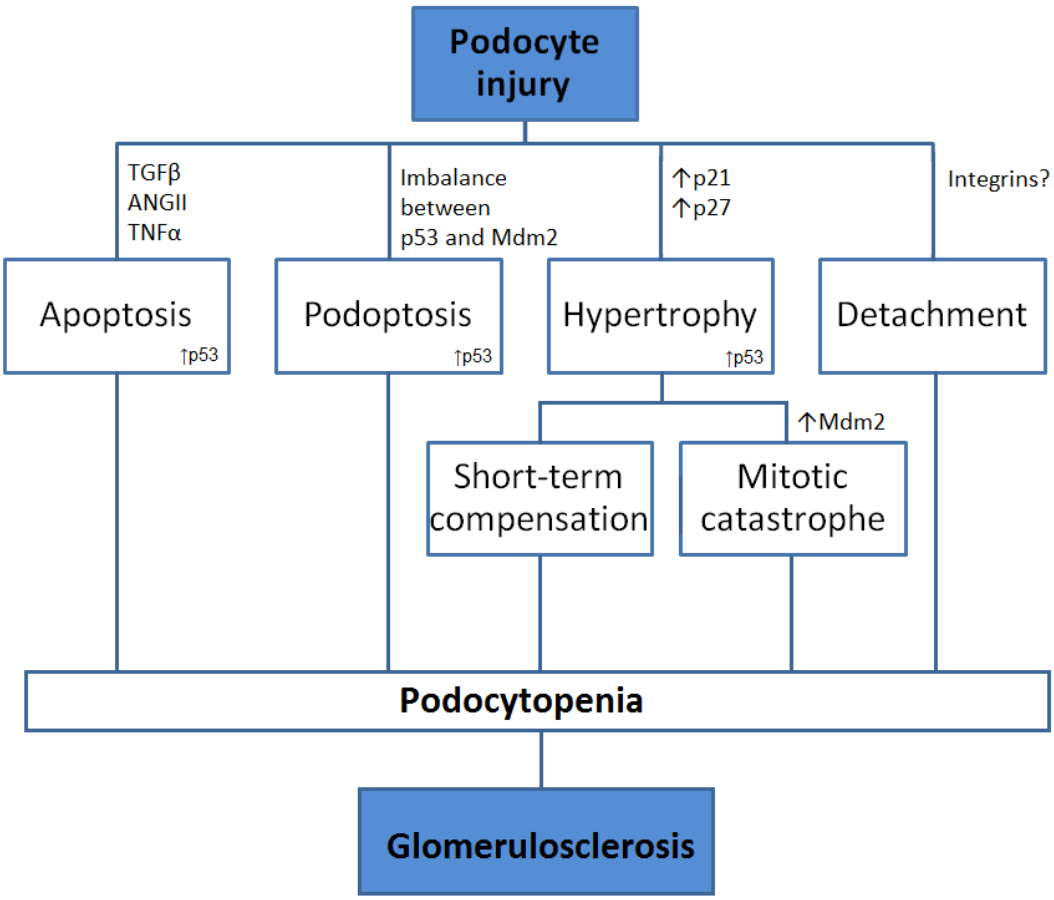

Figure 37. Causes of podocytopenia. The mechanisms underlying podocytopenia are still being elucidated. It has been shown that after injury, podocytes can undergo apoptosis as a result of increased transforming growth factor beta (TGFβ), angiotensin II (ANGII) and tumour necrosis factor α (TNFα). Podoptosis has also been described as a caspase-independent form of cell death ascribed to low levels of Mdm2 and consequent overexpression of p53. After podocyte injury, cells can also undergo cell cycle arrest and hypertrophy through upregulation of the cyclin-dependent kinase inhibitors (CDKI) p21 and p27. This response compensates shortly podocyte loss but can be truncated, if Mdm2 levels raise and mitosis is promoted; leading to an aberrant mitosis and eventually cell death (mitotic catastrophe). Detachment of viable podocytes has been also described after injury, but the underlying mechanisms are not known. Adapted from (Mundel P 2002).

The opposite effect of Nutlin-3a upon db/db mice, where on one hand podocytes damage and loss is induced and on the other hand inflammation is attenuated, could possibly explain why the histological structure was not significantly different between groups. Yet, the overall renal function was in terms of BUN significantly aggravated in Nutlin-3a-treated mice compared to vehicle, possibly due to the increased podocytopenia and tubular damage.

The worsening of DKD in this model could also be explained by an extra role of Mdm2 in diabetic disease. Saito and colleagues recently revealed by means of a computational network associating data from metabolomic analysis (MetabPPI) that Mdm2 presents a significant high number of interactions with enzymes associated with metabolites that are altered in DKD (Saito R 2016). The relevance of Mdm2 was further proved in two independent human cohorts, in which mRNA levels of Mdm2 appeared downregulated in both glomeruli and tubules. Still it is not known yet, by which means Mdm2 is downregulated and whether this molecular modification has an important association with the pathophysiology of DKD or it is rather a consequence of one or more activated pathways. This study could however explain why the administration of Nutlin-3a in healthy mice features some pathological marks of DKD, such as albuminuria and mesangial expansion (figure 19A).

In summary the results observed in diabetic mice treated with Nutlin-3a showed that the blockade of Mdm2 prompts aggravation of podocytopenia and renal function and, at the same time, attenuates renal inflammation and fibrosis. Together, these results reveal a deleterious effect of Mdm2 blockade upon podocytes in healthy mice as well as in a DKD model, in contrast to acute kidney injury models. At the same time, an advantageous effect upon inflammation through inhibition of the NF-κB pathway was observed. A direct inhibition of NF-κB, for example with celastrol, could therefore offer a novel therapeutic strategy in DKD without a negative effect upon podocyte loss, as shown by Kim et al in a db/db mouse model (Kim JE 2013). In addition, further research on Mdm2 and its role in DKD could contribute to the better understanding of its complex pathophisiology and thereby to its treatment.

5.3 Limitations of the study and future perspectives

The present study includes however certain limitations. An important hindrance was the use of a mouse model to study the human DKD. As commented above, this always results in a big constraint to infer conclusions of the disease in humans, since this model (like other diabetic mouse models) cannot fully resemble the disease. As a consequence, the study displays a very restricted external validity. The role of the activated RAAS system and the consequent systemic hypertension is for both T1D and T2D, though in different extent, a hallmark and important factor of the DKD progression. However, the db/db mouse model presents low blood pressure, as opposed to humans. To closely resemble human diabetic features from T2D, the db/db diabetic model was stressed with both uninephrectomy and high fat diet; this caused high mortality, resulting in a much reduced group size that presented high variability. For that reason and the above mentioned, a new study is intended with different diabetic models that will complement the results of the present one and offer a wider interpretation.

The evaluation of renal function was indirectly measured in terms of BUN and serum creatinine. Despite being these two parameters orientative for the GFR, other methods have been proved more precise, for example inulin-clearance. Additionally, a more meticulous analysis on the effect of Nutlin-3a on the tubular compartment should be performed, since this work focused mainly on the glomeruli.

In vitro studies were also limited by the use of mouse cell lines instead of primary cells. Besides, a more detailed study on the gene and protein expression alterations after Nutlin-3a stimulation would render more information on the molecular pathways that are modified and how these may affect tissue function.

5.4 Conclusions

In brief, therapeutic blockade of Mdm2 with Nutlin-3a may hold the risk of increased podocyte and tubular cell death within the kidney. While tubular epithelium has a high potential of renewal, the regeneration of podocytes is limited and might affect the glomerular filtration barrier function and eventually cause impaired renal function. In diabetic kidney disease, where these two compartments are already impaired, Nutlin-3a can further aggravate the disease.

REFERENCES

ACCORD Study Group, Gerstein HC, Miller ME, Byington RP, Goff DC Jr, Bigger JT, Buse JB Cushman WC, Genuth S, et al. (2008). “Effects of intensive glucose lowering in type 2 diabetes”. N Engl J Med **358**(24): 2545-59.

ADVANCE, Collaborative Group, et al. (2008). "Intensive blood glucose control and vascular outcomes in patients with type 2 diabetes." N Engl J Med **358**(24): 2560-2572.

Allam R, Syyed SG, Kulkarni OP, Lichtnekert J, Anders HJ (2011). "Mdm2 promotes systemic lupus erythematosus and lupus nephritis." J Am Soc Nephrol **22**(11):2016-27.

Allen DA, Harwood S, Varagunam, Raftery MJ, Yaqoob MM (2003). "High glucose-induced oxidative stress causes apoptosis in proximal tubular epithelial cells and is mediated by multiple caspases." FASEB J **17**(8): 908-910.

Alpers CE, Fogo AB. (2007). "The Kidney and Its Collecting System." Robbins Basic Pathology(14): 541-577.

Anders HJ, Jayne DRW, Rovin BH. (2016). "Hurdles to the introduction of new therapies for immune-mediated kidney diseases." Nature Reviews Nephrology **12**:205-16.

Atkins, R. (2005). "The epidemiology of chronic kidney disease." Kidney Int Suppl(94): s14-s18.

Ayala JE1, Samuel VT, Morton GJ, Obici S, Croniger CM, Shulman GI, Wasserman DH, McGuinness OP (2010). "NIH Mouse Metabolic Phenotyping Center Consortium. Standard operating procedures for describing and performing metabolic tests of glucose homeostasis in mice." Dis Model Mech **3**(9-10): 525-534.

Ayala JE, Bracy.DP, OP McGuiness, DH Wasserman (2006). "Considerations in the design of hyperinsulinemic-euglycemic clamps in the conscious mouse." Diabetes **55**(2): 390-397.

Aylon Y, Oren M. (2007). "Living with p53, dying of p53." Cell **130**(4): 597-600.

Baigent C, Ladray MJ, Reith C, Emberson J, Wheeler DC, Tomson C, et al. (2011). "The effects of lowering LDL cholesterol with simvastatin plus ezetimibe in patients with chronic kidney disease (Study of Heart and Renal Protection): a randomised placebo-controlled trual." Lancet **377**(9784):2181-92.

Barak Y, Juven T, Haffner R, Oren M (1993). "*mdm2* expression is induced by wild type p53 activity." The EMBO Journal **12**(2): 461-468.

Benigni A, Gagliardini E, Tomasoni S, Abbate M, Ruggenenti P, Kalluri R, Remuzzi G. (2004). "Selective impairment of gene expression and assembly of nephrin in human diabetic nephropathy." Kidney Int **65**(6): 2193-2200.

Birn H, Christensen E. (2006). "Renal albumin absorption in physiology and pathology." Kidney Int **69**(3): 440-449.

Brosius FC, He JC. (2015). "JAK Inhibition and progressive kidney disease." Curr Opin Nephrol Hypertens **24**(1):88-95.

Brown ET, Umino Y, T Loi, E Solessio, R Barlow (2005). "Anesthesia can cause sustained hyperglycemia in C57/BL6J mice." Vis Neurosci **3**: 525-534.

Bueso-Ramos CE, Manshouri T, Haidar MA, Huh YO, Keating MJ, Albitar M. (1995). "Multiple patterns of MDM-2 deregulation in human leukemias: implications in leukemogenesis and prognosis." Leuk Lymphoma **17**(1-2): 13-18.

Bueso-Ramos CE, Manshouri T., Haidar MA, Yang Y, McCown P, Ordonez N, Glassman A, Sneige N, Albitar M. (1996). "Abnormal expression of MDM-2 in breast carcinomas." Breast Cancer Res Treat **37**(2): 179-188.

Bunz F, Dutriaux A, Lengauer C, Waldman T, Zhou S, Brown JP, Sedivy JM, Kinzler KW, Vogelstein B. (1998). "Requirement for p53 and p21 to sustain G2 arrest after DNA damage." Science **282**(5393): 1497-1501.

Cahilly-Snyder L, Yang-Feng T, Francke U, George DL (1987). "Molecular analysis and chromosomal mapping of amplified genes isolated from a transformed mouse 3T3 cell line." Somat Cell Mol Genet **13**(3): 235-244.

Candeias MM, Malbert-Colas L, Powell DJ, Daskalogianni C, Maslon MM, Naski N, Bourougaa K, Calvo F, Fahraeus R (2008). "*p53* mRNA controls p53 activity by managing Mdm2 functions." Nat Cell Biol **10**(9): 1098-1105.

Caruso-Neves C, Kwon SH, Guggino WB. (2005). "Albumin endocytosis in proximal tubule cells is modulated by angiotensin II through an AT2 receptor-mediated protein kinase B activation." Proc Natl Acad Sci U S A **102**(48): 17513-17518.

Castedo M, Perfettini JL, Roumier T, Andreau K, Medema R, Kroemer G. (2004). "Cell death by mitotic catastrophe: a molecular definition." Oncogene **23**(16): 2825-2837.

Chen J, Marechal V, Levine AJ. (1993). "Mapping of the p53 and mdm-2 interaction domains." Mol Cell Biol **13**(7): 4107-4114.

Chène, P. (2003). "Inhibiting the p53-MDM2 interaction: an important target for cancer therapy." Nat Rev Cancer **3**(2): 102-109.

Cheney MD, McKenzie PP, Volk EL, Fan L, Harris LC (2008). "MDM2 displays differential activities dependent upon the activitation status of NFkappaB." Cancer Biol Ther **7**(1): 38-44.

Chiarelli F, Gaspari S, Marcovecchio ML. (2009). "Role of growth factors in diabetic kidney disease." Horm Metab Res **41**:585-93.

Clegg HV, Ithana K., Zhang Y (2008). "Unlocking the Mdm2-p53 loop: Ubiquitin is the key." Cell Cycle **7**(3): 1-6.

Dalla Vestra M, Masiero A, Roiter AM, Saller A, Crepaldi G, Fioretto P. (2003). "Is podocyte injury relevant in diabetic nephropathy? Studies in patients with type 2 diabetes." Diabetes **52**(4): 1031-1035.

DCCT/EDIC, Research Group. (2011). "Intensive diabetes therapy and glomerular filtration rate in type 1 diabetes." N Engl J Med **365**(25): 2366-2376.

DeFronzo, R. (1995). "Diabetic nephropathy: etiologic and therapeutic considerations." Diabetes Rev **3**: 510-564.

de Zeeuw D, Bekker P, Henkel E, Hasslacher C, Gouni-Berthold I, Mehling H, Potarca A, Tesar V, Heerspink HJ, Schall TJ, CCX140-B Diabetic Nephropathy Study Group. (2015). "The effect of CCR2 inhibitor CCX140-B on residual albuminuria in patients with type 2 diabetes and nephropathy: a randomised trial." Lancet Diabetes Endocrinol **3**(9):687-96.

de Zeeuw D, Akizawa T, Audhya P, Bakris GL, Chin M, Schmidt HC, Goldsberry A, Houser M, Krauth M, et al. (2013). "Bardoxolne Methyl in Type 2 Diabetes nd Stage 4 Chronic Kidney Disease." N Engl J Med **369**(26): 2492-503.

Diabetes Cntrol and Complications Trial Research Group. (1993). "The effect of intensive treatment of diabetes on the development and progression of long-term complications in insulin-dependent diabetes mellitus." N Engl J Med **329**(14): 977-986.

Dluhy RG, McMahon GT. (2008). "Intensive glycemic control in the ACCORD and ADVANCE trials." N Engl J Med **358**(24): 2630-2633.

Dong Z, Wang Y, Qiu Q, Zhang X, Zhang L, Wu J, Wei R, Zhu H, et al. (2016). “Clinical predictors differentiating non-diabetic renal diseases from diabetic nephropathy in a large population of type 2 diabetes patients.”. Diabetes Res Clin Pract **121**:112-118.

Dunkler D, Gao P, Lee SF, Heinze G, Clase CM, Tobe S, Teo KK, Gerstein H, Mann JFE, Oberbauer R. (2015). “Risk Prediction for Early CKD in Type 2 Diabetes”. Clinical Journal of the American Society of Nephrology **10**(8):1371-9.

Ebrahim M, Mulay SR, Anders HJ, Thomasova D. (2015). "MDM2 beyond cancer: podoptosis, development, inflammation, and tissue regeneration." Hitol Histopathol **30**(11): 1271-1282.

ECDCDM, Expert Committee on the Diagnosis and Classification of Diabetes Mellitus. (2002). "Report of the Expert Committee on the Diagnosis and Classification of Diabetes Mellitus." Diabetes Care **25**(1): s5-s20.

EDIC Study. (2003). "Sustained effect of intensive treatment of type 1 diabetes mellitus on development and progression of diabetic nephropathy: the Epidemiology of Diabetes Interventions and Complications (EDIC) study." JAMA **290**(16): 2159-2167.

Eid AA, Gorin Y, Faqq BM, Maalouf R, Barnes JL, Block K, Abboud HE (2009). "Mechanisms of podocyte injury in diabetes: role of cytochrome P450 and NADPH oxidases. ." Diabetes **58**(5): 1201-1211.

Eischen CM, Lozano G. (2009). "p53 and MDM2: antagonists or partners in crime?" Cancer Cell **15**(3): 161-162.

Fakharzadeh SS, Trusko S, George SL (1991). "Tumorigenic potential associated with enhanced expression of a gene that is amplified in a mouse tumor cell line." Embo J **10**(6): 1565-1569.

Fang S, Jensen JP, Ludwig RL, Vousden KH, Weissman AM. (2000). "Mdm2 is a RING finger-dependent ubiquitin protein ligase for itself and p53." J Biol Chem **275**(12): 8945-8951.

Foijer F, t. Riele H. (2006). "Check, double check: the G2 barrier to cancer." Cell Cycle **5**(8): 831-836.

Freedman DA, Wu L, Levine AJ. (1999). " Functions of the MDM2 oncoprotein." Cell Mol Life Sci **55**(1): 93-107.

Fullerton B, Jeitler K, Seitz M, Horvath K, Berghold A, Siebenhofer A. (2014). "Intensive glucose control versus conventional glucose control for type 1 diabetes mellitus." Cochrane Database Syst Rev: 2:CD009122.

Gannon HS, Donehower L, Lyle S, Jones SN. (2011). "Mdm2-p53 signaling regulates epidermal stem cell senescence and premature aging phenotypes in mouse skin." Dev Biol **353**(1): 1-9.

García-García PM, Getino-Melián M, Domínguez-Pimentel V, Navarro-González JF. (2014). "Inflammation in diabetic kidney disease." World J Diabetes **5**(4): 431-443.

Gentile G, Mastroluca D, Ruggenenti P, Remuzzi G (2014). "Novel effective drugs for diabetic kidney disease? or not?" Expert Opin Investig Drugs **19**(4): 571-601.

Geyer RK, Yu ZK, Maki CG. (2000). "The MDM2 RING-finger domain is required to promote p53 nuclear export." Nat Cell Biol **2**(9): 569-573.

Grassi G. (2016). "ME 02-3 EXTENDING SPRINT RESULTS TO DIABETICS." J Hypertens **34** Suppl1.

Grier JD, Xiong S, Elizondo-Fraire AC, Parant JM, Lozano G. (2006). "Tissue-specific differences of p53 inhibition by Mdm2 and Mdm4." Mol Cell Biol **26**(1): 192-198.

Habib SL (2013). "Diabetes and renal tubular cell apoptosis." World J Diabetes **4**(2): 27-30.

Hagiwara S, McClelland, Kantharidis P. (2013). "MicroRNA in DIabetic Nephropathy: Renin Angiotensin, AGE/RAGE, and Oxidative Stress Pathway." Journal of Diabetes Research **2013**:11 Pages.

Hainaut P, Hollstein M. (2000). "p53 and human cancer: the first ten thousand mutations." Adv Cancer Res **77**: 81-137.

Han DC, Hoffman BB, Hong SW, Guo J, Ziyadeh FN. (2000). "Therapy with antisense TGF-β oligodeoxynucleotides reduces kidney weight and matrix mRNAs in diabetic mice." Am J Physiol Ren Physiol **278**:628-34.

Haraldsson B., Nyström J, Deen WM. (2008). "Properties of the Glomerular Barrier and Mechanisms of Proteinuria." Physiol Rev **88**: 451-487.

Hashimoto T, Ichiki T, Ikeda J, Narabayashi E, Matsuura H, Miyazaki R, Inanaga K, Takeda K, Sunagawa K. (2011). "Inhibition of MDM2 attenuates neointimal hyperplasia via suppression of vascular proliferation and inflammation." Cardiovasc Res **91**(4): 711-719.

Haupt Y, Maya R, Kazaz A, Oren M (1997). "Mdm2 promotes the rapid degradation of p53." Nature **387**(6630): 296-299.

Hayashi K, Epstein M, Loutzenhiser R, Forster H (1992). "Impaired myogenic responsiveness of the afferent arteriole in streptozotocin-induced diabetic rats: role of eicosanoid derangements." J Am Soc Nephrol **2**(11): 1578-1586.

Haynes R, Lewis D, Emberson J, Reith C, Agodoa L, Cass A, et al. (2014). "Effects of lowering LDL cholesterol on progression of kidney disease."

Honda R, Tanaka H, Yasuda H (1997). "Oncoprotein MDM2 is a ubiquitin ligase E3 for tumor suppressor p53." FEBS Lett **420**(1): 25-27.

Honda R, Yasuda H (2000). "Activity of MDM2, a ubiquitin ligase, toward p53 or itself is dependent on the RING finger domain of the ligase." Oncogene **19**(11): 1473-1476.

Hoshi S, Shu Y, Yoshida F., Inagaki T., Sonoda J., Watanabe T., Nomoto K., Nagata M. (2002). "Podocyte injury promotes progressive nephropathy in zucker diabetic fatty rats." Lab Invest **82**(1): 25-35.

Hostetter, T. (2003). "Hyperfiltration and glomerulosclerosis." Semin Nephrol **23**(2): 194-199.

Huang JS, Chuang LY, Guh JY, Huang YJ. (2007). "Antioxidants attenuate high glucose-induced hypertrophic growth in renal tubular epithelial cells." Am J Physiol Ren Physiol **293**: 1072-82.

Ismail-Beigi F, Craven T, Banerji MA, Basile J, Calles J, Cohen RM, Cuddihy R, Cushman WC, Genuth S, Grimm RH Jr, Hamilton BP, Hoogwerf B, Karl D, Katz L, Krikorian A, O'Connor P, Pop-Busui R, Schubart U, Simmons D, Taylor H, Thomas A, Weiss D, Hramiak I; ACCORD trial group. (2010). "Effect of intensive treatment of hyperglycaemia on microvascular outcomes in type 2 diabetes: an analysis of the ACCORD randomised trial." Lancet **376**(9739): 419-430.

Iwakuma T, Lozano G. (2003). "MDM2, An Introduction." Molecular Cancer Research **1**: 993-1000.

Jenkins AJ, Lyons TJ, Zheng D, Otvos JD, Lackland DT, McGee D, Garvey WT, Klein RL; DCC/EDIC Research Group. (2003). "Serum lipoproteins in the diabetes control and complications trial/epidemiology of diabetes intervention and complications cohort: associations with gender and glycemia." Diabetes Care **26**(3): 810-818.

Jones SN, Hancock AR, Vogel H, Donehower LA, Bradley A. (1998). "Overexpression of Mdm2 in mice reveals a p53-independent role for Mdm2 in tumorigenesis." Proc Natl Acad Sci USA **95**(26): 15608-15612.

Jones SN, Roe AE, Donehower LA, Bradley A (1995). "Rescue of embryonic lethality in Mdm2-deficient mice by absence of p53." Nature **378**(6553): 206-208.

Ju W, Smith S, Kretzler M. (2012). "Genomic biomarkers for chronic kidney disease." Transl Res **159**(4): 290-302.

Kanwar, YS, Sun L, Xie P, Liu FY, Chen S. (2011). "A Glimpse of Various Pathogenic Mechanisms of Diabetic Nephropathy2. Annu Rev Pathol **6**:395-423.

KDIGO (2012). "KDIGO 2012 Clinical Practice Guideline for the Evaluation and Management of Chronic Kidney Disease." Kidney Int **3**(1).

Kelly KJ, Plotkin Z, Vulgamott SL, Dagher PC. (2003). "P53 mediates the apoptotic response to GTP depletion after renal ischemia-reperfusion: protective role of a p53 inhibitor." J Am Soc Nephrol **14**(1): 128-138.

Keswani SG, Katz AB, Lim FY, Zoltick P, Radu A, Alaee D, Herlyn M, Crombleholme TM. (2004). "Adenoviral mediated gene transfer of PDGF-B enhances wound healing in type I and type II diabetic wounds." Wound Repair Regen **12**(5): 497-504.

Kim JE, Lee MH, Nam DH, Song HK, Kang YS, Lee JE, Kim HW, et al. (2013). "Celastrol, an NF-kB inhibitor, improves insulin resistance and attenuates renal injury in db/db mice." PLoS One **8**(4):e62068.

Klag MJ, Whelton PK, Randall BL, Neaton JD, Brancati FL, Ford CE, Shulman NB, Stamler J. (1996). "Blood pressure and end-stage renal disease in men." N Engl J Med **334**(1): 13-18.

Kruiswijk F, Labuschagne C, Vousden KH. (2015). "p53 in survival, death and metabolic health: a lifeguard with a licence to kill." Nat Rev Mol Cell Biol. **16**(7): 393-405.

Kubbutat MH, Jones SN, Vousden KH (1997). "Regulation of p53 stability by Mdm2." Nature **387**(6630): 299-303.

Lachin, J. (2010). "Point: Intensive glycemic control and mortality in ACCORD--a chance finding?" Diabetes Care **33**(12): 2719-2721.

Lasagni L, Lazzeri E, Shankland SJ, Anders HJ, Romagnani P. (2013). "Podocyte Mitosis - A Catastrophe." Current Molecular Medicine **13**: 13-23.

Lee MJ, Feliers D, Mariappan MM, Sataranna tarajan K, Mahimainathan L, et al. (2007). "A role for AMP-activated protein kinase in diabetes-induced renal hypertrophy." Am J Ren Physiol **292**:617-27.

Lengner CJ, Steinman H, Gagnon J, Smith TW, Henderson JE, Kream BE, Stein GS, Lian JB, Jones SN. (2006). "Osteoblast differentiation and skeletal development are regulated by Mdm2-p53 signaling." J Cell Biol **172**(6): 909-921.

Levey AS, Astor BC, Stevens LA, Coresh J. (2010). "Chronic kidney disease, diabetes, and hypertension: what's in a name?" Kidney Int **78**(1): 19-22.

Levey AS, Coresh J. (2012). "Chronic kidney disease." Lancet **379**(9811): 165-180.

Levey AS, Eckardt KU, Tsukamoto Y, Levin A, Coresh J, Rossert J, De Zeeuw D, Hostetter TH, Lameire N, Eknoyan G. (2005). "Definition and classification of chronic kidney disease: a position statement from Kidney Disease: Improving Global Outcomes (KDIGO)." Kidney Int **67**(6): 2089-2100.

Levey AS, Tangri N, Stevens LA. (2011). "Classification of chronic kidney disease: a step forward." Ann Intern Med **154**(1): 65-67.

Li M, Brooks CL, Wu-Baer F, Chen D, Baer R, Gu W. (2003). "Mono- versus polyubiquitination: differential control of p53 fate by Mdm2." Science **302**(5652): 1972-1975.

Li Q, Zhang Y, El-Naggar AK, Xiong S, Yang P, Jackson JG, Chau G, Lozano G. (2014). "Therapeutic efficacy of p53 restoration in Mdm2-overexpressing tumors." Mol Cancer Res **12**(6): 901-911.

Linares LK, Kiernan R, Triboulet R, Chable-Bessia C, Latreille D, Cuvier O, Lacroix M, Le Cam L, Coux O, Benkirane M. (2007). "Intrinsic ubiquitination activity of PCAF controls the stability of the oncoprotein Hdm2." Nat Cell Biol **9**(3): 331-338.

Liu G, Park YJ, Tsuruta Y, Lorne E, Abraham E. (2009). "p53 Attenuates lipopolysaccharide-induced NF-kappaB activation and acute lung injury." J Immunol **182**(8): 5063-5071.

Ma T, Zhu J, Chen X, Zha D, Singhal PC, Ding G (2013). "High glucose induces autophagy in podocytes." Exp Cell Res **319**(6): 779-789.

Marine JC, Lozano G. (2010). "Mdm2-mediated ubiquitylation: p53 and beyond." Cell Death Differ. **17**(1): 93-102.

McNicholas BA, Griffin MD. (2012). "Double-edged sword: a p53 regulator mediates both harmful and beneficial effects in experimental acute kidney injury." Kidney Int **81**(12): 1161-1164.

Mendrysa SM, McElwee MK, Michalowski J, O'Leary KA, Young KM, Perry ME (2003). "mdm2 is critical for inhibition of p53 during lymphopoiesis and the response to ionizing irradiation." Mol Cell Biol **23**(2): 462-472.

Menne J, Eulberg D, Beyer D, Baumann M, Saudek F, Valkusz Z, Wiecek A, Haller H. (2016). "C-C motif-ligand 2 inhibition with emapticap pegol (NOX-E36) in type 2 diabetic patients with albuminuria." Nephrol Dial Transplant (Epub ahead of print).

Meyer TW, Bennett P, Nelson RG. (1999). "Podocyte number predicts long-term urinary albumin excretion in Pima Indians with Type II diabetes and microalbuminuria." Diabetologia **42**(11): 1341-1344.

Michaels J, Churgin SS, Blechman KM, Greives MR, Arabi S, Galiano RD, Gurtner GC. (2007). "db/db mice exhibit severe wound-healing impairments compared with other murine diabetic strains in a silicone-splinted excisional wound model." Wound Repair Regen **15**(5): 665-670.

Mirzayans R, Andrais B, Scott A, Murray D. (2012). "New insights into p53 signaling and cancer cell response to DNA damage: implications for cancer therapy." J Biomed Biotechnol. **2012**(170325. doi: 10.1155/2012/170325).

Mogensen CE, Christensen CK, Vittinghus E. (1983). "The stages in diabetic renal disease. With emphasis on the stage of incipient diabetic nephropathy." Diabetes **32**(Suppl 2): 64-78.

Molitoris BA, Dagher PC, Sandoval RM, Campos SB, Ashush H, Fridman E, Brafman A, Faerman A, Atkinson SJ, Thompson JD, Kalinski H, Skaliter R, Erlich S, Feinstein E. (2009). "siRNA targeted to p53 attenuates ischemic and cisplatin-induced acute kidney injury." J Am Soc Nephrol. **20**(8): 1754-1764.

Momand J, Zambetti GP, Olson DC, George D, Levine AJ (1992). "The mdm-2 oncogene product forms a complex with the p53 protein and inhibits p53-mediated transactivation." Cell **69**(7): 1237-1245.

Montes de Oca Luna R, Wagner DS, Lozano G (1995). "Rescue of early embryonic lethality in mdm2-deficient mice by deletion of p53." Nature **378**(6553): 203-206.

Moran O., Phillip M. (2003). "Leptin: obesity, diabetes and other peripheral effects-a review." Pediatr Diabetes **4**(2): 101-109.

Mulay SR, Thomasova D., Ryu M, Anders HJ (2012). "MDM2 (murine double minute-2) links inflammation and tubular cell healing during acute kidney injury in mice." Kidney Int **81**(12): 1199-1211.

Mulay SR, Thomasova D, Ryu M, Kulkarni OP, Migliorini A, Bruns H, Gröbmayr R, Lazzeri E, Lasagni L, Liapis H, Romagnani P, Anders HJ. (2013). "Podocyte loss involves MDM2-driven mitotic catastrophe." J Pathol **230**(3): 322-335.

Mulay SR, Romoli S, Kumar S, Desai J, Anders HJ, Thomasova D. (2016). "Murine double minute-2 inhibition ameliorates established crescentic glomerulonephritis." Am J Pathol **186**(6):1442-53.

Mundel P, Shankland SJ. (2002). "Podocyte Biology and Response to Injury." J Am Soc Nephrol **13**: 3005-3015.

Mundel P, Reiser J, Zúñiga Mejía Borja A, Pavenstädt H, Davidson GR, Kriz W, Zeller R. (1997). "Rearrangements of the cytoskeleton and cell contacts induce process formation during differentiation of conditionally immortalized mouse podocyte cell lines." Exp Cell Res **236**(1): 248-258.

Naski N, Gajjar M, Bourougaa K, Malbert-Colas L, Fahraeus R, Candeias MM (2009). "The p53 mRNA-Mdm2 interaction." Cell Cycle **8**(1): 31-34.

Navarro-González JF, Mora-Fernández C, Muros de Fuentes M, García-Pérez J. (2011). "Inflammatory molecules and pathways in the pathogenesis of diabetic nephropathy." Nat Rev Nephrol **7**(6): 327-340.

NKF, National Kidney Foundation. (2012). "KDOQI Clinical Practice Guideline for Diabetes and CKD: 2012 Update." Am J Kidney Dis **60**(5): 850-886.

Oliner JD, Pietenpol JA, Thiagalingam S, Gyuris J, Kinzler KW, Vogelstein B (1993). "Oncoprotein MDM2 conceals the activation domain of tumour suppressor p53." Nature **362**(6423): 857-860.

O'Shea JJ, Kontzias A, Yamaoka K, Tanaka Y, Laurence A. (2013). "Janus kinase Inhibitors in autoimmune diseases." Ann Rheum Dis **72**(2):ii111-ii115.

Pätäri A, Forsblom C, Havana M, Taipale H, Groop PH, Holthöfer H. (2003). "Nephrinuria in diabetic nephropathy of type 1 diabetes." Diabetes **52**(12): 2969-2974.

Patel S, Player MR. (2008). "Small-molecule inhibitors of the p53-HDM2 interaction for the treatment of cancer." Expert Opin Investig Drugs **17**(12): 1865-1882.

Perez-Gomez MV, Sanchez-Niño MD, Sanz AB, Zheng B, Martín-Cleary C, Ruiz-Ortega M, et. al. (2016). "Targeting inflammation in diabetic kidney diasease: early clinical trials." Expert Opinion on Investigational Drugs **25**(9):1045-58.

Perry ME, Piette J., Zawadzki JA, Harvey D, Levine AJ (1993). "The mdm-2 gene is induced in response to UV light in a p53-dependent manner." Proc. Natl. Acad. Sci. USA **90**: 11623-11627.

Petermann AT, Pippin J, Durvasula R, Pichler R, Hiromura K, Monkawa T, Couser WG, Shankland SJ. (2005). "Mechanical stretch induces podocyte hypertrophy in vitro." Kidney Int **67**(1): 157-166.

Picksley SM, Spicer JF, Barnes DM, Lane DP. (1996). "The p53-MDM2 interaction in a cancer-prone family, and the identification of a novel therapeutic target." Acta Oncol **35**(4): 429-434.

Poremba C, Yandell DW, Metze D, Kamanabrou D, Böcker W, Dockhorn-Dworniczak B. (1995). "Immunohistochemical detection of p53 in melanomas with rare p53 gene mutations is associated with mdm-2 overexpression." Oncol Res **7**(7-8): 331-339.

Powers AC (2008). "Diabetes Mellitus." Harrison's Principles of Internal Medicine **II**(15): 2275-2304.

Rahmoune H, Thompson PW, Ward JM, Smith CD, Hong G, Brown J. (2005). "Glucose Transporters in human renal proximal tubular cells isolated from the urine of patients with non-insulin-dependent diabetes." Diabetes **54**:3427-34.

Rees DA, Alcolado JC. (2005). "Animal models of diabetes mellitus." Diabet Med **22**(4): 359-370.

Reifenberger G, Liu L, Ichimura K, Schmidt EE, Collins VP. (1993). "Amplification and overexpression of the MDM2 gene in a subset of human malignant gliomas without p53 mutations." Cancer Res **53**(12): 2736-2739.

Remuzzi G, Macia M, Ruggenenti P. (2006). "Prevention and treatment of diabetic renal disease in type 2 diabetes: the BENEDICT study." J Am Soc Nephrol **17**(4 Suppl 2): s90-s97.

Riddle, M. (2010). "Counterpoint: Intensive glucose control and mortality in ACCORD--still looking for clues." Diabetes Care **33**(12): 2722-2724.

Ringshausen I, O'Shea CC, Finch AJ, Swigart LB, Evan GI (2006). "Mdm2 is critically and continously required to supress lethal p53 activity in vivo." Cancer Cell **10**(6): 501-514.

Roth J, D. M., Freedman DA, Shenk T, Levine AJ. (1998). "Nucleo-cytoplasmic shuttling of the hdm2 oncoprotein regulates the levels of the p53 protein via a pathway used by the human immunodeficiency virus rev protein." Embo J **17**(2): 554-564.

Ruggenenti P, Cravedi P, Remuzzi G. (2010). "The RAAS in the pathogenesis and treatment of diabetic nephropathy." Nat Rev Nephrol **6**(6): 319-330.

Ruiz-Ortega M, Esteban V, Rupérez M, Sánchez-López E, Rodríguez-Vita J, Carvajal G, Egido J. (2006). "Renal and vascular hypertension-induced inflammation: role of angiotensin II." Curr Opin Nehrol Hypertens **15**(2): 159-166.

Ryu M, Mulay SR, Miosge N, Gross O, Anders HJ (2012). "Tumour necrosis factor-a drives Alport glomerulosclerosis in mice by promoting podocyte apoptosis." J Pathol **226**(1): 120-131.

Sabounjian L, Graham P, Wu L, Braman V, Cheng C, Liu J, Shipley J, Neutel J, Dao . (2016). "A First-in-Patient, Multicenter, Double-Blind, 2-Arm, Placebo-Controlled, Randomized Safety and Tolerability Study of a Novel Oral Drug Candidate, CTP-499, in Chronic Kideny Disease." Clin Pharmacol Drug Dev **5**(4):314-25.

Saito R, Rocañín-Arjó A, You YH, Darshi M, Van Espen B, Miyamoto S, Pham J, Pu M, et al. (2016). "Systems biology analysis reveals role of MDM2 in diabetic nephropathy." JCI insight **1**(17):e87877.

Sanchez AP, Sharma K. (2009). "Transcription factors in the pathogenesis of diabetic nephropathy." Expert Rev Mol Med **11**(e13).

Satriano J, Vallon V. (2006). "Primary kidney growth and its consequences at the onset of diabetes mellitus." Amino Acids **31**:1-9.

Satriano J, Mansoury H, Deng A, Sharma K, Vallon V, et al. (2010). "Transition of kidney tubule cells to a senescent phenotype in early experimental diabetes." Am J Physiol Cell Physiol **299**:374-80.

Schiffer M., Bitzer M, Roberts IS., Kopp J.B., ten Dijke P., Mundel P., Böttinger E.P. (2001). "Apoptosis in podocytes induced by TGF-beta and Smad7." J Clin Invest **108**(6): 807-816.

Schmid H, Boucherot A, Yasuda Y, Henger A, Brunner B, Eichinger F, Nitsche A, Kiss E, Bleich M, Gröne HJ, Nelson PJ, Schlöndorff D, Cohen CD, Kretzler M, European Renal cDNA Bank (ERCB) Consortium (2006). "Modular activation of nuclear factor-kappaB transcriptional programs in human diabetic nephropathy." Diabetes **55**(11): 2993-3003.

Shangary S, Wang S. (2009). "Small-molecule inhibitors of the MDM2-p53 protein-protein interaction to reactivate p53 function: a novel approach for cancer therapy." Annu Rev Pharmacol Toxicol. **49**: 223-241.

Shankland SJ, Pippin JW, Reiser J, Mundel P. (2007). "Podocytes in culture: past, present and future." Kidney Int **72**(1): 26-36.

Shankland, S. (2006). "The podocyte's response to injury: role in proteinuria and glomerulosclerosis." Kidney Int **69**(12): 2131-2147.

SPRINT Research Group, Wright JT Jr, Williamson JD, Whelton PK, Snyder JK, Sink KM, Rocco MV, Reboussin DM, et al. (2015). "A Randomized Trial of Intensive versus Standard Blood-Pressure Control." N Engl J Med **373**(22):2103-16.

Stommel JM, Marchenko ND, Jimenez GS, Moll UM, Hope TJ, Wahl GM. (1999). "A leucine-rich nuclear export signal in the p53 tetramerization domain: regulation of subcellular localization and p53 activity by NES masking." Embo J **18**(6): 1660-1672.

Sung SH, Zizadeh FN, Wang A, Pyagay PE, Kanwar YS, Chen S. (2006). "Blockade of vascular endothelial growth factor signaling ameliorates diabetic albuminuria in mice." J Am Soc Nephrol **17**(11): 3093-3104.

Susztak K, Raff AC, Schiffer M, Böttinger E (2006). "Glucose-Induced Reactive Oxygen Species Cause Apoptosis of Podocytes and Podocyte Depletion at the Onset of Diabetic Nephropathy." Diabetes **55**: 225-233.

Tabatabai NM, Sharma M, Blumenthal SS, Petering DH. (2009). "Enhanced expressions of sodium-glucose cotransporters in the kidneys in diabetic Zucker rats." Diabetes Res Clin Pract **83**:e27-30.

Taylor WR, Stark GR. (2001). "Regulation of the G2/M transition by p53." Oncogene **20**(15): 1803-1815.

Thomasova D., Bruns HA, Kretschmer V, Ebrahim M, Romoli S, Liapis H, Kotb AM, Endlich N, Anders HJ. (2015). "Murine Double Minute-2 Prevents p53-Overactivation-Related Cell Death (Podoptosis) of Podocytes." J Am Soc Nephrol **26**(7): 1513-1523.

Thomasova D, Mulay SR, Bruns H, Anders HJ (2012). "p53-Independent Roles of MDM2 in NF-kB Signaling: Implications for Cancer Therapy, Wound Healing, and Autoimmune Diseases." Neoplasia **14**(12): 1097-1101.

Tolonen N, Forsblom C, Thorn L, Wadén J, Rosengård-Bärlund M, Saraheimo M, Feodoroff M, Mäkinen VP, Gordin D, Taskinen MR, Groop PH; FinnDiane Study Group (2009). "Lipid

abnormalities predict progression of renal disease in patients with type 1 diabetes." Diabtologia **52**(12): 2522-2530.

Tone A, Shikata K, Matsuda M, Usui H, Okada S, Ogawa D, Wada J, Makino H. (2005) “Clinical features of non-diabetic renal diseases in patients with type 2 diabetes”. Diabetes Research and Clinical Practice **69**(3):237–242.

Tonolo G, Velussi M, Brocco E, Abaterusso C, Carraro A, Morgia G, Satta A, Faedda R, Abhyankar A, Luthman H, Nosadini R. (2006). "Simvastatin maintains steady patterns of GFR and improves AER and expression of slit diaphragm proteins in type II diabetes." Kidney Int **70**(1): 177-186.

Tozawa M, Iseki K, Iseki C, Kinjo K, Ikemiya Y, Takishita S. (2003). "Blood pressure predicts risk of developing end-stage renal disease in men and women." Hypertension **41**(6): 1341-1345.

UKPDS, UK Prospective Diabetes Study Group. (1998). "Intensive blood-glucose control with sulphonylureas or insulin compared with conventional treatment and risk of complications in patients with type 2 diabetes (UKPDS 33)." Lancet **352**(9131): 837-853.

USRDS (United States Renal Data System) (2015). "CKD in the United States". Annual Data Report Volume 1: 13-24.

Valentin-Vega YA, Okano H, Lozano G. (2008). "The intestinal epithelium compensates for p53-mediated cell death and guarantees organismal survival." Cell Death Differ. **15**(11): 1772-1781.

Vallon V. (2010). "The proximal tubule in the pathophysiology of the diabetic kidney". Am J Physiol Regul Integr Comp Physiol **300**:R1009-22.

Vallon V, Thomson SC. (2012). "Renal Function in Diabetic Disease Models: The Tubular System in the Pathophysiology of the Diabetic Kidney." Annu Rev Physiol **74**:351-75.

Vallon V. (2015). "The mechanisms and therapeutic potential of SGLT-2 inhibitors in diabetes mellitus." Annual review of medicine **66**:255-70.

Vassilev LT, Vu B, Graves B, Carvajal D, Podlaski F, Filipovic Z, Kong N, Kammlott U, Lukacs C, Klein C, Fotouhi N, Liu EA (2004). "In Vivo Activation of the p53 Pathway by Small-Molecule Antagonists of MDM2." Science **303**: 844-848.

Verzola D, Bertolotto M, Villaggio B, Ottonello L, Dallegri F, Salvatore F, Berruti V, Gandolfo MT, Garibotto G, Deferrari G (2004). "Oxidative stress mediates apoptotic changes induced by hyperglycemia in human tubular kidney cells." J Am Soc Nephrol **Suppl 1**: s85-s87.

Vestri S, Okamoto MM, De Freitas HS, Aparecida Dos Santos R, Nunes MT, et al. (2001). "Changes in sodium or glucose filtration rate modulate expression of glucose transporters in renal proximal tubular cells of rat." J Membr Biol **182**:105-12.

Vidotti DB, Amoni CP, Maquigussa E, Boim MA. (2008). "Effect of long-term type 1 diabetes on renal sodium and water trasnporters in rats."Am J Npehrol **28**:107-14.

Wada J, Makino H. (2013). "Inflammation and the pathogenesis of diabetic nephropathy." Clinical Science **124**: 139-152.

Wang B., Chandrasekera C, Pippin J.J. (2014). "Leptin- and Leptin Receptor-Deficient Rodent Models: Relevance Human Type 2 Diabetes." Current Diabetes Reviews **10**: 131-145.

Wanner C, Inzucchi SE, Lachin JM, et al. (2016). Empagliflozin and Progression of Kidney Disease in Type 2 Diabetes." The New England Journal of medicine **375**(4):323-34.

Watanabe T, Hotta T, Ichikawa A, Kinoshita T, Nagai H, Uchida T, Murate T, Saito H. (1994). "The MDM2 oncogene overexpression in chronic lymphocytic leukemia and low-grade lymphoma of B-cell origin." Blood **84**(9): 3158-3165.

Wei CC, Zhang SL, Chen YW, Guo DF, Ingelfinger JR, Bomsztyk K, Chan JS. (2006). "Heterogeneous nuclear ribonucleoprotein K modulates angiotensinogen gene expression in kidney cells." J Biol Chem **281**(35): 25344-25355.

White KE, Bilous RW, Diabiopsies Study Group. (2004). "Structural alterations to the podocyte are related to proteinuria in type 2 diabetic patients." Nephrol Dial Transplant **19**(6): 1437-1440.

WHO (2015). "Diabetes. Fact sheet." World Health Organization **312**.

Wolf G, Schroeder R, Ziyadeh FN, Stahl RA. (2004). "Albumin up-regulates the type II transforming growth factor-beta receptor in cultured proximal tubular cells." Kidney Int **66**(5): 1849-1858.

Wolf G, Ziyadeh FN. (2008). "Cellular and molecular mechanisms of proteinuria in diabetic nephropathy". Nephron Physiol **106**:26-31.

Yang B, Hodgkinson A, Oates PJ, Millward BA, Demain AG. (2008). "High glucose induction of DNA-binding activity of the transcription factor NF-κB in patients with diabetic nephropathy." Biochem Biophys Acta **1782**:295-302.

Yang JY, Zong CS., Xia W, Yamaguchi H, Ding Q, Xie X, Lang JY, Lai CC, Chang CJ, Huang WC, Huang H, Kuo HP, Lee DF, Li LY, Lien HC, Cheng X, Chang KJ, Hsiao CD, Tsai FJ, Tsai CH, Sahin AA, Muller WJ, Mills GB, Yu D, Hortobagyi GN, Hung MC. (2008). "ERK promotes tumorigenesis by inhibiting FOXO3a via MDM2-mediated degradation." Nat Cell Biol **10**(2): 138-148.

Yin Y, Sthephen C, Luciani MG, Fahraeus R (2002). "p53 stability and activity is regulated by Mdm2-mediated induction of alternative p53 translation products." Nat Cell Biol **4**(6): 462-467.

Zhang F, Tagen M, Throm S, Mallari J, Miller L, Guy RK, Dyer MA, Williams RT, Roussel MF, Nemeth K, Zhu F, Zhang J, Lu M, Panetta JC, Boulos N, Stewart CF. (2011). "Whole-

body physiologically based pharmacokinetic model for nutlin-3a in mice after intravenous and oral administration." Drug Metab Dispos. **39**(1): 15-21.

Zhang XP, Liu F, Cheng Z, Wang W. (2009). "Cell fate decision mediated by p53 pulses." Proc Natl Acad Sci U S A **106**(30): 12245-12250.

Zhao Y, Yu H, Hu W. (2014). "The regulation of MDM2 oncogene and its impact on human cancers." Acta Biochim Biophys Sin **46**(3): 180-189.

Zimmet P, A.lberti KG, Shaw J. (2001). "Global and societal implications of the diabetes epidemic." Nature **414**(6865): 782-787.

Zinman B, Wanner C, Lachin JM, et al. (2015). "Empagliflozin, Cardiovacular Outcomes, and Mortality in Type 2 Diabetes." The New England journal of medicine **373**:2117-28.

Ziyadeh, F. (2004). "Mediators of diabetic renal disease: the case for tgf-Beta as the major mediator." J Am Soc Nephrol **15**(Suppl 1): s55-s57.

Ziyadeh FN, Wolf G. (2008). "Pathogenesis of the podocytopathy and proteinuria in diabetic glomerulopathy." Curr Diabetes Rev **4**(1): 39-45.

Zuurbier CJ, Keijzers P, Koeman A, Van Wezel HB, Hollmann MW (2008). "Anesthesia's effects on plasma glucose and insulin and cardiac hexokinase at similar hemodynamics and without major surgical stress in fed rats." Anesth Analg **106**(1): 135-142.

ABBREVIATIONS

A	
ACTA1	Actin alpha 1
AGE/RAGE	Advanced Glycation Endproduct / Receptors of AGE
AKI	Acute kidney injury
ANGII	Angiotensin II
aSMA	Actin, alpha skeletal muscle
B	
Bcl-2	B-cell Lymphoma 2
BUN	Blood Urea Nitrogen
C	
CCL x	Chemokine Ligand x
CCR x	Chemokine Receptor x
CD2AP	CD2 associated protein
CKD	Chronic kidney disease
Col 1/4	Collagen 1/4
D	
db/db	Leptin receptor deficient mice
DKD	Diabetic kidney disease
DM	Diabetes mellitus
DMSO	Dimethyl-sulfoxide
DNA	Desoxyribonucleic acid
E	
ESRD	End stage renal disease
F	
FSGS	Focal segmental glomerulosclerosis

G	
GFB	Glomerular filtration barrier
GFR	Glomerular filtration rate
GS	Glomerular score
H	
HDL	High density lipoprotein
I	
ICAM x	Intercellular adhesion molecule
IL x	Interleukine x
iNOS	Inducible nitric oxide synthase
i.p.	intraperitoneal
J	
JAK/STAT	Janus kinase / Signal transducers and activators of transcription
L	
LDH	Lactate dehydrogenase
LDL	Low density lipoprotein
M	
Mdm2	Murine double minute 2
MTC	Mouse tubular cells
mRNA	Messenger RNA
N	
NF-κB	Nucear factor ‘kappa light chain enhancer’ of activated Bcells
P	
PAS	Periodic Acid Schiff
PCR	Polymerase chain reaction
PEC	Parietal epithelial cells

PKC	Proteinkinase C
PUMA	p53 upregulator of apoptosis
R	
RAAS	Renin Angiotensin Aldosterone System
RITA	Reactivation of p53 and induction of tumour cell apoptosis
RNA	Ribonucleic acid
ROS	Reactive oxygen species
RT-PCR	Real time PCR
S	
SGLT 1/2	Sodium glucose transporter 1/2
SNGFR	Single nephron GFR
siRNA	Small interfering RNA
T	
T1/2D	Type 1/2 Diabetes
TGF	Tubuloglomerular feedback
TGFβ	Transforming growth factor beta
TNFα	Tumour necrosis factor alpha
V	
VEGF	Vascular endothelial growth factor
W	
WT1	Wilms tumour 1

LIST OF FIGURES AND TABLES

SGLT2 = sodium glucose cotransporter-2, *RAAS = Renin Angiotensin Aldosterone System, SNGFR= Single-Nephron glomerular filtration rate.*

Figure 3. Schematic drawing of the glomerular filtration barrier, composed of podocytes and its pseudopods, the glomerular basement membrane (GBM) and the endothelium. Adapted from (Haraldsson B. 2008).

Figure 4. Autorregulatory feedback loop. In conditions of no stress, Mdm2 inhibits p53 in three ways: 1) blocks transactivation of p53, 2) favours nuclear export, and 3) induces p53 degradation. However, upon DNA damage, p53 levels increase and transactivation of p53 targets takes place. Among p53 target genes, there is Mdm2. If the DNA damage is repaired, the increasing levels of Mdm2 will again inhibit p53 and restore its levels. Adapted from (Chène 2003).

Figure 5. Mdm2 protein domains. The conserved domains of Mdm2 are the p53 interaction domain in the aminoterminus, the nuclear localization signal (NLS) and the nuclear export signal (NES), the acidic domain and Zinc finger, which interact with ribosomal proteins, and in the carboxiterminus the RING finger domain with E3 ubiquitin ligase activity. Adapted from (Iwakuma T 2003).

Figure 6. p53 stabilization and response. In non-stressed cells, p53 exists in very low concentrations. Under cellular stress, the levels of p53 raise and p53 mediates the transcription of genes involved in apoptosis, cell cycle arrest, and DNA repair. Adapted from (Chène 2003).

Figure 7. Inhibitors of the Mdm2-p53 interaction. Schematic representation of the Mdm2 and p53 proteins. Nutlin binds Mdm2 in the p53 binding domain in the aminoterminus, HLI98 binds Mdm2 in the RING domain, and RITA binds p53 in the transactivation domain. Adapted from (Marine JC 2010).

Figure 8. Immunofluorescence staining for Nephrin and Mdm2 of a glomerulus. In the first picture on the left, nephrin stains in green the cytoplasm of podocytes. In the second one, expression of Mdm2 inside the glomerulus is stained in red. In the last picture, on the

Figure 13. **A-B) Viability (MTT assay) and C-D) cytotoxicity (LDH assay) in mouse tubular cells. A)** Stimulation with Nutlin-3a reduced tubular cell viability after 12 hours and **B)** after 24 hours post-stimulation compared to control and vehicle, being statistically significant at the later time point. **C-D)** Nutlin-3a stimulation increased significantly cytotoxicity in a dose-dependent manner after 6 and 24 hours. Triton X was used as negative control for the MTT assay and as positive control and reference for the cytotoxicity assay. Podocytes cultured in media with 5% serum served as survival control. n = 5 for each group. *NG = normal glucose media (5,5mM); NG+10 = normal glucose media with 10µM of Nutlin-3a; NG+15 = normal glucose media with 15µM of Nutlin-3a; NG+20 = normal glucose media with 20µM of Nutlin-3a; NG+DMSO = normal glucose with 20µl/ml of DMSO*. Data was analyzed using 1-way ANOVA with Tukey's Multiple Comparison Test. * = p<0,05; ** = p<0,005; *** = p<0,0005.

Figure 14. Viability (MTT assay) and cytotoxicity (LDH assay) in mouse podocytes and mouse tubular cells exposed to normal (5,5-11mM) or high glucose media (45mM). A) An environment rich in glucose increases mouse podocyte viability and reduces significantly cell death after 48 hours. **B)** Mouse tubular cells presented by contrast no statistical difference in viability but again they did in cytotoxicity in the later time point, being significantly greater in a normal glucose than in high glucose media. Data was analyzed with t-test.n = 10 in each group. *NG = normal glucose media (5-10mM)*; *HG = high glucose media (25mM)*. * = p<0,05; ** = p<0,005; *** = p<0,0005.

Figure 15. Viability (MTT assay) and cytotoxicity (LDH assay) in mouse podocytes cultured in high glucose media (45mM). A) Podocyte stimulation with Nutlin-3a in a high glucose media reduces significantly cell viability in a dose-dependent manner compared to control after 12 hours and **B)** after 24 hours, which was significantly different compared to vehicle. **C-D)** Nutlin-3a stimulation in podocytes exposed to high glucose media increases significantly the cytotoxicity in a dose-dependent manner compared to control and vehicle after 6 and 24 hours. Triton X was used as negative control in the viability assay and as positive control and reference for the cytotoxicity assay. Manitol (25mM) was used as control of osmolarity for the high glucose environment. No statistical differences were found between manitol and high glucose that could suggest a negative effect of high glucose media in cell osmolarity. Data was analyzed with 1 way ANOVA withTukey's Multiple

Comparison Test. n = 5 per group. *HG = high glucose media; HG+10 = high glucose media with 10µM of Nutlin-3a; HG+15 = high glucose media with 15µM of Nutlin-3a; HG+20 = high glucose media with 20µM of Nutlin-3a; HG+DMSO = high glucose with 20µl/ml of DMSO*. * = p<0,05; ** = p<0,005; *** = p<0,0005.

Figure 16. Viability (MTT assay) and cytotoxicity (LDH assay) in mouse tubular cells cultured in high glucose media (45mM). A) Stimulation of mouse tubular cells with Nutlin-3a of exposed to high glucose media reduced significantly the cell viability in a dose-dependent manner compared to control after 12 hours. **B)** After 24 hours, viability was also significantly reduced after Nutlin-3a stimulation compared to control but not to vehicle. **C)** Cytotoxicity in MTCs exposed to high glucose media increased in the Nutlin-3a-treated groups compared to control after 6 hours, but the difference was not significant compared to vehicle. **D)** After 24 hours of stimulation with Nutlin-3a no significant differences were seen among the groups. Triton X was used as negative control in the viability assay, and as positive control and reference for the cytotoxicity assay. Manitol (25mM) was used as control of osmolarity for the high glucose environment. No statistical differences were found between manitol and high glucose that could suggest a negative effect of high glucose meda in cell osmolarity. Data was analyzed with 1-way ANOVA with Tukey's Multiple Comparison Test. n = 5 per group. *HG = high glucose media; HG+10 = high glucose media with 10µM of Nutlin-3a; HG+15 = high glucose media with 15µM of Nutlin-3a; HG+20 = high glucose media with 20µM of Nutlin-3a; HG+DMSO = high glucose with 20µl/ml of DMSO*. * = p<0,05; ** = p<0,005; *** = p<0,0005.

Figure 17. Body weight, blood glucose levels and survival percentage. A) Body weight monitoring during treatment with Nutlin-3a. While body weight in vehicle and control mice increased progressively with age, Nutlin-3a-treated mice lost weight from the moment that the treatment was established. **B)** At the end of the study, the body weight of Nutlin-3a-treated mice was significantly lower compared to control and vehicle (p<0.0005). **C)** 100% of control (n=3) and vehicle (n=6) mice survived until the end of the study while only 72% of Nutlin-3a-treated mice did (n=11). The difference is however no significant (p=0.2). Survival curves were compared with Mantel-Cox test. **D)** Glycaemia at the end of the study was significantly lower in Nutlin-3a-treated mice compared to vehicle (p<0.05) but not compared to control mice (p>0.05).

Figure 18. Renal functional parameters. A) Plasma creatinine levels increased in the Nutlin-3a group (2.8 ± 1.4 mg/dl) compared to vehicle and control (1.8 ± 0.7 and 1.7 ± 0.6 mg/dl, respectively), but not significantly. **B)** Blood urea nitrogen (BUN) levels at the end of the study significantly increased in Nutlin-3a-treated group (36.2 ± 3.6 mg/dl) compared to vehicle (23.9 ± 3.2 mg/dl) ($p<0,05$), but not to control (26.7 ± 1.7 mg/dl). **C-D)** Albumin/creatinine ratio increased slightly after the first week of treatment and strikingly at the end of the treatment, being significantly higher compared to vehicle and control ($p<0.05$). Data were analysed with 1-way ANOVA with Tukey's Multiple Comparison Test. n(Control) = 3; n(Vehicle) = 6; n(Nutlin-3a) = 5. *ns = statistically not significant; * = p<0,05.*

Figure 19. Glomerular PAS score and mRNA expression. A) Representative pictures of each group. Original magnification 40x. (Arrow: mild mesangial expansion). **B)** Semiquantification of glomerular damage in PAS stained slides of paraffin-fixed kidney tissue. While control and vehicle mice have an average of 0.11±0.05 and 0.20±0.13, being 0 considered as normal and 1 as mild mesangial proliferation, Nutlin-3a-treated mice present a significant higher score with an average of 0.50±0.14. **C)** Gene expression of tubular injury markers appear upregulated in Nutlin-3a mice. Data was analysed with 1 way ANOVA with Tukey's Multiple Comparison Test. n(Control) = 3; n(Vehicle) = 6; n(Nutlin-3a) = 5. *ns = statistically not significant; * = p<0,05.*

Figure 20. p53 immunostaining and gene expression of MDM2 and p53. **A)** Representative pictures of p53 immunostaining. In the Nutlin-3a group, overexpression of p53 in the periphery of the glomeruli and in some tubular cells was seen, as shown in the picture (white arrow), whereas no p53 staining was observed in vehicle and control treated mice. **B)** Quantification of the percentage of stained area that shows significantly higher p53 levels in the Nutlin-3a group compared to vehicle ($p<0,05$). **C)** Both *Mdm2* and *p53* expression is upregulated in Nutlin-3a-treated mice compared to control and vehicle ($p<0.05$). Data was analysed with 1 way ANOVA with Tukey's Multiple Comparison test. *ns = statistically not significant*; *** = p<0,05; ** = p<0,005.*

Figure 21. Gene expression of p53-related target genes. The pro-apoptotic genes Bcl-2 and Bax are upregulated in the Nutlin-3a group compared to vehicle and control ($p<0,05$),

whereas mRNA levels of PUMA did not differ between groups. The gene expression of cyclin-dependent kinase inhibitor p21 is also upregulated in the Nutlin-3a-treated group compared to vehicle (p<0,05), but not to control. Data was analysed with 1-way ANOVA with Tukey's Multiple Comparison Test. *ns = statistically not significant*; ** = p<0,05; ** = p<0,005.*

Figure 22. Wt-1/Nephrin staining and podocyte count. **A)** Representative pictures of each group. In red, Wt1; in green, Nephrin. **B)** Quantification. The number of podocytes in the Nutin-3a-treated group was significantly lower (11,55 ± 0,48) than the one in the vehicle group (13,66 ± 0,68) and control group (15,87 ± 0,35). Data was analysed with the average of podocytes per glomerulus in each kidney, involving a minimum of 20 glomeruli for each kidney. 1-way ANOVA with Tukey's Multiple Comparison Test was applied. *ns = statistically not significant*; ** = p<0,05; ** = p<0,005*.

Figure 23. Gene expression of NFκB and inflammatory markers. A) mRNA levels of the NFκB subunits, p50 and p65, appear significantly upregulated in the Nutlin-3a-treated group compared to control and vehicle (p<0,05). **B)** mRNA levels of CCL5, CCL2, IL-1β, TNFα, iNOS, IL-12a and IL-6 are significantly upregulated in Nutlin-3a-treated mice compared to vehicle (p<0.05). Data was analysed with 1-way ANOVA with Tukey's Multiple Comparison Test. *ns = statistically not significant; * = p<0,05; ** = p<0,005.*

Figure 24. Glomerular macrophage infiltration. A) Representative pictures of Mac2 staining of kidney sections from vehicle and Nutlin-3a-treated mice. Arrows point at stained macrophages. **B)** Quantification. The average number of macrophages in the Nutlin-3a-treated group (0,98 ± 0,11) is significantly higher than that observed in the vehicle group (0,57 ± 0,11) (p<0,05). The difference however with the control group (0,61 ± 0,13) is not statistically significant. On the left a picture of a representative glomerulus for the vehicle and Nutlin—3a group is displayed. Arrows point at stained macrophages. Data was analysed with 1-way ANOVA with Tukey's Multiple Comparison Test. *ns = statistically not significant; * = p<0,05..*

Figure 25. Gene expression of fibrosis markers. There are no significant differences between groups in the gene expression of fibrotic markers such as Fibronectin, aSMA,

Col1a1 and Coll4a1. However, expression of Laminin ($p<0,05$) and TGFβ ($p<0,05$) are significantly upregulated compared to vehicle and control. Data was analysed with 1-way ANOVA with Tukey's Multiple Comparison Test. *ns = statistically not significant; * = p<0,05; ** = p<0,005*

Figure 26. Collagen 1 immunohistochemistry. **A)** Representative pictures of collagen 1 staining for each group. No significant differences were observed between groups. Pictures were analysed with Image J. **B)** Quantification of the percentage of stained area. Data was analyzed using 1 way ANOVA and Tukey's Multiple Comparison Test. *ns = statistically not significant.*

Figure 27. Percentage of survival and glycaemia. **A)** In both groups, mortality during the treatment was very high but no significant differences were seen between survival rates. **B)** Plasma glucose levels were steadily high in both groups, and no significant difference was observed between groups. S*urvival curves were compared with Mantel Cox Test and glycaemia was analysed with 2-Way-ANOVA.*

Figure 28. Cholesterolemia and triacylgliceridemia. A high fat diet (10% fat content) was employed in the study, to emulate closer the human environmental factors of diabetes type II. As a control, blood of diabetic mice with the same background and age, which also underwent uninephrectomy, was concurrently analysed with a colorimetric assay. **A)** Triacylgliceride levels increased significantly over time ($p<0,0001$) but were not affected by a diet richer in fat content ($p=0,36$); however, **B)** cholesterolemia was significantly higher in these mice than in those fed with a normal diet ($p<0,0001$) . Data were analysed with 2-Way-ANOVA. *UNI = uninephrectomized; ND = normal diet (4,5% fat content); HFD = high fat diet (10% fat content); ns = statistically not significant; * = p<0,05; ** = p<0,005; *** = p<0,0005.*

Figure 29. Renal functional parameters. **A)** Plasma creatinine levels are increased in Nutlin-3a group (2.10 ± 0.23 mg/dl) compared to vehicle (1.33 ± 0.06 mg/dl), but not significantly ($p=0,09$). **B)** Blood urea nitrogen (BUN) levels increased overtime, being significantly higher after four weeks of treatment with Nutlin-3a ($p<0,05$).. **C-D)** Albuminuria as means of albumin/creatinine ratio appeared not significantly different between groups.

Data was analysed with Man Whitney Test for A and D, and with 2-Way-ANOVA for B. n(Vehicle) = 4, n(Nutlin-3a) = 6. *ns = statistically not significant; * = p<0,05*

Figure 30. Glomerular PAS score. **A)** Representative pictures of each group. Glomerulus presents an important mesangial proliferation and mild to severe sclerosis. **B)** Glomerular score showed no significant difference between groups. Data was analyzed with Man Whitney test. *ns = statistically not significant.*

Figure 31. p53 immunostaining and gene expression of Mdm2 and p53. **A)** Representative pictures of p53 immunostaining. No significant differences were seen between groups. **B)** Quantification of the percentage of stained area that shows no significant differences between the Nutlin-3a group and vehicle group. **C)** p53 gene expression is downregulated in Nutlin-3a-treated mice compared to vehicle ($p<0.05$), without being significant for Mdm2 mRNA levels. Data was analysed with Man Whitney test. *ns = statistically not significant*; ** = p<0,05.*

Figure 32. Gene expression of p53-tanscription dependent genes. The proapoptotic genes Bcl-2 and Bax are downregulated in the Nutlin-3a-treated group compared to vehicle ($p<0,05$) whereas mRNA levels of PUMA show no difference between groups. The gene expression of cyclin-dependent kinase inhibitor p21 is also downregulated in the Nutlin-3a-treated group compared to vehicle ($p<0,05$). Data was analysed with Mann Whitney Test. *ns = statistically not significant*; ** = p<0,05..*

Figure 33. Wt-1/Nephrin staining and podocyte count. **A)** Representative images of immunofluorescence with Wt-1/Nephrin in vehicle and Nutlin-3a-treated group. The number of podocytes is considerably reduced compared to healthy mice due to diabetic nephropathy. **B)** The number of podocytes in the Nutin-3a treated group was significantly lower (5,84 ± 0,22) than in the vehicle group (6,59 ± 0,07). Data was analysed with the average of podocytes per glomerulus in each kidney, counting a minimum of 20 glomerules for each kidney. Data was analysed with Man Whitney test. ** = p<0,05.*

Figure 34. Gene expression of podocyte markers. mRNA levels of podocyte markers, such as nephrin, Wt-1, synaptopodin, podocin, Podocalyxin, and CD2AP are downregulated

in the Nutlin-3a group compared to control and vehicle (p<0,05). Data was analysed with Mann Whitney Test. *ns = statitstically not significant*; ** = p<0,05; ** = p<0,01*.

Figure 35. Glomerular macrophage infiltration and gene expression of NFκB and inflammatory markers. A) Representative pictures of Mac2 staining for each group. **B)** Quantification of number of macrophages per glomerulus in each group. A minimum of 20 glomerules were scored for each kidney. While vehicle group presents an average of 2,97 ± 0,12 macrophages per glomerulus, Nutlin-3a-treated group displayed 1,81 ± 0,05 (p<0,05). **C)** mRNA levels of the NFκB subunits p50 and p65 are downregulated in the Nutlin-3a-treated group compared to vehicle; difference is not statistically significant (p=0,07 and p=0,11, respectively). **D)** mRNA levels of inflammatory markers are not significantly reduced in the Nutlin-3a group, except for CCL5 (p<0.05). Data was with Mann Whitney Test. N(Vehicle) = 4; n(Nutlin-3a)=6. *ns = statistically not significant; * = p<0,05.*

Figure 36. Collagen 1 staining and gene expression of fibrosis markers. **A)** Immunohistochemistry. Representative pictures of collagen 1 staining of kidney sections from db/db mice treated with Nutlin-3a or vehicle. **B)** Quantification of the stained area. Nutlin-3a mice displayed a significant lower expression of collagen 1 than the vehicle group (p<0,005). **C)** mRNA levels of fibronection, laminin, TGFβ, aSMA and collagen 4 a1 are downregulated in the Nutlin-3a-treated group compared to vehicle (p<0,05). Collagen 1, however, does not reach statistical significance. Data was analysed with Mann Whitney Test. *ns = statistically not significant; * = p<0,05; ** = p<0,01.*

EIDESSTATTLICHE VERSICHERUNG

Ich erkläre hiermit an Eides statt,

dass ich die vorliegende Dissertation mit dem Thema

Role of murine double minute-2 in diabetic kidney disease

selbständig verfasst, mich außer der angegebenen keiner weiteren Hilfsmittel bedient und alle Erkenntnisse, die aus dem Schrifttum ganz oder annähernd übernommen sind, als solche kenntlich gemacht und nach ihrer Herkunft unter Bezeichnung der Fundstelle einzeln nachgewiesen habe.

Ich erkläre des Weiteren, dass die hier vorgelegte Dissertation nicht in gleicher oder in ähnlicher Form bei einer anderen Stelle zur Erlangung eines akademischen Grades eingereicht wurde.

München, 06.11.2017	Anaïs Rocañín Arjó
Ort, Datum	Unterschrift

PUBLICATIONS

Part of the work has been published in:

Saito R, Rocanin-Arjo A, You YH, Darshi M, Van Espen B, Miyamoto S, Pham J, Pu, M, Romoli S, Natarajan L, Ju W, Kretzler M, Nelson R, Ono K, Thomasova D, Mulay SR, Ideker T, D'Agati V, Beyret E, Belmonte JC, Anders HJ, Sharma K. (2016). "Systems biology analysis reveals role of MDM2 in diabetic nephropathy." JCI insight **1**(17):e87877.

Part of the work was presented in

- *Kongress für Nephrologie 2015 von der DGfN.*
- *Kidney Week 2015 from the ASN (*SA-OR040)

ACKNOWLEDGEMENTS

Many people have supported me during this year and made this dissertation possible; thank you all for being there.

Firstly, I would like to thank my 'Doktorvater' **Prof. Hans-Joachim Anders** to give me the opportunity to work with him and to show me the backstage of science progress. Thank you very much. To all my **lab buddies** I would also like to show my gratitude, for their help and the wonderful time I spent with them in and outside the lab: Julia, Julian, Santosh, Dana, Mohsen, Bea, Severin, Franzi, Satish, Shrikant, Kirstin, Martrez, Jyaysi, Alexander, Marc, Melissa, Nina, Lukas, Yajuan and Tomo. Thanks for everything you showed me and for your willingness to always help. I thank also Dan and Jana for providing technical assistance to carry out the research work successfully. And to **Simone Romoli** and **Steffi Steiger** I would like to dedicate a special mention, not only for giving me constant support, but also to guide me through all this year. Thank you all for giving me unforgettable memories.

I would also like to express my gratitude to **Kumar Sharma**, Young You, Manjula Darshi, Jessica Pham and Rintairo Saito from the Centre for Renal Translational Medicine in UCSD in Sand Diego, California, for their support and help during my stay with them and for the wonderful collaboration and teamwork.

For **my family**, there are not enough words to express my love and gratitude. To my sister and my mum, who despite the distance are always there for me, I am profoundly grateful. I also thank my father, who stays even much much further, for all his valuable lessons that along with his love will remain always in my heart. Und ich bedanke mich auch bei meiner liebevollen und warmherzigen deutschen Familie. Vielen Dank Heinrich, Monika und Katrin für eure Unterstützung und Liebe.

And last but not least, I want to thank my friend and partner **Michael**. Thank you for your constant help and dedication, for making me smile and laugh, for comforting me in blue moments and for your love and affection.